Hydrological response of the Ötztal glacierized catchments to future climate change

R.R. Wijngaard
Utrecht University & alpS GmbH

Master Thesis

Hydrological response of the Ötztal glacierized catchments to future climate change

August 2014

Written by:
René Reijer Wijngaard
3346005
R.R.Wijngaard@students.uu.nl

Graduate School of Geosciences
Faculty of Geosciences
Utrecht University

Supervised by:
Prof. Dr. Ir. M.P.F. (Marc) Bierkens
M.P.F.Bierkens@uu.nl

Dr. M. (Matthias) Huttenlau
huttenlau@alps-gmbh.com
Dr. K. (Katrin) Schneider
scheider@alps-gmbh.com

Department of Physical Geography
Faculty of Geosciences
Utrecht University

alpS GmbH
Centre for Climate Change Adaptation

Acknowledgements

First of all I would like to thank sincerely my supervisors Prof. Dr. Ir. M.F.P. (Marc) Bierkens, Dr. M. (Matthias) Huttenlau and Dr. K. (Katrin) Schneider. Prof. Dr. Ir. Marc Bierkens initiated this internship by giving a lot of valuable ideas and by creating the first contacts with the host institution alpS GmbH. During the internship his valuable suggestions and feedback were essential for improving my thesis. Dr. Matthias Huttenlau and Dr. Katrin Schneider helped me with the set-up of this research. Without them this internship would not be possible. They also supplied me with a lot of valuable suggestions and feedback for improving my thesis.

I would like to thank alpS GmbH for the supply of data, which made this research possible. Special thanks to Paul Schattan, Kay Helfricht, Dr. K. (Kristian) Förster, Klaus Schneeberger, Johannes Bellinger, Dr. C. (Christian) Georges and Florian Hanzer. Paul Schattan greatly helped me with introducing HBV Light and GIS. His advice was valuable to have a better understanding of modelling and working with GIS. Kay Helfricht made it possible to work with his glaciological model and helped me with glaciology-related questions. Klaus Schneeberger was always there to help me if I had problems with Matlab. Also he supplied me with valuable advice and ideas in relation with hydrological statistics. Johannes Bellinger was always available for questions in relation with data sets used for this research. Paul Schattan, Dr. Kristian Förster, Klaus Schneeberger, Dr. Christian Georges and Florian Hanzer provided me with valuable feedback and suggestions for improving my Master Thesis or were there to give some advice.

I would like to thank the Faculty of Geosciences. They provided me in the last two years with valuable knowledge about Hydrology, Water Management, Earth Sciences and many other relevant skills. I would like to express special appreciation to Dr. Ir. W.W. (Walter) Immerzeel. During my Master study I got inspired by his work and his valuable contribution to science. His work helped me to get better understandings in the field of mountain hydrology.

At last, I would like to thank my parents, my brother, my sister and my friends who always supported me during the internship and writing my Master Thesis. Without them it would not be possible to complete the Master Thesis.

"*The truth is: the natural world is changing. And we are totally dependent on that world. It provides our food, water and air. It is the most precious thing we have and we need to defend it.*"

Sir David Attenborough

Abstract

For people living in and around glacierized catchments runoff that originates from glaciers and snow is a valuable water resource. Especially in arid/semi-arid mountainous regions and during dry periods runoff derived from glaciers and snow can be the only substantial source of water supply. In the European Alps, where most glacierized catchments are characterized by high runoff conditions during summer and low runoff conditions during winter, dry periods are not so common. The expectation however is that climate will change and dry periods will be more common in summer, since temperature is expected to increase and precipitation is expected to decrease. Moreover climate change is expected to affect glacial evolution and likewise the expectation is that climate change will alter the runoff characteristics of these catchments, which will have serious consequences for the water resources and water management of these catchments. Thus, it is important to know how glacierized catchments respond hydrologically to future climate change.

In order to investigate the hydrological response of Alpine catchments to future climate change the semi-distributed hydrological model 'HBV Light' is used to model future runoff for gauging stations Brunau (Ötztaler Ache), Obergurgl (Gurgler Ache) and Vent (Venter Ache), which are located in the Ötztal Alps. To understand the functioning of the model, first a sensitivity analysis is conducted in order to investigate the effect of parameter changes on simulated discharge. Subsequently the model is calibrated, validated and forced by separate and combined glacier and climate scenarios. For glacier scenarios, present, near future, mid future and far future glacial area distributions are used. These glacial area distributions are extracted from a model, which is able to derive future ice thickness, glacial area and volume distributions as a result of climate change. For climate scenarios climate projections of daily precipitation and daily temperature for 1985-2100 are used, which are realizations of an ensemble of three RCM's (ALADIN, RegCM3 and REMO) based on SRES A1B. These projections are subsequently used in a "delta change approach" on a daily basis for (i) near future, (ii) mid future and (iii) far future, using the meteorological data series of 1983-2012 as reference period. Finally, the results of the HBV Light runs are used to analyse changes in the seasonality of high runoff conditions, absolute changes, relative changes, and peak and low flow characteristics.

The glacier scenarios show a stronger rate of ice-thickness reduction than area reduction until ~2040. After 2040 the reduction rate of ice-thickness becomes smaller, while reduction rates of area and volume are predicted to increase. At the end of the 21st century the expectation is that less than 20% of the glacier area and volume of 2006 will be left. Future runoff simulations, under glacier-only scenarios, show a decrease in runoff during summer period with relative decreases up to 45%. Also the expectation is that highest runoff conditions will shift from July to June for the gauging stations Obergurgl and Brunau. For climate-only scenarios future runoff simulations show an increase in spring runoff up to 300%. For combined scenarios (glacier and climate change) increases up to 125% for spring and decreases up to 55% for July-August are projected. The highest runoff conditions are expected to shift from July to May-June. The changing runoff conditions may implicate that flood risk will increase during late spring and early summer and therefore result in changing flood seasonality. Moreover low flow conditions will become more frequent during summer months towards the end of the 21st century. These predictions are however uncertain due to uncertainties in meteorological data, glacial evolution, climate projections and model-related aspects, such as parameter uncertainties.

The results of this study help to better understand the future impact of climate change and the associated reduction of glacier volumes on the water cycle of alpine catchments. It may contribute to the development of adaptation measures, reducing the impact of changing runoff characteristics and improving the sustainability of alpine catchments.

Key Words: hydrological response, climate change, glacier change, HBV Light, Ötztaler Ache.

Samenvatting

Voor bewoners die in en rondom vergletsjerde stroomgebieden leven, vormt de afvoer afkomstig van gletsjers en sneeuw een waardevolle waterbron. Deze afvoer kan in het bijzonder in aride en semi-aride gebergten of gedurende droge perioden de enigste substantiële bron zijn voor de watervoorziening. In de Europese Alpen, waar vergletsjerde stroomgebieden meest gekarakteriseerd worden door hoge afvoerconcentraties in de zomer en lage afvoerconcentraties in de winter, komen droge perioden momenteel zelden voor, maar door de verwachte klimaatverandering zullen droge perioden vaker optreden. De verwachting is dat gedurende de zomer de temperatuur zal toenemen en dat neerslag zal afnemen. Daarnaast zal klimaatverandering effect hebben op de ontwikkeling van gletsjers en de afvoerkarakteristieken van alpine stroomgebieden. Dit kan mogelijkerwijs serieuze gevolgen hebben voor het waterbeheer van deze stroomgebieden. Daarom is het relevant om te onderzoeken wat de mogelijke effecten van klimaatverandering kunnen zijn op de hydrologie van vergletsjerde stroomgebieden.

Om de hydrologische veranderingen als gevolg van klimaatverandering te kunnen modelleren wordt het semi-verdeelde hydrologische model “HBV Light” gebruikt. Het onderzoeksgebied is het stroomgebied van de Ötztaler Ache (Tirol, Oostenrijk) waarbij de afvoermeetstations Brunau (Ötztaler Ache), Obergurgl (Gurgler Ache) en Vent (Venter Ache) gebruikt worden voor gedetailleerde analyses. Om een beter beeld te krijgen in hoe het model functioneert, wordt er eerst een sensitiviteitsanalyse uitgevoerd waarbij de effect van parameterveranderingen op de gesimuleerde afvoer onderzocht wordt. Vervolgens wordt het model gekalibreerd, gevalideerd en voor het opstellen van afvoertijdseries toegepast. Het model wordt gerund met gescheiden gletsjer- en klimaatscenario’s en met gecombineerde scenario’s welke rekening houden met zowel gletsjerveranderingen als ook klimaatveranderingen. De gletsjerscenario’s zijn gebaseerd op toekomstige gletsjeroppervlakteverdelingen die gemodelleerd zijn voor veranderende klimaatcondities. Voor de klimaatscenario’s worden klimaatprojecties op basis van dagelijkse temperatuur- en neerslagwaarden voor de periode 1985-2100 gebruikt. Deze projecties zijn realiseringen uit een ensemble van drie RCMs (ALADIN, RegCM3 en REMO, gebaseerd op SRES A1B) die in een “delta change approach“ toegepast worden. Als referentieperiode worden meteorologische data uit 1983-2012 gebruikt. Tot slot worden de resultaten uit “HBV Light” gebruikt om seizoensgebonden veranderingen van hoge afvoercondities, absolute veranderingen, relatieve veranderingen en hoog- en laagwaterkarakteristieken te analyseren.

De gletsjerscenario’s laten tot ~2040 een sterke reducering in ijsdikten en een geringere afname in oppervlakteverdelingen zien. Vanaf ~2040 wordt de reducering van ijsdikten geringer. Echter is een sterke teruggang van gletsjeroppervlakte en -volume te verwachten. De verwachting is dat aan het einde van de 21e eeuw minder dan 20% van de gletsjeroppervlakte en -volume van 2006 over is. Onder aanname van gletsjerscenario’s laten toekomstige afvoersimulaties een relatieve afname tot 45% zien in de zomer. Daarnaast is de verwachting dat de hoogste afvoercondities van juli naar juni verschuiven waarbij dit geldt voor meetstations Brunau en Obergurgl. Onder aanname van klimaatscenario’s laten toekomstige afvoersimulaties een verhoging van 300% zien in de lente. Voor de gecombineerde scenario’s is een verhoging tot 125% in de lente en een reducering tot 55% in juli-augustus te verwachten. Daarnaast zullen naar verwachting de hoogste afvoercondities van juli naar mei – juni verschuiven. De veranderingen in de afvoerkarakteristiek impliceren dat mogelijkerwijs het hoogwaterrisico toe zal nemen in het voorjaar en het begin van de zomer. Bovendien zal laagwater naar het einde van de 21^{e} eeuw toe vaker gaan optreden. Deze voorspellingen moeten echter voorzichtig benaderd worden door onzekerheden in de meteorologische data, de gletsjerontwikkelingen, de klimaatprojecties en model gerelateerde aspecten zoals parameter onzekerheden.

De resultaten van deze studie helpen een beter beeld te krijgen van de mogelijke impact van gletsjer- en klimaatveranderingen op de watercyclus van alpine stroomgebieden. De gewonnen kennis kan een bijdrage leveren in de ontwikkeling van adaptatiemaatregelen met als doel de impact van veranderende afvoerkarakteristieken te reduceren en de duurzaamheid van alpine regio’s te bevorderen.

Trefwoorden: afvoerkarakteristiek, gletsjerverandering, klimaatverandering, HBV Light, Ötztaler Ache.

Kurzfassung

Der durch Gletscher- und Schneeschmelze dominierte Abfluss im alpiner Einzugsgebiete stellt für deren Bewohner eine wertvolle Wasserressource dar. Speziell in ariden und semi-ariden Gebirgsregionen und während Trockenperioden kann dieser Abfluss die einzige substantielle Quelle für die Wasserversorgung sein. Grundsätzlich sind vergletscherte Einzugsgebiete meist charakterisiert durch eine höhere Abflusskonzentration im Sommer und eine Niedrige im Winter. Momentan treten Trockenperioden in weiten Teilen der Europäischen Alpen eher selten auf, jedoch wird sich durch den erwarteten Klimawandel die Situation verschärfen. Generell sind eine Zunahme der Temperatur und eine Abnahme des Niederschlags im Sommer zu erwarten. Außerdem hat der Klimawandel Auswirkungen auf die Gletscherentwicklung und die Abflusscharakteristik alpiner Einzugsgebiete. Dies kann möglicherweise zu Engpässen im Bereich der Wasserversorgung führen. Daher ist die Erforschung der möglichen Auswirkungen des Klimawandels auf die Hydrologie vergletscherter Einzugsgebiete von hoher Relevanz.

In der vorliegenden Arbeit wird das halbverteilte hydrologische Modell „HBV Light“ verwendet, um die möglichen klimatisch induzierten Auswirkungen auf das Abflussregime zu modellieren. Als Untersuchungsregion dient das Einzugsgebiet der Ötztaler Ache (Tirol, Österreich), wobei detaillierte Analyse für die Pegelmessstellen Brunau (Ötztaler Ache), Obergurgl (Gurgler Ache) und Vent (Venter Ache) durchgeführt werden. Um ein besseres Modellverständnis zu erhalten, wird eine Sensitivitätsanalyse ausgeführt, wobei die Auswirkung der Parameteränderungen auf den simulierten Abfluss untersucht wird. Anschließend wird das Modell kalibriert, validiert und für die Erstellung von Abflusszeitreihen verwendet. Das Modell wird sowohl mit separaten Gletscher- und Klimaszenarien als auch mit kombinierten Szenarien der Gletscheränderungen und des Klimawandels betrieben. Die Gletscherszenarien basieren auf zukünftigen Gletscherflächenverteilungen, die für geänderte Klimabedingungen modelliert wurden. Für die Klimaszenarien werden Klimaprojektionen auf Basis täglicher Niederschlags- und Temperaturdaten für die Periode 1985-2100 verwendet. Diese Projektionen sind Realisierungen aus einem Ensemble von drei RCMs (ALADIN, RegCM3 und REMO, basierend auf SRES A1B), die in einem „delta change“ Ansatz verwendet werden. Als Referenzperiode werden meteorologische Daten der Periode 1983-2012 verwendet. Zuletzt werden die Ergebnisse aus „HBV Light“ ausgewertet, um die Änderungen der Saisonalität hoher Abflusskonditionen, der absoluten Änderungen, der relativen Änderungen und der Hoch- und Niedrigwassercharakteristiken zu analysieren.

Die Gletscherszenarien zeigen bis ~2040 eine starke Reduzierung der Eisdicken und eine geringere Abnahme der Flächenverteilungen. Ab ~2040 wird die Reduzierung der Eisdicken geringer jedoch zeigen die Flächen und das Volumen einen starken Rückgang. Bis Ende des 21. Jahrhunderts ist zu erwarten, dass weniger als 20% der Vergletscherung von 2006 verbleiben wird. Unter Verwendung der Gletscherszenarien zeigen die zukünftigen Abflusssimulationen eine relative Abnahme bis zu 45% im Sommer. Dazu wird sich voraussichtlich das Juli-Maximum der mittleren monatlichen Abflusshöhen in den Juni verschieben, wobei dies für die Pegelmessstellen Brunau und Obergurgl gilt. Unter Verwendung der Klimaszenarien zeigen die zukünftigen Abflusssimulationen eine Erhöhung um bis zu 300% im Frühling. Für die kombinierten Szenarien ist eine Erhöhung von bis zu 125% im Frühling und eine Abnahme von bis zu 55% im Juli-August zu erwarten. Dazu wird sich voraussichtlich das Juli-Maximum der mittleren monatlichen Abflusshöhen in den Mai-Juni verschieben. Die Änderungen der Abflusscharakteristik implizieren, dass möglicherweise das Hochwasserrisiko im Frühjahr und Frühsommer zunehmen wird. Außerdem werden bis Ende des 21. Jahrhunderts Perioden mit Niedrigwasserführung der Flüsse im Sommer häufiger. Die Prognosen sind jedoch mit Vorsicht zu betrachten, da es große Unsicherheiten im Bereich der meteorologischen Daten, der Gletscherentwicklung und den Klimaprojektionen gibt. Ebenso gibt es Unsicherheiten im Bereich des Modells sowie Unsicherheiten in Beziehung mit der Parametrisierung.

Die Ergebnisse dieser Arbeit helfen die Auswirkung der Gletscheränderungen und des Klimawandels auf den Wasserkreislauf alpiner Einzugsgebiete besser zu verstehen. Das gewonnene Wissen hilft bei der Entwicklung von Anpassungsmaßnahmen, um die negativen Auswirkungen sich ändernden Abflusscharakteristika zu begrenzen und um nachhaltige Entwicklungen in alpinen Regionen sicherzustellen.

Schlüsselwörter: Abflusscharakteristika, Gletscheränderung, Klimawandel, HBV Light, Ötztaler Ache

Table of Contents

List of Figures

List of Tables

1. Introduction

1.1 Background and Problem Description

For civilizations living in mountain ranges and surrounding regions runoff originating from glaciers and snow is a valuable water resource. So-called 'mountain runoff', which can partly consist of melt water deriving from glaciers and snow, forms an important resource for drinking water supply, agricultural and other purposes (e.g. energy production from hydropower). Especially for arid and semi-arid regions mountain runoff can be a very important water supplier, which can be illustrated by rivers located in arid/ semi-arid regions like the Nile, the Euphrates, the Indus, the Ganges or the Colorado. Figures from Viviroli and Weingartner (2004) show that runoff from adjacent mountain ranges can contribute over 90% to the total runoff of these rivers. In a similar way the significance of mountain runoff (only glacial runoff) is illustrated by Kaser et al. (2010), which introduced a population impact index number as a relation between population density in a certain altitude band and the maximum monthly contribution of mountain runoff to the total runoff in the same altitude band. With this number Kaser et al. (2010) found out that human interdependence of mountain runoff is strongest in the intermediate altitude bands since these areas still experience relatively high contributions of mountain runoff (generally decreases in downstream direction) in combination with relatively high population numbers (generally increases in downstream direction). The importance of contributions from mountain ranges to their lowland areas makes that these mountain ranges can be defined as the 'water towers' of these areas (Viviroli et al., 2007). In this way mountain ranges like the Central-Asian mountain ranges (e.g. Tibetan Plateau and Himalayas) and the European Alps can be interpreted to be 'water towers' of their surrounding lowlands. Central Asian mountain ranges, for example, are the main water suppliers for more than 1.4 billion citizens living in these mountain ranges and their surrounding lowlands (Immerzeel et al., 2010). This is not different for the European Alps. Millions of citizens living in the European Alps and surrounding lowlands are directly or partly dependent on the contribution of mountain runoff, which mainly exists of melt water originating from glacier and snow storages (Alpine Convention, 2009). The mean contribution of discharge from the Alps to the total discharge of rivers having their source in the Alps can vary between 26% and 53% for the rivers Danube (gauging station Ceatal Izmail, Romania) and Po (gauging station Pontelagoscuro, Italy) respectively. The magnitude of the contribution to total discharge depends on the proportion of the catchment covered by the Alps. For the Danube catchment this proportion is 10%, which results in lower mean contributions than the Po catchment, which has a proportion of 35%. This is also reflected in the contributions of the Alps to summer discharge. In the summer period high amounts of melt water deriving from glacier and snow storages located in the Alps in combination with an evapotranspiration surplus in lowland regions lead to higher contributions varying from 35% to 80% for the rivers Danube and Po respectively (Weingartner and Viviroli, 2004; Wehren et al., 2010). Especially during hot and dry periods, such as the summer periods of 1976 and 2003, the contributions deriving from glacier and snow storages are very important for water supply in the lowland regions. This can be illustrated by measurements in the Rhine catchment where contributions up to 95% were measured during the summer period of 1976 (Middelkoop, 2008, pp.283), while in the summer of 2003 contributions varied between 14.3 % and 55.7% at Lobith (catchment glacierization of 0.2%) and Bern (catchment glacierization of 6.4%) respectively. The difference with percentages observed in 1976 is that the percentages of 2003 were only based on contributions from glacial storages (Huss, 2011).

Although glacier and snow storages are important for lowland regions these storages are even more important in the headwater catchments (characterized by higher contributions from glacial and snow storages) located in the Alps since these storages may be the only substantial water suppliers for civilizations living in these catchments, especially during dry summer seasons (Schneeberger et al., 2003). According to the classification system of Pardé (1947) these headwater catchments are characterized by several runoff regimes varying from moderate nival regimes to glacial regimes (predominant in catchments with glacial cover of 15-20% or more) with the highest

runoff conditions occurring in May for moderate nival regimes (see Figure 1.1) and in July/August for glacial regimes (see Figure 1.2). The difference in the timing of highest runoff conditions is explained by the fact that moderate nival regimes are mainly dominated by snowmelt, which appears in May and June, where glacial regimes are dominated by glacial melt, which appears in July-September (Mader et al., 1996; Wehren et al., 2010). In winter period all regimes are characterized by low runoff conditions since most of the precipitation is stored temporally in the form of snow.

***Figure 1.1**: mean discharge (1952-1982) for Grossache, Tyrol. The plot illustrated here is typical for moderate nival regimes. Source: Mader et al., 1996.*

Climate change is expected to change the runoff regimes in the headwater catchments (Huss et al., 2008). Especially the catchments dominated by regimes characterized by glacial cover are highly vulnerable to climate change and therewith-related expected changes in runoff regimes. The expectation is that long-term climate change[1] (Schädler and Weingartner, 2010) will lead to glacier volume and area losses, something that already has been observed in the European Alps since the end of the Little Ice Age (±1850), with an exception of late 1970s, which was a short period accompanied with glacial advance (Abermann et al., 2009; Pellicciotti et al., 2010; Beniston, 2011). The general trend of glacial volume and area losses can be confirmed by inter alia the Austrian glacier inventories of 1969 and 1997. Based on these glacier inventories volume and area losses of 22% and 17% respectively were reported by Lambrecht and Kuhn (2007) relative to the initial glacial volume (22.78 km^3) and area (567 km^2) of 1969. A more recent glacier inventory (2006) of the Ötztaler Alps, containing almost one-third of all glaciers in the Austrian Alps with a glacier area of 151,2 km^2 (1997), illustrates relative area losses of 12.2% and 8.3% for the same reference period 1969-1997 and the period 1997-2006 respectively (Abermann et al., 2009).

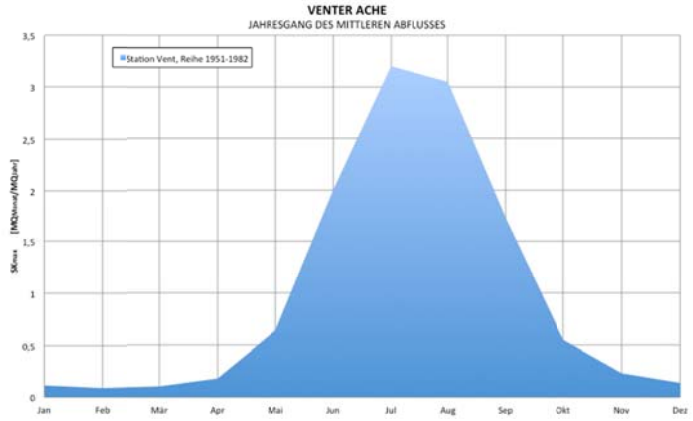

***Figure 1.2**: mean discharge (1952-1982) for Venter Ache. The plot illustrated here is typical for glacial regimes. Source: Mader et al., 1996.*

[1] Temperature increase of 3.9 °C for the Alps and 4.3 °C for the higher regions (>1500m) until 2100. Yearly precipitation decrease of 1 – 11%, with overall increase during spring period. Based on IPCC Scenario A1B.

It is likely that toward the future potential glacier volume losses will affect runoff characteristics. The expectation is that loss of glacier volume initially will lead to an increase in runoff, but will decrease on the long run (Braun et al., 2000; Helfricht et al., In Press; Huss et al., 2014). The explanation behind this pattern is that melting of glaciers initially is associated with thinning in combination with rise of the ELA (Equilibrium Line Altitude) and reduction of the AAR (Accumulation Area Ratio). Rising ELA/ Reducing AAR means that a larger area of bare ice is exposed, decreasing the albedo and eventually leading to a further enhancement of glacier melt. In this phase runoff as a result of glacial melt water increases. After some period of enhanced glacier melt a stage is reached, which can be associated with a stronger area reduction than thickness reduction. In this stage the ELA reaches the highest part of the glacier and the AAR becomes zero, meaning that the entire glacier area is exposed as bare ice. During this stage highest runoff conditions start to shift from July/ August to May/June implicating that, in combination with decreasing snow cover due to increase in temperature, glacial regimes will shift toward nivo-pluvial regimes (Braun et al., 2000; Casassa et al., 2009).

Changing runoff characteristics have a lot of consequences for the water resources management and water management of alpine valleys. A potential increase in runoff may lead to higher flood peaks and therefore increasing flood risk. Adaptation measures may be needed to reduce damages caused by flooding. A potential decrease in runoff may lead to increasing year-to-year runoff variability having consequences for the seasonal water availability of inter alia the drinking water supply, the agricultural sector and the energy sector (hydropower generation). For example, 50-60% of the Swiss electricity production and 60-75% of the Austrian electricity production currently rely on hydropower generation, which is possible due to high runoff rates, low year-to-year variability and high relief energy (Wehren et al., 2010). Decreasing runoff would mean that the capacity for hydropower generation decreases, having consequences for the electricity production in these countries. In order to project the impact of climate change on the water resources of alpine valleys, one needs to build hydrological models. Based on the analyses with these models adaptation measures can be developed, reducing the impact of changing runoff patterns and improving the sustainability of water resources in alpine valleys.

1.2 Previous Work

There have been quite a number of studies dedicated to assessing the effect of climate change on runoff characteristics in glacierized headwater catchments. In these studies conceptual hydrological models are most often used since these models are most feasible for areas with limited data availability (Middelkoop, 2008, pp. 272). Examples of conceptual hydrological models, that have been used, are:

- HBV (*Hydrologiska Byråns Vattenbalansavdelning*; Bergström and Forsman, 1973; Bergström et al., 1992, Bergström and Singh, 1995; Lindström et al., 1997). HBV has been used by inter alia Junghans et al. (2011) for the Silvretta catchment located on the Swiss/ Austrian border and the Rhine catchment upstream of Basel. In this study the HBV model was compared with the GERM model (Huss et al., 2008). Junghans et al. (2011) concluded that the HBV model is less suitable for glacierized catchments since the glacier routine present in the HBV is static, excluding the changes in glacier volume and area. Other widespread used versions of HBV are HBV3-ETH9 (Braun and Aellen, 1990; Braun and Renner, 1992), which is a modified version of the original HBV model with modifications in the snow and glacier routine, and HBV Light (Seibert, 1997, 1999; Seibert and Vis, 2012), which is developed for easy application of the HBV model. HBV3- ETH9 has been applied in the Central Asian mountain ranges (Braun et al., 1993; Hagg et al., 2007) and in the European Alps (Braun and Aellen, 1990; Braun and Renner, 1992; Hottelet et al., 1993; Braun et al., 2000). HBV Light has been applied in a few glacierized catchments located in the European Alps by Konz and Seibert (2010).

- PREVAH (*PREcipitation-Runoff-EVApotranspiration HRU (Hydrological Response Units) Model*; Gurtz et al., 1999, 2003; Viviroli et al., 2009). The PREVAH model uses the original HBV model as main foundation, but has several extensions and improvements, which were needed for inter alia developing a representative model for mountainous catchments. The extensions and improvements were mainly performed in the groundwater, glacier, interception and snow-and ice melt modules, and in relation with some parameters concerning soil moisture and evapotranspiration (Viviroli et al., 2009). The PREVAH model has mainly been used for flood forecasting or water balance modelling in the European Alps (Verbunt et al., 2007; Zappa et al., 2008), Russia (Oltchev et al., 2002) and China (Bosshard and Zappa, 2008). The PREVAH model has also been applied for runoff modelling in a few glacierized catchments located in the Austrian Alps (Koboltschnig et al., 2007, 2008).
- SRM (*Snowmelt Runoff Model*; Martinec, 1975). According to Martinec et al. (2008) the SRM has been applied in over 100 basins worldwide. The SRM is mainly used for the simulation of daily discharge as a result of snowmelt and rainfall. Immerzeel et al. (2010) extended the original SRM with application of glacier melt, which enabled the possibility to simulate daily discharge as a result of glacier melt.
- GERM (*Glacier Evolution Runoff Model*; Huss et al., 2008). GERM is a glacio-hydrological model that has been developed to combine runoff simulations of high-glacierized catchments with glacier mass balances. GERM has mainly been applied in the European Alps using RCM data input (Huss et al., 2008; Junghans et al., 2011; Farinotti et al., 2012) and the Central Asian mountain ranges (Sorg et al., 2013). Next to GERM also other glacio-hydrological models have been developed. Schneeberger et al. (2003) developed a glacier balance model and a glacier flow model for several glaciers and heavily glaciated areas in the world. GCM models were used as climatic input for the balance model. Similar approaches were applied for Central Asian catchments, e.g. Baltoro (Pakistan), Langtang (Nepal) and the Amu and Syr Darya catchments (Kyrgyzstan and Tajikistan) using downscaled GCM data (Immerzeel et al., 2012, 2013; Lutz et al., 2013).

Next to the widely used conceptual models there are also a few conceptual models, which have been developed for catchments in the Austrian Alps and which may be important in the context of this research. These conceptual models are the models:

- HQSIM (Kleindienst, 1996), which is a semi-distributed water balance model based on HRU's and using the BROOK model of Federer and Lash (1978) as foundation (Kirnbauer et al., 2009), containing internal reservoirs for snow, soil moisture and groundwater. HQSIM is mainly used for flood forecasting and water balance modelling in the non-glaciated catchments of Tyrol, Austria, but has recently also been used for glaciated catchments (Helfricht et al., In Press). Nowadays HQSIM forms an important part of an operational flood forecasting system for the Tyrolean part of the river Inn together with the SES model and a 1-D hydraulic model, called Flux$^{DSS/DESIGNER}$. This system, called HOPI (*HOchwasserPrognose für den Tiroler Inn*) has been developed by alpS GmbH on behalf of the Tyrolean government and the Tyrolean hydropower company, called TIWAG (*Tiroler Wasserkraft AG*) (Kirnbauer et al., 2009; Schöber et al., 2010).
- SES (Schnee- und Eis Schmelzmodel/ Snow and Glacier Melt Model; Asztalos, 2004; Asztalos et al., 2007), which is a fully distributed energy balance based model developed to simulate runoff in glaciated catchments (Achleitner et al., 2012). SES forms a relevant part of the HOPI system and has mainly been used in the glaciated catchments of the Ötztaler and Stubaier Alps in Austria (Kirnbauer et al., 2009; Schöber et al., 2010; Achleitner et al., 2012).

Next to conceptual hydrologic models there also have been other approaches to study the effect of climate change on the runoff characteristics, such as water balance models in a subcatchment located in the Indus catchment (Jeelani et al., 2012) and physically based models called TOPKAPI-ETH and WaSIM-ETH. TOPKAPI-ETH (Ragletti and Pellicciotti, 2012) is a modified version of the fully

distributed hydrological model TOPKAPI (*TOPographic Kinematic APproximation and Integration model*), which has mainly been applied in catchments located in the Andes and Karakorum (Ragletti and Pellicciotti, 2012; Ragletti et al., 2013). WaSIM-ETH (*Waterbalance Simulation Model ETH*) is a fully distributed catchment model originally developed by Schulla (1997) and expanded by Klok and Roelofsma (1999) with the glacial submodel of Hock (1999) to make the model feasible for simulating runoff in heavily glaciated catchments. WaSIM-ETH has mainly been applied in the European Alps (e.g. Klok et al., 2001; Verbunt et al., 2003), but also in other regions of the world, e.g. Iceland (Rögnvaldsson et al., 2007; Einarsson and Jónsson, 2010).

In the above-mentioned studies, assessing the effects of climate change on runoff characteristics in glacierized catchments, several trends have been reported. For instance in a glacierized catchment located in Iceland runoff increases have been projected for the winter, early summer (due to increase in snowmelt) and late summer periods (due to increase in ice melt) of 2021-2050 (Einarsson and Jónsson, 2010). In the Austrian and Swiss Alps increases in annual runoff (due to increase in ice melt) have been projected for the first decades of the 21st century, while for the second half of the 21st century annual runoff decreases have been projected with positive runoff changes in spring/ early summer (due to earlier onset of snowmelt) and negative runoff changes in July/ August, (due to decrease in ice melt, snowmelt and precipitation, and increase in evapotranspiration) (Huss et al., 2008; Junghans et al., 2011; Farinotti et al., 2012; Helfricht et al., In Press). Similar trends have been reported for a part of the Central Asian mountain ranges. For instance in the Tien Shan mountain range (Kyrgyzstan/ Tadzhikistan) runoff increases and decreases have been projected until 2050-2075 for the spring and summer periods respectively, assuming a doubling of present CO_2 concentrations and a total loss of glaciers (Hagg et al., 2007). Another study performed by Sorg et al. (2013), in the Tien Shan mountain range, projects a decrease in annual runoff on long term, which is mainly caused by a decrease in precipitation and glacial volume. However, in other parts of the Central Asian mountain ranges (e.g. Indus, Ganges and Brahmaputra catchments) annual runoff increases have been projected until at least 2050, which is mainly caused by an increase in precipitation and partly also by an increase in meltwater production (Immerzeel et al., 2012, 2013; Lutz et al., 2014). In other studies performed in the Andes and Canadian mountain ranges also changes in runoff have been projected for the future. For instance in the Andes (Cordillera Blanca, Peru) runoff increases (due to increase in direct runoff) and decreases (due to decrease in ice melt) have been projected for the wet (October-April) and dry (May- September) seasons of the second half of the 21st century respectively (Juen et al., 2007). In the Canadian mountain ranges (British Columbia, Canada) runoff decreases have been projected for the summer periods of 2050-2100, which are mainly caused by glacial retreat (Stahl et al., 2008).

The results of the different studies give valuable insight in possible future runoff changes, but should be treated with care since there can be a lot of uncertainties. These uncertainties, which are often associated with the different model approaches used in these studies, are (Seibert, 1997; Hagg et al., 2007; Steele-Dunne et al., 2008; Immerzeel et al., 2012; Ragletti et al., 2013; Huss et al., 2014):

- Parameter uncertainties (inter alia overparameterization and inter correlation between parameters. Uncertainty increases with the number of parameters),
- Model structure uncertainties,
- Internal inconsistencies (e.g. underestimation of precipitation and overestimation of melt)
- Scarcity of data (especially in mountainous regions),
- Climatic heterogeneity (inter alia related to heterogeneity in precipitation, especially for larger catchments),
- Climate projections (inter alia related with downscaling procedure and, accuracy and resolution of GCM and RCM outputs) and
- Uncertainties in relation with glacier and snow dynamics (e.g. feedback interactions between glacier change and runoff or the future evolution of glaciers and snow, which is often caused related to simplifications in modelling glacier change and snow melt).

1.3 Research Questions and Objective

The main research question is *how glacierized catchments in the Ötztal Alps (Austria) will respond hydrologically to future climate change*. In order to answer the main research question two subquestions will be investigated:

1. *How will the glaciers of the Ötztal/ Stubai Alps change as a result of climate change?*
2. *How will the catchments respond hydrologically to changes in glaciers and climate?*

The first subquestion is necessary to understand how the glaciers will evolve as a result of climate change. The answers resulting from this subquestion are subsequently needed for the second subquestion. The second subquestion is there to determine in what way runoff will alter in the 21st century as a result of changes in glaciers and climate. In this way it is possible to find out whether runoff will increase or decrease during the summer period, what the related timing of these changes may be and in what way the seasonality of runoff distribution will be altered.

The main research objective therefore is to study the hydrologic response of alpine catchments to changes in glaciers and climate. The outcomes of this research can be used for further detailed research to the consequences of climate change for water resources management (e.g. water availability) and water management (e.g. flood risk) of these catchments, and may form a basis for the development of adaptation strategies and/or measures.

1.4 Thesis Outline

The remaining part of this thesis possesses the following structure. In Section 2, a description will be given about the glacierized catchments of the Ötztal Alps covering the topics of topography, meteorology, glaciology and hydrology.

In Section 3, a description is given about the data and methods used for this research. There will be an extensive description about the model used for this research, which will be the HBV Light model (Seibert, 1997, 1999; Seibert and Vis, 2012). Furthermore the input data, the sensitivity analysis, the calibration/validation procedure, climate/glacier scenarios, and peak/low flow statistics will be described in more detail.

In Section 4, the results of this research will be presented. First the results of the sensitivity analysis and calibration/validation procedure will be presented. Then the results will be described, focusing on the scientific subquestions of 1.3. Finally results are described in relation with peak and low flow statistics.

In Section 5 the reliability of the HBV Light results will be discussed inter alia by comparing them with model results of HQSIM, which is a model that has been used in the alpS project StartClim2013. This project has been launched to model changes in runoff regimes as a result of glacier changes in the glacierized catchments of the Ötztal Alps. Then uncertainties concerning input data, scenarios and model performance will be discussed.

In Section 6 final conclusions will be given and subsequently in Section 7 management, policy and recommendations for further research will be provided.

2. Study Area: Catchments of the Ötztaler Alps

In this research the focus will be on the main catchment of the Ötztaler Alps: the Ötztaler Ache and its two sub catchments, which are the catchments of the Gurgler Ache and the Venter Ache, both located in the southern part of the Ötztaler Ache catchment. In order to describe these areas, the following topics will be covered: Topography, Meteorology, Glaciology and Hydrology.

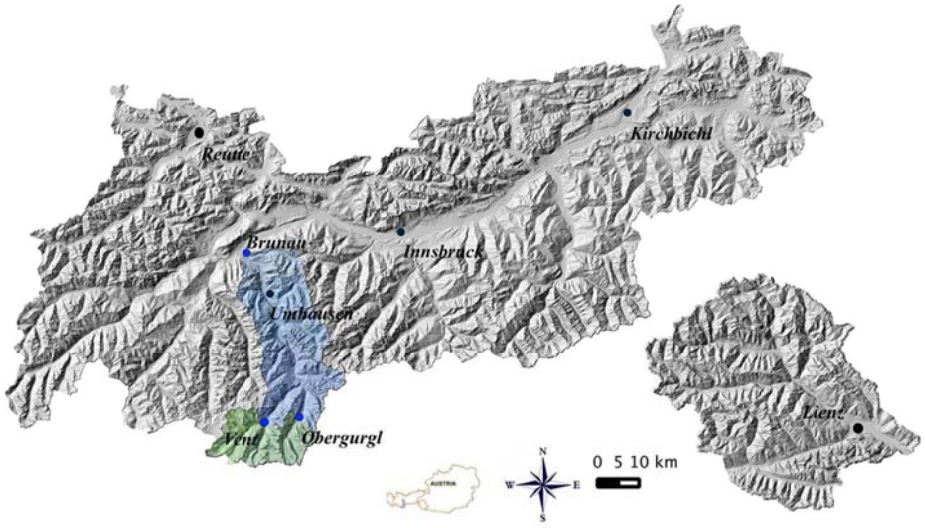

Figure 2.1: *Digital Terrain Model of Tyrol 2006 with the catchment of the Ötztaler Ache (blue) and the subcatchments of the Gurgler and Venter Ache (green). Dark blue dots represent the gauging stations Brunau, Vent and Obergurgl.*

2.1 Topography

The Ötztaler Ache located in Tyrol, Austria (see Figure 2.1) is a tributary of the Inn River and its catchment covers a total area of 891 km^2. The elevation range for the Ötztaler Ache is 710 – 3766 m a.s.l., with the lowest point at the entrance of the catchment (Brunau) and the highest in the subcatchment of the Venter Ache (Wildspitze). The two subcatchments of the Venter and Gurgler Ache have catchment areas of approximately 165 km^2 and 72 km^2 respectively. The elevation ranges for these catchments are 1740 – 3766 m a.s.l. and 1879 – 3537 m a.s.l. respectively. In the higher parts of the Ötztaler Ache catchment and its subcatchments glacial cover and bare vegetated rock surfaces are the main land cover types, where the lower parts are dominated by coniferous woodlands and alpine meadows (see Figure 2.2).

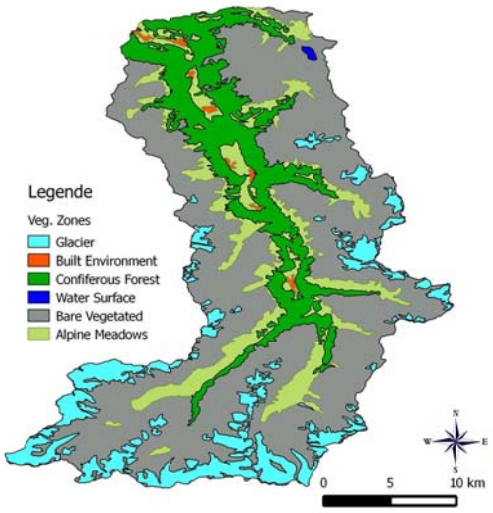

Figure 2.2: *Vegetation Map of the Ötztaler Ache catchment.*

2.2 Meteorology

The catchment of the Ötztaler Ache and its subcatchments generally experience a comparatively dry climate, which can be explained by its relative isolated position in the central Alps. Both from the north (Northern Calcareous Alps) and the south (the Alpine Main Range) the catchment of the Ötztaler Ache is shielded from precipitation deriving from the respective directions (Kuhn et al., 1982). This can be traced back in mean annual precipitation sums measured at weather stations of the ZAMG (*Zentralanstalt für Meteorologie and Geodynamik – Central Institution for Meteorology and Geodynamics*) over the period 1971-2000. In the Northern Calcareous Alps, for example, mean annual precipitation sums vary between 1100 mm and 1400 mm (Reutte (870 m a.s.l.): 1376,1 mm and Kirchbichl (498 m a.s.l.): 1135,2 mm), where in the catchment of the Ötztaler Ache mean annual precipitation sums are much lower with values in the range of 650–850 mm (Umhausen (1041 m a.s.l.): 692 mm and Obergurgl (1938 m a.s.l.): 819 mm) (ZAMG, 2013).

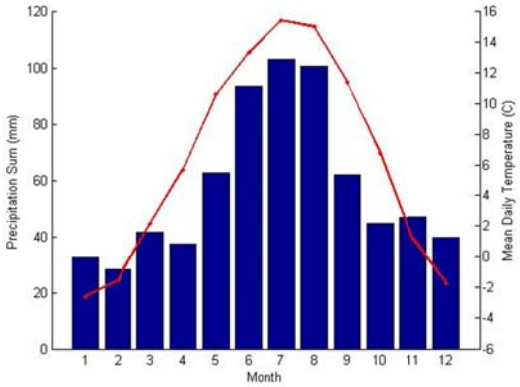

Figure 2.3: *Monthly Mean Temperature and Precipitation of the period 1971-2000 for the ZAMG station Umhausen (1041 m a.s.l.).*

In Figures 2.3 and 2.4 the monthly precipitation and temperature characteristics are illustrated for the stations Umhausen and Obergurgl. Observing the mean monthly precipitation sums it is obvious that there are precipitation maxima in the summer period and precipitation minima in the winter period. The maxima in the summer period are mainly caused by convective precipitation events (Hagg et al., 2003). The same Figures also illustrate an altitude dependent temperature distribution with lower daily mean temperatures for Obergurgl (mean annual temperature = 2.2 °C) than for Umhausen (mean annual temperature = 6.3 °C) with the lowest temperatures appearing in January – February and the highest in July – August (ZAMG, 2013).

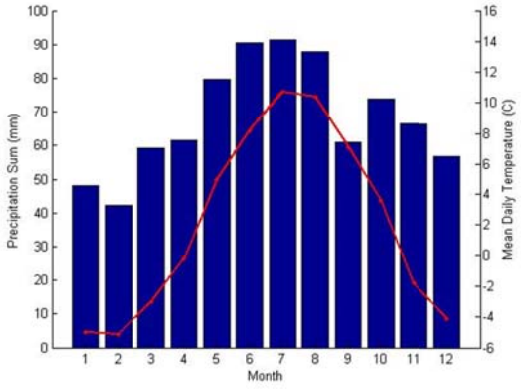

Figure 2.4: *Monthly Mean Temperature and Precipitation of the period 1971-2000 for the ZAMG station Obergurgl (1938 m a.s.l.).*

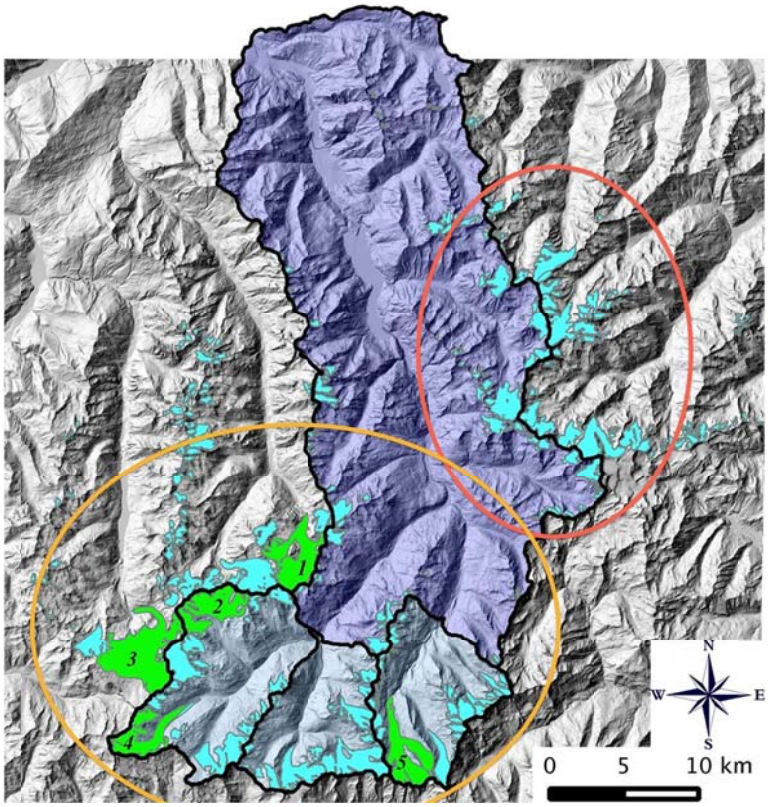

Figure 2.5: *Catchment of Ötztaler Ache and subcatchments of Gurgler (O) and Venter Ache (V) with glacier areas (blue) extracted from the glacier inventories of 2006. The glaciers inside the red circles represent the glaciers of the Stubaier Alps; the glaciers in orange circle represent the glaciers of the Ötztaler Alps. 1= Mittelberg Ferner, 2= Vernagtferner, 3= Gepatschferner, 4= Hintereisferner and 5= Gurgler Ferner.*

2.3 Glaciology

In Figure 2.5 the glacial areas of the Ötztaler Ache catchment are shown, based on the glacial inventories of 2006. The ratios of glacial area with total area were 11.7% for the entire catchment of the Ötztaler Ache, 29.4 % for the subcatchment of the Gurgler Ache and 32.2% for the subcatchment of the Venter Ache in 2006. The main part of the glaciers including the largest three glaciers, the Gepatschferner (46.81N 10.95E), the Mittelberg Ferner (46.55N 10.53E) and the Gurgler Ferner (46.47N 10.58E) with glacial areas of 16.75, 9.62 and 8.8 km^2 respectively, are located in the Ötztaler Alps (Abermann et al., 2012). The remaining part of the glaciers is located in the Stubaier Alps. In the Ötztaler and Stubaier Alps glaciers are mainly dominant in the elevation range of 2450 – 3600 m a.s.l. with largest glacial cover at elevations of about 3100 m a.s.l. (see Figure 2.6).

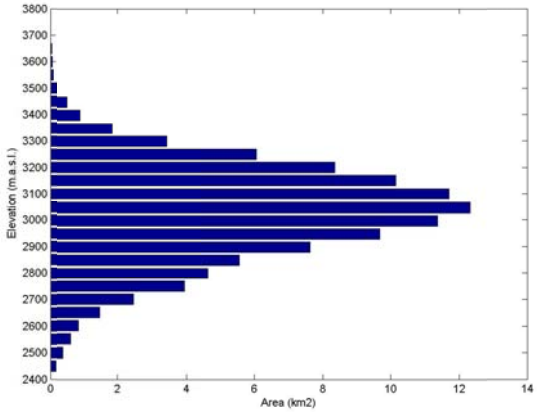

Figure 2.6: *Area-Elevation Distribution of Glaciers Ötztal 2006.*

2.4 Hydrology

The Ötztaler Ache is with a total length of 67 km the largest tributary of the Inn River (Achleitner et al., 2012). The Ötztaler Ache can be subdivided into two sections. The first section is the ~41 km section between the confluence with the Inn River, near Ötztal Bahnhof (685 m a.s.l.), and Zwieselstein (1470 m a.s.l.) where the Venter Ache confluences with the Gurgler Ache. The second section consists of the headwaters Gurgler Ache and the Venter Ache, which has another confluence of the headwaters Niedertalbach and Rofenache close to the village of Vent (1800 m a.s.l.). The Ötztaler Ache has next to the headwater tributaries also 9 other important tributaries. In Table 2.1 these tributaries (locations, see Appendix I) are given together with their length. Likewise the lengths of the headwater tributaries are also given.

***Table 2.1**: Tributaries and headwaters of the Ötztaler Ache with their lengths (km). Reference: HD Tirol, 2014.*

Tributary	*Length (km)*
Rettenbach	5.3
Pollesbach	9.8
Poltbach	5.2
Unterriederbach	4.8
Leierstalbach	6.8
Stuibenbach	14.2
Hairlachbach	16.7
Fischbach	12.2
Windache	10.5
Headwaters	
Rofen Ache	9.8
Niedertalbach	9.4
Venter Ache	13.3
Gurgler Ache	14.3

The catchment of the Ötztaler Ache and its subcatchments are dominated by glacial and glacio-nival runoff regimes with high runoff conditions in the period June-August and low runoff conditions in the winter period. In Figure 2.7 the Pardé coefficients (mean monthly discharge/mean annual discharge) of gauging stations Vent (Venter Ache), Obergurgl (Gurgler Ache) and Brunau (Ötztaler Ache) are given, based on monthly and annual mean discharges for periods 1971-2010, 1966-2010 and 1991-2010 respectively. When observing the Pardé coefficients it seems that the gauging stations Vent and Obergurgl experience glacial regimes since the coefficients observed in July or August are higher than in June. At gauging station Brunau observations are different with higher coefficients for July than for June/August. This implies that gauging station Brunau experiences a glacio-nival regime.

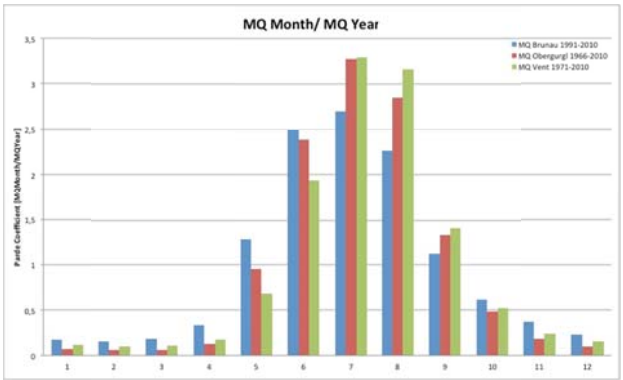

***Figure 2.7:** Pardé Coefficients of gauging stations Brunau (1991-2010; blue), Vent (1971-2010; green) and Obergurgl (1966-2010; red). Reference: (Lebensministerium (Austrian Ministry of Life) 2010).*

3. Methodological Approach

While describing the research methodology, the following set-up is used:

1. Description of the HBV Light Model.
2. Description of the Input Data used for calibrating HBV Light.
3. Description of the Sensitivity Analysis, Calibration and Validation Procedure.
4. Description of the Climate and Glacier Scenarios used for this research.
5. Description of Peak and Low Flow Statistics

3.1 Model Description of HBV Light

In this research the conceptual hydrological model 'HBV Light' was used to simulate daily discharge for the catchment of the Ötztaler Ache and the subcatchments of the Gurgler and Venter Ache. To enable the simulation of daily discharge; daily temperature, daily precipitation and potential evapotranspiration were used as input data. Additionally daily-observed discharge was also used as input data, which was needed for calibration and validation of the model.

HBV Light is a user-friendly version based on the HBV-96 model of Bergström (1992), a semi-distributed model (using the concept of Elevation Vegetation Units (EVUs), which enables the possibility to divide the catchment in several vegetation and elevation zones) that has been developed at the Swedish Meteorological and Hydrological Institute (SMHI). HBV Light, developed at the University of Zürich (Seibert, 1997, 1999; Seibert and Vis, 2012), has a structure (see Figure 3.1) containing a snow routine, soil moisture routine, response (groundwater) routine, routing (runoff) routine and in the more recent version also an aspect and glacier routine (which have been updated again more recently), enabling the possibility to include aspect factors and to simulate glacier melt (Seibert and Vis, 2012). Additional features of HBV Light, which are not in the HBV-96 model, are the application of a model warming-up period and the allowance of real values for the routing parameter MAXBAS (Seibert, 1997). In the following parts the routines and features of HBV Light, used for this research, are described in more detail.

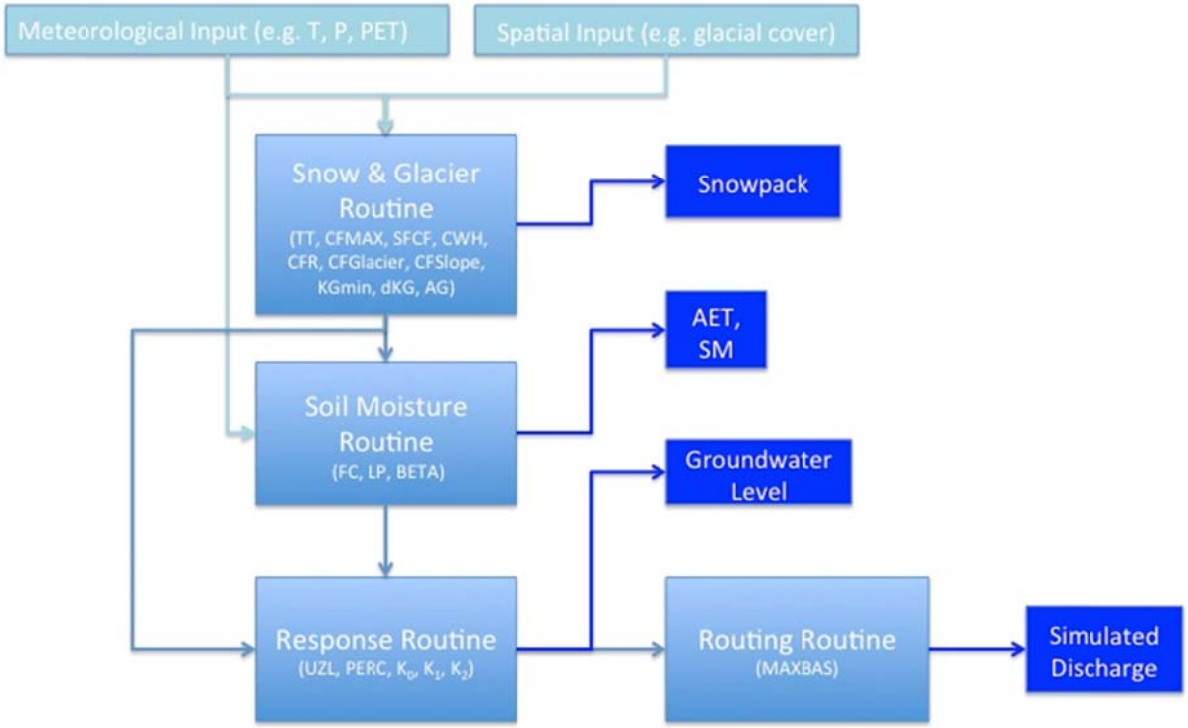

***Figure 3.1**: Schematic Structure of HBV Light.*

3.1.1 Snow and Glacier Routine

In order to simulate snow accumulation and -melt and glacier melt a degree-day approach was used, which implies that the amount of snowmelt is determined by the air temperature and the degree-day factor. The degree-day approach is expressed as follows (Seibert, 2005):

$$M = CFMAX * (T(t) - TT) \quad (3.1)$$

where CFMAX (mm °C^{-1} d^{-1}) is the degree day factor, T(t) (°C) is the temperature on day t, and TT (°C) is the critical temperature determining whether precipitation will fall in form of snow (TT>T) or rain (TT<T). According to Seibert (2005) CFMAX usually has values, in the range of 1.5 – 4 mm °C^{-1} d^{-1} where the lower values are mostly characteristic for forested vegetation zones. In case the influence of aspect is incorporated CFMAX is multiplied with the factor CFSlope (-) for south-facing aspects and divided for north-facing aspects. When glacier melt also is incorporated CFMAX is multiplied with the factor CFGlacier (-).

If precipitation falls in the form of snow, the precipitation has to be corrected with a snowfall correction factor, called SFCF, to avoid underestimation of snowfall caused by undercatch of snowfall at precipitation gages, which is subsequently caused by wind. This means that for forested areas SFCF is often assumed to be lower than for open areas.

The presence of a snowpack means that melt water or rain can be retained by the snowpack until it exceeds a certain fraction of the water equivalent of snow, which is indicated by CWH (-). Mostly CWH is assumed to be 0.1. A much smaller fraction of melt water or rain refreezes again if it is retained by the snowpack, and in case temperature is below the critical temperature. This fraction is indicated by CFR (-), which is mostly assumed to be 0.05.

In the most recent version of HBV Light (Seibert & Vis, 2014) the glacier routine has been updated by incorporating a glacial reservoir with glacial outflow. To simulate glacial outflow a relationship has been used from Stahl et al. (2008), which is expressed as follows:

$$Q_g(t) = \left(KG_{min} + dKG * e^{-AG*SWE(t)}\right) * S(t) \quad (3.2)$$

where Q_g (t) (mm d^{-1}) represents the glacial outflow at day t, KG_{min} (d^{-1}) is the minimum outflow coefficient representing deep snow conditions and poorly developed glacial drainage, KG_{min} + dKG (d^{-1}) is the maximum outflow coefficient representing conditions with well-developed glacial drainage, AG (mm^{-1}) is a calibration parameter, SWE (mm) is the water equivalent of snow covering the glacial reservoir and S(t) (mm) is the storage of the glacial reservoir itself. KG_{min}, dKG and AG are the parameters, which have to be calibrated in the glacier routine.

3.1.2 Soil Moisture Routine & Response (Groundwater) Routine

In case there is no capacity to retain more melt water or rain in the snowpack, melt water and rain are added to the soil reservoir (leading to an increase in the actual storage of the soil reservoir) or to the groundwater reservoirs. In which way melt water and rain are divided over the soil and groundwater reservoirs is described by the following equation (Seibert, 2005; Seibert and Vis, 2012):

$$\frac{F(t)}{I(t)} = \left(\frac{SM(t)}{FC}\right)^{BETA} \quad (3.3)$$

where F(t) (mm d^{-1}) represents the groundwater recharge on day t, I(t) represents the input (sum of melt water and rain) to the soil reservoir on day t, SM (mm) is the actual storage of the soil reservoir on day t, FC (mm) is the maximum storage of the soil reservoir and BETA (-) is a parameter that determines the relative contribution to runoff from melt water or rain (Konz and Seibert, 2010). If SM exceeds FC, water is not stored in the soil reservoir any more, but will proceed as groundwater

recharge. Another important parameter, which is included in the soil moisture routine, is LP. LP (-) is a parameter representing a soil moisture value above which the actual evapotranspiration is equal to the potential evapotranspiration. The way by which LP is related to actual and potential evapotranspiration, and other soil reservoir characteristics is described in the following equation (Seibert, 2005):

$$E_{act} = E_{pot} * \min\left(\frac{SM(t)}{FC*LP}, 1\right) \quad (3.4)$$

where E_{act} (mm d^{-1}) is the actual evapotranspiration, E_{pot} (mm d^{-1}) is the potential evapotranspiration and LP is given as a fraction of FC. In case the ratio between SM and FC * LP is equal to 1 then actual evapotranspiration is equal to potential evapotranspiration. Otherwise a linear reduction of actual evapotranspiration is assumed (Konz and Seibert, 2010).

Groundwater recharge is entering the response routine in the upper groundwater reservoir, called SUZ (mm). The amount of water entering the lower groundwater reservoir, SLZ (mm), depends on the parameter PERC (mm d^{-1}), which represents the maximum percolation to the lower groundwater reservoir SLZ. The outflow of the lower groundwater reservoir SLZ is determined by one linear reservoir equation, where the outflow of the upper groundwater reservoir SUZ is determined by one or two linear reservoir equations depending on the threshold value UZL (mm), which means if SUZ exceeds UZL a second linear reservoir equation is added. Assuming that SUZ exceeds UZL, the outflow from groundwater reservoirs is expressed as:

$$Q_{GW}(t) = K_0 * (SUZ - UZL) + K_1 * SUZ + K_2 * SLZ \quad (3.5)$$

where K_0, K_1 and K_2 (d^{-1}) are outflow coefficients representing quickflow (overland flow and subsurface flow) and baseflow respectively, and Q_{GW} (t) (mm d^{-1}) is the total outflow from the groundwater reservoirs on day t. In case SUZ does not exceed UZL, the outflow from the groundwater reservoirs is expressed as:

$$Q_{GW}(t) = K_1 * SUZ + K_2 * SLZ \quad (3.6)$$

3.1.3 Routing Routine

In order to simulate discharge at the outlet of the catchment, the runoff resulting from the response routine is passed to the routing routine representing channel retention and flow. The routing routine consists of a triangular weighting function with base length MAXBAS (d), which is there to transform the runoff values derived from the response routine. This transformation is expressed as (Seibert, 2005):

$$Q_{sim}(t) = \sum_{i=1}^{MAXBAS} c(i) * Q_{GW}(t - i + 1) \quad (3.7)$$

where Q_{sim} (mm d^{-1}) is the simulated discharge on day t and

$$c(i) = \int_{i-1}^{i} \frac{2}{MAXBAS} - \left|u - \frac{MAXBAS}{2}\right| * \frac{4}{(MAXBAS)^2} du. \quad (3.8)$$

In Figure 3.2 a transformation of runoff values, deriving from the response routine, is illustrated for MAXBAS = 5 d. MAXBAS = 5 d means that the base of the triangular weighting function is 5 days with greatest weight at 3 days. This means that the peak discharge deriving from the response routine is shifted with 3 days and is reduced with the weight at 3 days. This transformation can be observed in the right figure of Figure 3.2.

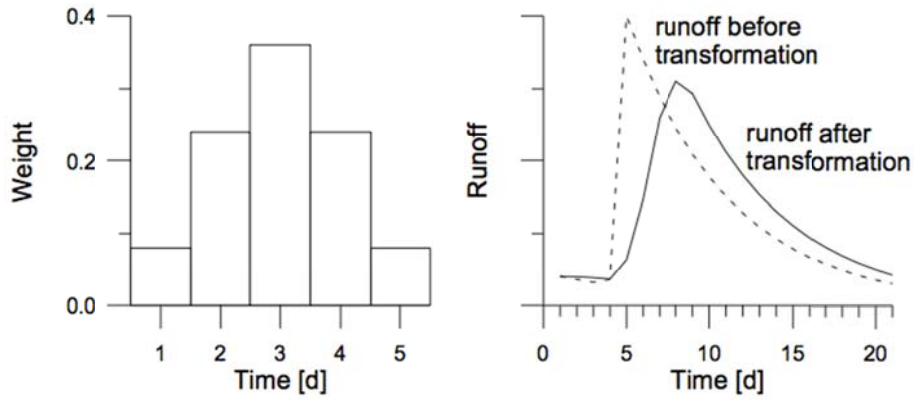

Figure 3.2: *MAXBAS Weight Distribution (left) and MAXBAS Discharge Transformation (right). Reference: Seibert, 2005.*

3.1.4 Elevation Zones: Temperature and Precipitation

In case there is more than one elevation zone, the changes in temperature and precipitation with elevation have to be calculated. To calculate the change in precipitation with elevation the following expression is used (Seibert, 2005):

$$P(z) = P_0 * \left(1 + \frac{PGrad(z-PElev)}{10000}\right) \quad (3.9)$$

where P(z) (mm) is the amount of precipitation at elevation z, P_0 (mm) is the amount of precipitation at elevation PElev, PGrad (% / 100m) is the precipitation gradient and PElev is the reference elevation of precipitation data. To calculate the change in temperature with elevation the following expression is used (Seibert, 2005):

$$T(z) = T_0 - \left(\frac{TGrad(z-TElev)}{100}\right) \quad (3.10)$$

where T(z) (°C) is the temperature at elevation z, T_0 (°C) is the temperature at elevation TElev, TGrad (°C / 100m) is the temperature gradient and TElev is the reference elevation of temperature data.

3.1.5 Model Calibration

When calibrating 'HBV Light' the parameter values are sought that result in the best fit between observed and simulated discharge. In order to get the best-fit 'HBV Light' uses the so-called coefficient of efficiency R_{eff} of Nash and Sutcliffe (1970) as main efficiency criterion, which is expressed as follows:

$$R_{eff} = 1 - \frac{\sum(Q_{obs}(t)-Q_{sim}(t))^2}{\sum(Q_{obs}(t)-\overline{Q_{obs}})^2} \quad (3.11)$$

where R_{eff} (-) is the coefficient of efficiency (R_{eff} = 1 → best possible fit; R_{eff} <0 → poor fit), Q_{obs} (t) (mm d^{-1}) is the observed discharge on day t and $\overline{Q_{obs}}$ (mm d^{-1}) is the mean of the observed discharge over the entire calibration period. Next to the Nash-Sutcliffe efficiency criterion there are also other efficiency criteria that can be used. Examples of these criteria are:

- Coefficient of Determination:

$$r^2 = \frac{\left(\sum(Q_{obs}-\overline{Q_{obs}})(Q_{sim}-\overline{Q_{sim}})\right)^2}{\sum(Q_{obs}-\overline{Q_{obs}})^2 \sum(Q_{sim}-\overline{Q_{sim}})^2} \quad (3.12)$$

where r^2 (-) is the coefficient of determination (r^2 = 1 → best fit),

- Efficiency for log(Q) (that puts more focus on low flows):

$$LogReff = 1 - \frac{\sum(lnQ_{obs}(t) - lnQ_{sim}(t))^2}{\sum(lnQ_{obs}(t) - \overline{lnQ_{obs}})^2} \quad (3.13)$$

where LogReff (-) represents the efficiency for log(Q) (LogReff = 1 → best fit),

- Lindström Measure:

$$LindströmMeasure = Reff - 0.1 \frac{|\sum(Q_{obs} - Q_{sim}|}{\sum(Q_{obs})} \quad (3.14)$$

where LindströmMeasure (-) represents the Lindström Efficiency Measure (LindströmMeasure = 1 → best fit), and

- Volume Error:

$$VE = 1 - \frac{|\sum(Q_{obs} - Q_{sim})|}{\sum(Q_{obs})} \quad (3.15)$$

where VE (-) is the volume error (VE = 1 → best fit). The volume error is more or less related with the mean difference between observed and simulated discharge, which is another criteria that can be used to fit simulated discharge with observed discharge. For a good fit it is important that the mean difference is small as possible. Further it is also possible to use visual correspondence between the plots of observed and simulated discharge as criteria.

In order to calibrate the model sufficiently a calibration period between 5 and 10 years is necessary (Seibert, 2005), which can be implemented by using following techniques: manual calibration using trial – and – error technique, automatic calibration using Monte Carlo analyses or GAP (genetic calibration algorithm) optimization.

3.2 Input Data

3.2.1 Topography

For HBV Light application the (sub)catchments were divided into elevation zones with an interval of 250 m. For the Ötztaler Ache 14 elevation zones were used, starting at an elevation of 500 m a.s.l, and for the subcatchments of the Gurgler and Venter Ache 8 and 9 elevation zones respectively were used, starting at an elevation of 1750 m a.s.l. In order to specify the elevation zones in HBV Light Digital Terrain Models (DTMs) were used of the Airborne Laserscan (ALS) recordings of 2006 (Land Tirol, 2006). Next to elevation zones also vegetation zones were used in HBV Light. For this research the maximum number of 3 vegetation zones was applied, representing glacial cover, bare vegetated rock surfaces and vegetated areas (woodlands and meadows). In order to get the distribution of areas related to elevation zones, aspect and vegetation zones the DTMs were used in combination with vegetation cover grid data to determine the aspect-elevation area distribution for the different vegetation zones. The vegetation cover grid data were extracted from the vegetation cover grids used for HOPI (originally extracted from the Bundesministerium für Land- und Forstwirtschaft (Austrian Ministry of Life), 2005).

3.2.2 Meteorological Data

HBV Light uses daily temperature, daily precipitation and potential evapotranspiration data for the simulation of daily discharge. Daily temperature and daily precipitation data were extracted from

StartClim 2013. In this project these data were used as input for HQSIM using 1983-2012 as reference period and were extracted from the meteorological stations of the ZAMG, TIWAG AG, the Hydrographical Service Tyrol and the Commission of Glaciology, Bavarian Academy of Sciences for the period 1986 -2012. In order to get the full series of daily temperature and daily precipitation data for the reference period 1983-2012 the daily data of the period 1986-1988 have been used to fill the period 1983-1985. The reason for this procedure is the lack of data before 1986, which enabled the possibility to use meteorological data before 1986.

For the application in HQSIM a single time series of daily temperature data was required for the entire catchment of the Ötztaler Ache. This series was composed by simple linear regression analysis using the daily temperature data of the meteorological stations as input, resulting in a series of temperatures considering a reference elevation of 0 m a.s.l. and a series of daily temperature gradients. An example of a linear regression is given for the 26th of September 1988 (see Figure 3.3) when 14 meteorological stations were available. Based on the linear regression in this example, the temperature is determined to be 14.7 °C on 0 m a.s.l. (intercept trendline with y-axis) with a temperature gradient of 0.26 °C/ 100 m (slope trendline).

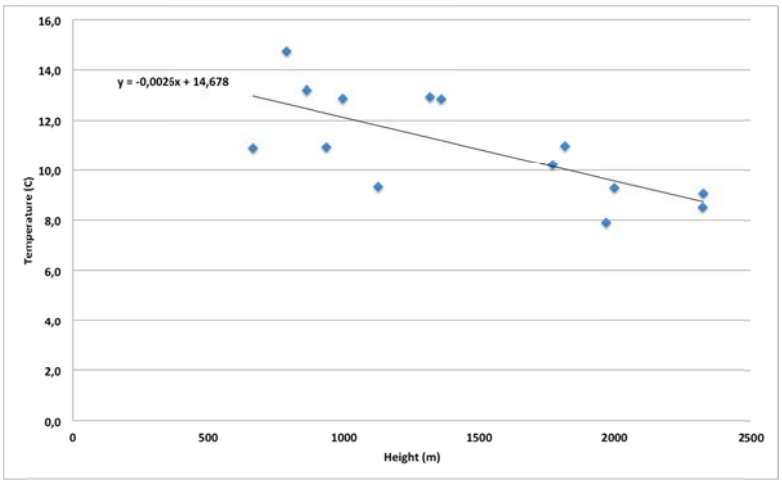

Figure 3.3: *Linear Regression of Temperature Data for 26-09-1988.*

The resulting series of daily temperatures and temperature gradients were subsequently adopted in HQSIM and were also used for HBV Light. However, the series of temperature gradients was not adopted in HBV Light, since HBV Light requires only one value for temperature gradient TGrad. Therefore TGrad was calibrated (in the range 0.45- 0.65 °C / 100m) and used by HBV Light for the calculation of temperature in the different elevation zones (see Section 3.1.4, Eq. 3.10).

In HQSIM the daily precipitation data were projected onto a 5 km x 5 km grid (which is also used in the HOPI system) using Inverse Distance Weighting (IDW) as methodological approach to interpolate precipitation data from meteorological stations to the grid points (see Figure 3.4). In order to implement IDW the following expression has been used (Kirnbauer et al., 2007):

$$p_j = \sum_i \omega_{ji} * p_i \tag{3.16}$$

where p_j (mm) is the determined precipitation for grid point j, p_i (mm) is the measured precipitation for station i and ω_{ji} (-) is a weight based on distance between station and grid point, which is determined by the following expression:

$$\omega_{ji} = \frac{1}{d_i^{\alpha}} \tag{3.17}$$

where d_j^{α} represents the distance between a station and a grid point, α represents the IDW power (α>1, where α = 2 is most common and has been used for IDW) and $\Sigma\omega_{ji} = 1$. Because HBV Light

cannot work with a grid system and requires a single time series of daily precipitation data, the daily precipitation data of the grid points were used to calculate a single time series of daily precipitation data for the entire catchment area of the Ötztaler Ache and for the subcatchment areas of the Gurgler and Venter Ache separately. Because of the large size of the area and therewith-related heterogeneity in precipitation patterns it is difficult to use a series of precipitation gradients. Therefore also (and also because of the fact that HBV Light only requires one value) one value is used in HBV Light for precipitation gradient PGrad. In consequence PGrad is calibrated (in the range 7.5 - 20% / 100 m) and subsequently used by HBV Light for the calculation of precipitation in the different elevation zones (see Section 3.1.4, Eq. 3.9).

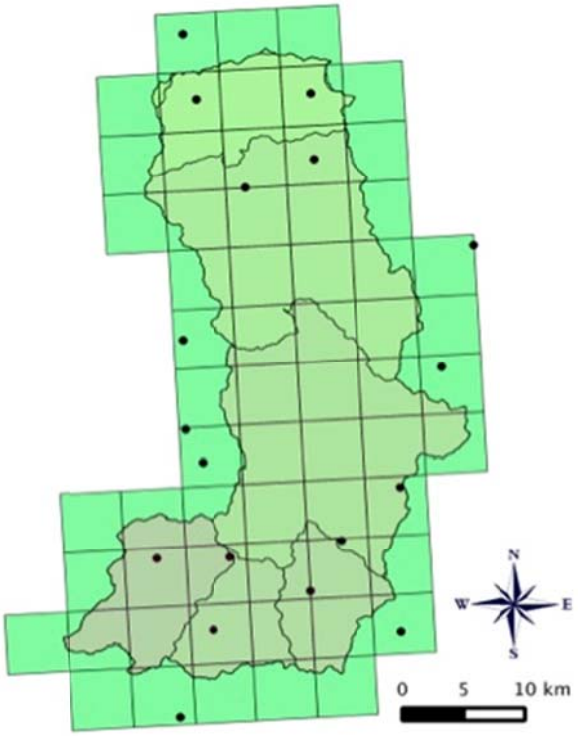

Figure 3.4: *HOPI grid system and locations of meteorological precipitation stations used for IDW.*

For potential evapotranspiration, long-term daily means were used on a monthly basis. Potential evapotranspiration was determined using the method of Hamon (1961) based on the daily temperature series of HOPI for the period 1983-2012. The expression of Hamon is as follows:

$$E_{pot} = 0.1651 * N * KPEC * 216.7 * \frac{e_s}{T+273,3} \quad (3.18)$$

where E_{pot} (mm d^{-1}) is the potential evapotranspiration, T (°C) is the daily mean temperature, KPEC (-) is a calibration coefficient, N is the daytime length in multiples of 12 hours and e_s (mb) is the saturation vapour pressure. Daytime length N and saturation vapour pressure e_s can be further expressed as:

$$N = \frac{24}{\pi} * \cos^{-1}[-\tan\left(1 + 0.033\cos\left(\frac{2\pi}{365}J\right)\right)\tan(\varphi)] \quad (3.19a)$$

and

$$e_s = 6.108 * e^{\left(\frac{17.27T}{T+237.3}\right)} \quad (3.19b)$$

where J is the Julian Day of the year and φ (radians) is the latitude (47°N/ ±0.82 for Ötztal). Using the Hamon method results in daily mean potential evapotranspiration values. These values were

subsequently used to calculate the long-term daily means on monthly basis. In contradiction with temperature and precipitation HBV Light does not calculate potential evapotranspiration for each elevation zone separately. The potential evapotranspiration applies for the entire catchment of the Ötztaler Ache.

3.2.3 Hydrological Data

In order to calibrate and validate the model daily-observed discharge data were used. Likewise for daily temperature and daily precipitation daily-observed discharge was extracted from StartClim 2013. In this project daily-observed discharge was used to calibrate and validate the model HQSIM. Originally the daily-observed discharge data were extracted from the gauging stations Brunau, Vent and Obergurgl (which are in possession of TIWAG AG) for the period 1983-2012.

3.3 Sensitivity Analysis, Calibration and Validation

Before HBV Light was calibrated and validated a sensitivity analysis was conducted in order to understand what kind of effect different parameters have on simulated discharge values. In this manner it is possible to gain insight in how HBV Light reacts to parameter changes and to get a better understanding on how the model works. The sensitivity analysis was performed for gauging station Brunau and Vent (only for glacier routine parameters) on 15 routine parameters, which are the parameters TT, CFMAX, SFCF, FC, LP, BETA, KGmin, dKG, AG, PERC, UZL, K_0, K_1, K_2 and MAXBAS, and 2 gradient parameters (TGrad and PGrad) using minimum, maximum and default values of Table 3.1. The other parameters were excluded from the sensitivity analysis, because these parameters are constant (CWH and CFR) or strengthen (CFGLAC and CFSlope for south-facing aspects) or weaken (CFSlope for north-facing aspects) the effect of other parameters (CFMAX).

Calibration and validation of HBV Light can be implemented in two ways: manual using trial and error techniques, and automatic using Monte Carlo analysis or GAP optimization. In order to calibrate and validate HBV Light for the catchments of the Ötztaler Ache and the subcatchments of Gurgler and Venter Ache the manual technique was used. The manual technique is assumed to be the best way to find parameter sets with highest efficiency, smallest mean difference and best visual similarity between the plots for observed and simulated discharge, taking the variability of parameters between the different vegetation zones into account. However, disadvantage is that manual calibration can lead to over-parameterization of the parameters and inter-correlation can appear between parameters due to interactions between these parameters (Steele-Dunne et al., 2008). The parameters and the ranges (minimum/maximum) for which these were calibrated are summarized in Table 3.1. To calibrate and validate HBV Light a warming-up period of one year was used since this is assumed to be enough for filling all the reservoirs in the model.

In Table 3.2 the calibration and validation periods are given for the Ötztaler, Gurgler and Venter Ache. The reason for starting the calibration in the late 90's is the low data quality and availability of the 80s and the beginning of the 90s, which makes this period less feasible for calibration. An additional advantage of having the calibration period in late 90s and the beginning of the 21st century is that it makes it possible to use 2003 as a calibration year. Since 2003 is known as an extreme year with absence of snow cover (Parajka and Blöschl, 2006) in the mountain regions, this year can be used as a calibration year for simulation of snow and in this manner also for simulation of discharge. For the Venter Ache 2003 cannot be used as a calibration year together with 2004, 2005 and 2006 since observed discharge data is missing for this period. Therefore the period 2003-2006 was deemed unsuitable for the calibration of HBV Light. In order to validate HBV Light for the different catchments two validation periods were used. The reason for choosing two validation

periods was to get an idea about what kind of effect data quality and availability[2] would have on the model performance, something that will be discussed later in Section 5.2.1.

Table 3.1: *Parameters, their units, their ranges used for calibration and their HBV Light default values (Based on Steele-Dunne et al., 2008; Konz & Seibert, 2010; Seibert & Vis, 2014)*

Parameter	Unit	Minimum Value	Maximum Value	**HBV-L Default**
Gradient				
PGrad	% / 100 m	7.5	20	10
TGrad	°C / 100 m	0.45	0.65	0.6
Snow Routine				
TT	°C	-2	2	0
CFMAX	mm d^{-1} °C^{-1}	2	6	3
SFCF	-	0.8	1.2	1
CFGlacier	-	1.5	3	1
CFSlope	-	1.5	2	1
SoilMois Routine				
FC	mm	100	500	200
LP	-	0.4	1	1
BETA	-	1	6	1
Glacier Routine				
KG_{min}	d^{-1}	0.01	0.2	0.05
dKG	d^{-1}	0.01	0.5	0.1
AG	mm^{-1}	0	10	1
Response Routine				
PERC	mm d^{-1}	0	6	1
UZL	mm	0	100	20
K_0	d^{-1}	0.05	0.5	0.2
K_1	d^{-1}	0.01	0.4	0.1
K_2	d^{-1}	0.005	0.2	0.05
Routing Routine				
MAXBAS	d	1	7	1

Table 3.2: *Calibration and Validation Periods.*

(Sub)Catchment	***Calibration Period***	***Validation Period 1***	***Validation Period 2***
Ötztaler Ache	*1998-2007*	*1987-1997*	*2008-2012*
Gurgler Ache	*1998-2007*	*1987-1997*	*2008-2012*
Venter Ache	*1993-2002*	*1987-1992*	*2008-2012*

[2] Mainly referring to quality and availability of precipitation data since precipitation has the most heterogeneous character, which makes it therefore important to have a regular area cover from precipitation gaging stations with complete series of measurements.

3.4 Climate and Glacier Scenarios

In order to find out how the catchments in the Ötztaler Alps respond hydrologically to changes in climate and glaciers, climate and glacier scenarios were used. The climate scenarios used for this research are climate scenarios constructed by the University of Natural Resources and Life Sciences, Vienna (BOKU) in cooperation with alpS GmbH. The scenarios contain climate projections of daily temperature and daily precipitation on a 1 km x 1 km grid for the period 1985-2100 and are realizations of an ensemble of three RCMs based on SRES A1B. The three RCMs used are:

- ARPEGE – ALADIN (from the CNRM (Centre National de Recherches Météorologiques)).
- ECHAM5 - RegCM3 (from the ICTP (International Centre for Theoretical Physics)).
- ECHAM5 – REMO (from the MPI (Max Planck Institut)).

These projections were subsequently used in a so-called "Delta Change Approach" on daily basis (Bosshard et al., 2011). In order to implement the "Delta Change Approach" the following steps were conducted (Helfricht et al., In Press):

1. Estimation of the mean annual cycle of precipitation and temperature on daily base for the reference period 1985-2014 and the scenario periods 2010-2039 (near future), 2040-2069 (mid future) and 2070-2099 (far future).
2. Estimation of relative precipitation and absolute temperature changes on daily base, between the reference period and scenario periods.
3. Application of a low-pass filter (equivalent to Bosshard et al., 2011).
4. Estimation of natural variability (±σ of the low-pass filtered signals using a window of 31 days) of low-pass filtered signals.

In Figure 3.5a and 3.5b the low-pass filtered signals and natural variabilities are given of the absolute temperature changes and relative precipitation changes in relation with the different RCMs. The mean of the signals was used as temperature and precipitation changes in order to determine the daily temperatures and precipitation rates for the scenario periods using the original meteorological data series of the 1983-2012 as reference period. The estimated future daily temperatures and precipitation rates were then used in HQSIM and HBV Light (via pre-processing), and to estimate future potential evapotranspiration (see Section 3.2.2).

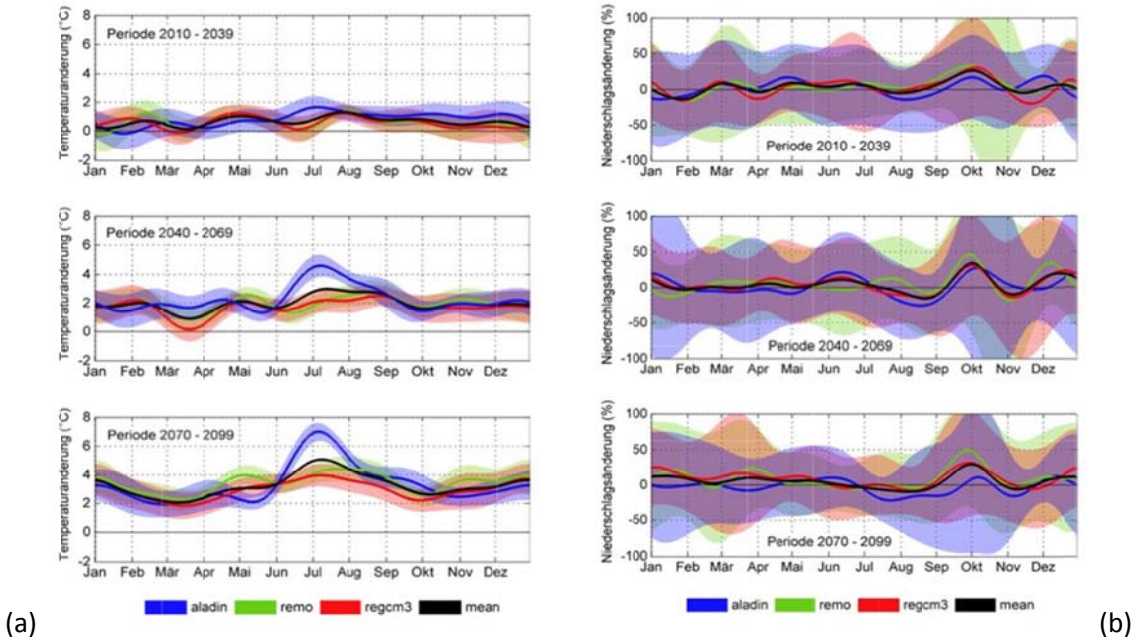

***Figure 3.5**: Low-pass filtered signals and natural variabilities (±σ) of absolute temperatures (a) and relative precipitation (b) changes for 2010-2039, 2040-2069 and 2070-2099. Reference: Helfricht et al., In Press.*

For glacier scenarios, glacier area distributions were used, which were extracted from a model developed by Helfricht (2013). This model is able to generate future ice thickness, glacial area and volume distributions on a 50m x 50m grid as a result of changing climate conditions, and uses photogrammetric elevation models (PEMs) of glaciers of 1997, DTMs of the Airborne Laser Scan (ALS) recordings of 2006 taken in the Ötztaler Alps and the ice thickness distributions of 2006 as input.

The ice thickness distributions of 2006 were developed according to the ice thickness estimation method (ITEM) of Farinotti et al. (2009), which is a method, based on glacier mass turnover and ice flow mechanisms. ITEM can be shortly described as follows (Farinotti et al., 2009; Gabbi et al., 2012): (1) apparent mass balances have to be estimated for each ice-flow catchment using vertical mass balances and an ELA; (2) the apparent mass balances are used to determine ice volume fluxes for defined ice flow lines; (3) the ice volume fluxes are used in an integrated form of Glen's flow law' (Glen, 1955) to derive the ice thicknesses for each ice flow line; (4) the derived ice thicknesses are interpolated over the entire glacier and are adjusted for the effects of the local surface slope, which eventually result in an ice thickness distribution for the entire glacier. An example of an ice thickness distribution is given in Figure 3.6.

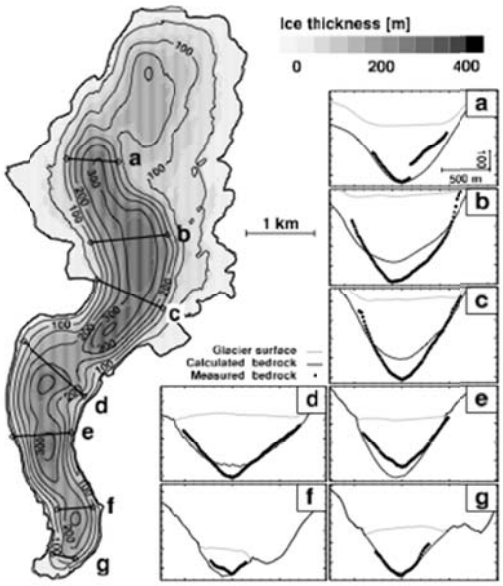

Figure 3.6: *Estimated Ice Thickness Distribution of the Rhone Glacier (Switzerland). At the right side of the figure the cross section a-g. Reference: Farinotti et al. (2009).*

In order to derive future ice thickness, glacial and volume distributions according to the model of Helfricht (2013) the following steps were conducted (which are illustrated in Figure 3.7):

1. Using the DTMs of 2006 and the PEMs of 1997, ice thickness losses were calculated relative to the measured elevations of the PEMs of 1997, using the following expression:

$$\Delta z_{2006-1997} = z_{2006} - z_{1997} \tag{3.20}$$

where z_{2006} (m) represents the glacial surface elevation of 2006, z_{1997} represents the glacial surface elevation of 1997 and Δz (m) represents the glacial surface elevation difference.

2. Using the DTMs of 2006 and the ice thickness distributions of 2006 the bedrock surface elevations were calculated using the following expression:

$$UG_{2006} = z_{2006} - h_{2006} \tag{3.21}$$

where UG (m) is the bedrock surface elevation and h_{2006} (m) represents the ice thickness of 2006.

3. Based on the difference in elevation between 1997 and 2006 an annual mean elevation difference was calculated. This annual mean elevation difference functioned as a fixed mass loss and was used to estimate the glacial surface elevation of 2005, which was taken as starting point for the estimation of new glacial surface elevations from 2005 onward until 2105 with intervals of 10 years. The estimation of the new glacial surface elevations was conducted in combination with an assumption of a loss (which is of application for the entire glacier area) of 0.8 m w.e. per 1 °C temperature increase (in the model of Helfricht (2013) minimum, mean and maximum temperature increases of 0.9 °C, 2 °C and 3 °C respectively are assumed until ~2060, which has been extracted from the climate projections for 2040-2069; see p.22).
4. The new glacial surface elevations were subsequently used, in combination with bedrock surface elevations, to estimate new ice thickness distributions (h_{new}). Thereby the assumption was made that when the ice thickness would have become negative that the bedrock surface had to be assumed ice-free. In terms of HBV this means that a glacial vegetation zone shifts to a bare vegetated zone. Based on this information new glacial areas (HRU New) were calculated for inter alia 2025(near future), 2055 (mid future) and 2085 (far future). Next to glacial area also glacial volume was calculated by multiplying the ice-thickness with the glacial area of each grid cell.

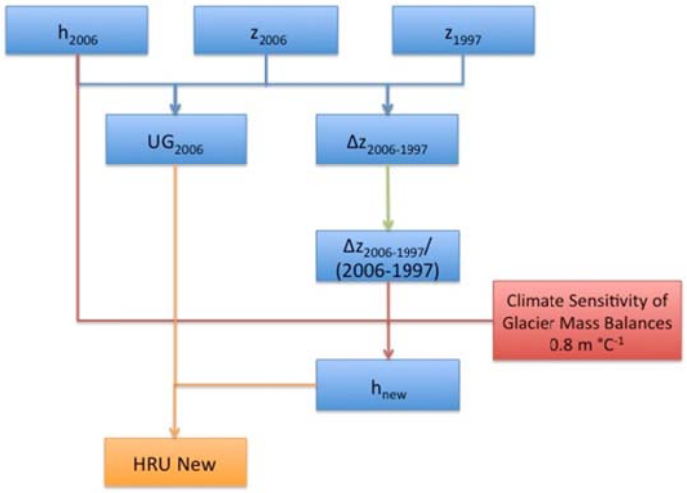

***Figure 3.7**: Schematic Structure of model used for estimation of ice-thickness distributions and subsequently the new areas covered by glaciers. Reference: Helfricht et al., In Press.*

To gain insight into what kind of effect climatic and glacier changes have on the hydrologic response of the catchments, climate and glacier scenarios were applied separately and combined. This means that HBV Light was run using 3 different scenario classes, which are (see Table 3.3):

- Class A: Combination of reference climate scenario, using the original meteorological data of 1986-2012, and glacier scenarios (using glacial area distributions of 2025, 2055 and 2085, assuming a mean temperature increase of 2 °C until ~2060),
- Class B: Combination of climate scenarios and reference glacier scenario based on the glacier areas of 2006, and
- Class C: Combination of climate and glacier scenarios.

Additional there is also a reference class, including the reference glacier and climatic scenarios.

***Table 3.3**: Classes of Scenario Combinations used for HBV Light*

	Glacier 2006	**Glacier 2025**	**Glacier 2055**	**Glacier 2085**
Basis 1986-2012	REF	A1	A2	A3
CC1 2010-2039	B1	C1		
CC2 2040-2069	B2		C2	
CC3 2070-2099	B3			C3

3.5 Peak & Low Flow Statistics

In order to understand implications of possible changing runoff characteristics the output of HBV Light was used for the implementation of peak and low flow statistics. Peak flow statistics involved determining the annual maximum series (AMS) of the reference period and the scenario periods belonging to A3, B3, C1, C2 and C3. The reason for choosing these 5 scenario periods is to compare changes in high runoff characteristics on long term for three different scenarios and to compare changes in high runoff characteristics on medium and long-term for combined climate and glacier scenarios. After determination of the annual maximum series, the time of occurrence was determined, which was subsequently used to create rose plots (example rose plot, see Figure 3.8). The reason for developing rose plots is that rose plots are efficient tools to say something about the period of occurrence of high runoff conditions and about the frequency of high runoff conditions in a certain period.

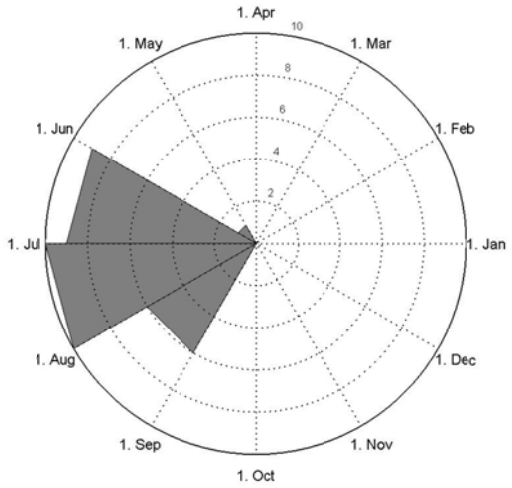

Figure 3.8: *Example of a rose plot. This rose plot contains the AMS of observed discharge values (1987-2012) for gauging station Brunau (Ötztaler Ache). The radius of the circle represents the frequency of occurrence. From this rose plot there it is evident that high flow conditions are most frequent in July followed by June. This pattern is typical for glacio-nival regimes.*

Low flow statistics were derived from Flow Duration Curves (FDCs) for the observed discharges and simulated discharges of the reference and scenario periods A3, B3, C1, C2 and C3 with a focus on the summer months June, July and August. The reason for choosing the summer months is the assumption that low flow are expected to become more frequent in summer time where it is expected to become a problem for the water management of glacierized catchments. Low flow conditions were determined by taking the 70-percentile (Q_{70}) and 95-percentile (Q_{95}) exceedance discharges of observed discharge values, which are mostly, used as low flow indices (Smakhtin, 2001; WMO, 2008). Using these values as reference levels, a prediction was made for the exceedance frequency of these discharges for the scenario periods.

4. Results

In order to present and to describe the results of this research the following set-up is used:

- Description of results sensitivity analysis.
- Description of results calibration and validation procedure.
- Description of results in relation with glacier changes.
- Description of results in relation with hydrologic response of catchments to climate and glacier changes.
- Description of results in relation with peak and low flow statistics.

4.1 Sensitivity Analysis – Results

In this section the results are given of the sensitivity analysis. The results will be given in the following sequence: 1) gradient parameters, 2) snow and glacier routine parameters, 3) soil moisture and response routine parameters and 4) routing routine parameters. To understand what kind of effect parameters have on simulated discharge values it is important to have a reference condition using HBV Light default values. In this manner it is possible to explain possible changes in simulated discharge relative to reference condition. The simulated discharge values characterizing this condition are given in Figure 4.1 together with simulated snow values and measured precipitation values. From this Figure there it is evident that snowmelt mainly appears between May and July with subsequently more or less constant snow conditions between the end of July and the end of September. It is likely that these snow conditions will mainly be concentrated to the higher elevation zones. In the same period (May-September) it is also evident that high runoff conditions occur from the end of May to the end of August (see Figure 4.1, bottom) with several runoff peaks. These peaks have their existence because of relatively large precipitation volumes in May, June/July and August (see Figure 4.1, central). In Sep/Oct there has also been a large precipitation event, but it had small effect on runoff since most of this precipitation fell as snow. This can be concluded by the observation that the increase in snow depth happened around the same time.

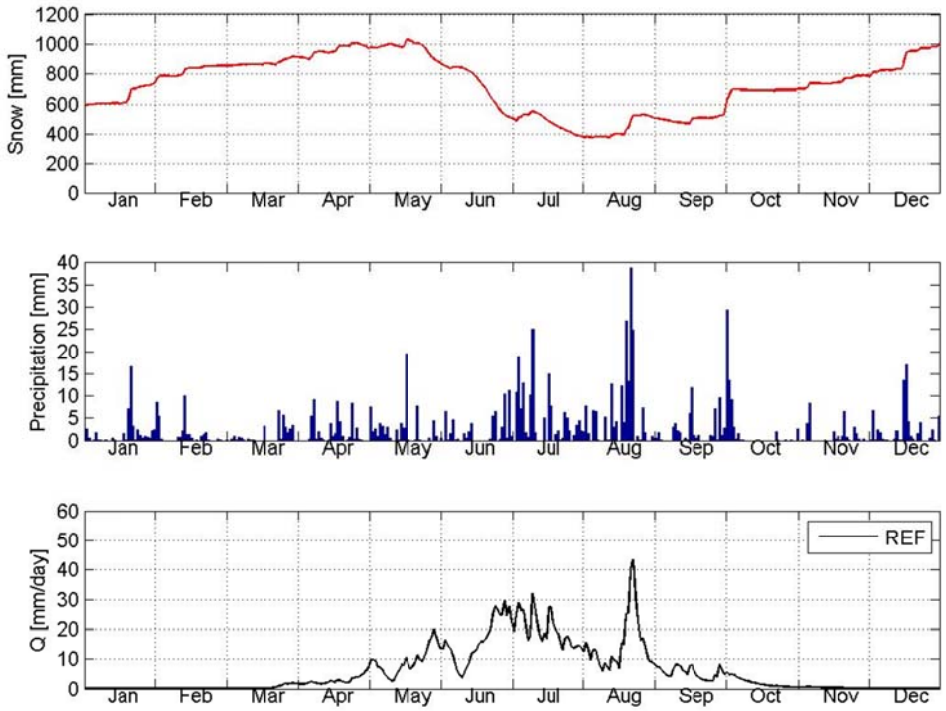

Figure 4.1: *Simulated snow, measured precipitation and simulated discharge of reference condition for gauging station Brunau.*

Gradient Parameters

It can be expected that simulated discharge will increase with increasing precipitation gradient PGrad and decreasing temperature gradient TGrad under the assumption that the reference elevation of precipitation and temperature measurements is at sea level or below the mean catchment elevation. In Figure 4.2 the simulated discharge is given for two values of PGrad (top) and two values of TGrad (bottom) under assumption of a reference elevation at sea level.

When PGrad increases it means that precipitation increases with a higher rate per 100 m elevation increase. This means more precipitation is entering the catchment and that therefore also more water has to be discharged, leading to an increase in simulated discharge values relative to the reference condition. This is different for a reference elevation that is higher than the mean catchment elevation. In such conditions the overall change in simulated discharge is negative since less water is entering the catchment.

Decreasing TGrad means that temperature decreases with a lower rate per 100 m elevation increase. This means that less precipitation falls in the form of snow and that less water is stored temporally and is released as melt water later on. Additionally the average temperature is higher meaning that snow-melting season has an earlier onset (March instead of May; see Figure 4.2, below). This implies in turn that snow quantities may be small during summer period and that discharge will be more rain- and ice melt dominated. It may explain why the peak discharge in August has a higher magnitude for low temperature gradients than for the reference condition. Over the entire period the sum of decreasing snowmelt and increasing ice melt and rain domination will lead to an increase in simulated discharge. This is however not the case if the reference elevation is higher than the mean catchment elevation. In such a situation the mean catchment temperature is lower instead of higher resulting in lower simulated discharge.

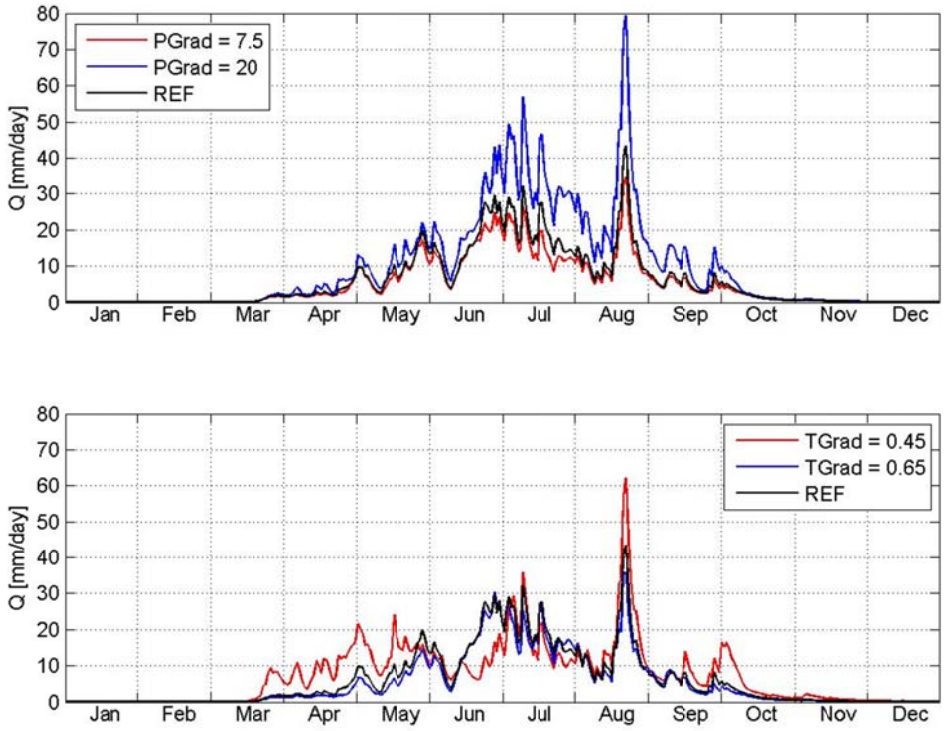

Figure 4.2: *HBV Light Simulations for PGrad = 7.5 %/100m , PGrad = 20 %/100m (top), TGrad = 0.45 °C/100m and TGrad = 0.65 °C/100m (bottom). PElev = 0 m a.s.l. ; TElev = 0 m a.s.l..*

Snow and Glacier Routine Parameters

It can be expected that simulated discharge will increase with decreasing TT (see Figure 4.3, top), increasing CFMAX (see Figure 4.3, bottom) and increasing SFCF (see Figure 4.4).

TT is decisive in the amount of precipitation falling as snow and the duration of the snowfall season. This means that if TT < 0 °C a smaller snowpack is produced and the snowfall season is shorter than when TT ≥ 0 °C. Consequently the melting season has an earlier onset for TT < 0 °C causing snow to melt away earlier and that discharge during summer period is more rain- and ice melt dominated. This explains in general the higher discharge values for low TT (see Figure 4.3, top).

CFMAX is an important parameter concerning production of melt water. Higher CFMAX values implicate that more melt water is produced during melting season. In Figure 4.3 (bottom) this can especially be observed in the period May-June where simulated discharge is higher for CFMAX = 6 than for the reference condition or CFMAX = 2.

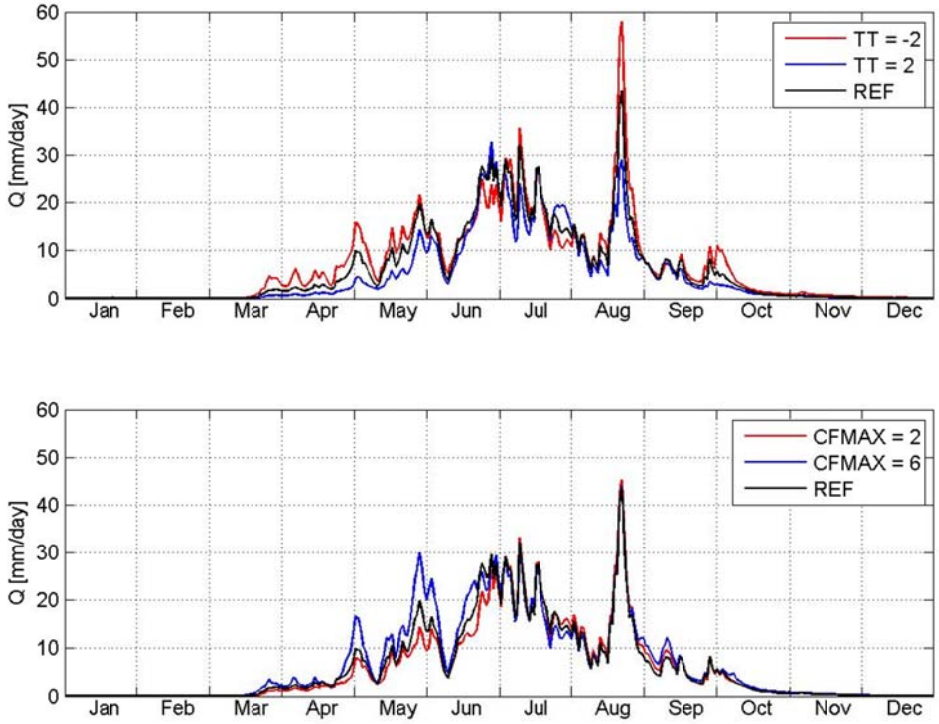

Figure 4.3: *HBV Light Simulations Brunau for TT = -2 °C, TT = 2 °C (top), CFMAX = 2 mm d^{-1} C^{-1} and CFMAX = 6 mm d^{-1} C^{-1} (bottom).*

SFCF is an important parameter in the simulation of snow. A higher SFCF value indicates a thicker snowpack is simulated over the entire period, which means higher volumes of melt water are available. These results in higher discharge values during melting season with the highest increases in June and July (see Figure 4.4).

In Figure 4.5 and 4.6 the results are given for the sensitivity analysis performed on KGmin (Figure 4.5, top), dKG (Figure 4.5, bottom) and AG (Figure 4.6) at gauging station Brunau.

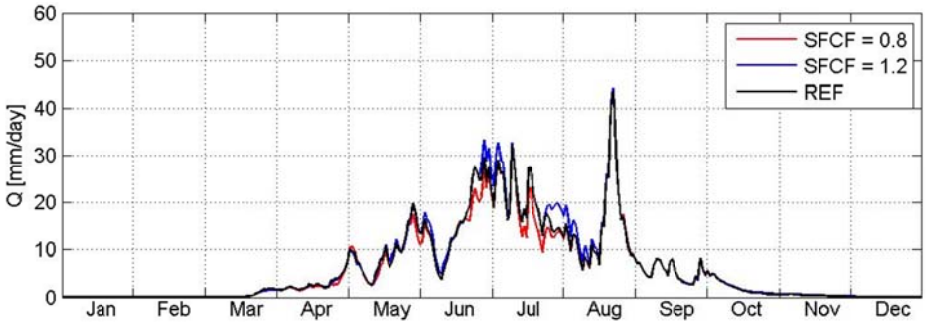

Figure 4.4: *HBV Light Simulations Brunau for SFCF = 0.8 and SFCF = 1.2 .*

When observing simulated discharge values for two different KGmin values it is evident that simulated discharge increases with increasing KGmin during summer period (June/July) and decreases during winter period. The changes are however small. The explanation for this pattern may be that during summer period the glacial drainage system is better developed meaning that dKG becomes operative. This results, in combination with higher KGmin, in higher glacial outflow and therefore also higher simulated discharge values. Because outflow is higher the glacial reservoir will be emptying faster meaning that during winter period less water is available for outflow. Therefore a decrease in simulated discharge appears during winter period.

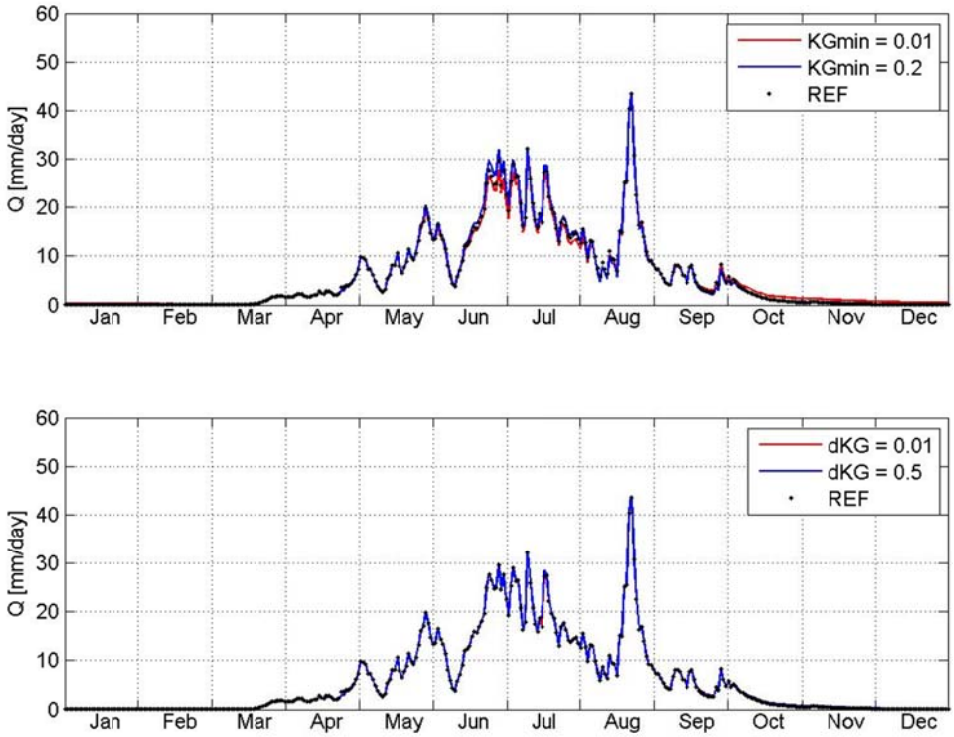

Figure 4.5: *HBV Light Simulations Brunau for KGmin = 0.01 d^{-1}, KGmin = 0.2 d^{-1} (top), dKG = 0.01 d^{-1} and dKG = 0.5 d^{-1} (bottom).*

When observing simulated discharge values for two different values of dKG and AG one can observe that there are no changes in simulated discharge with changing parameters. A possible reason is that the influence of glacial outflow at station Brunau is more limited since glaciation has a smaller ratio in the Ötztaler Ache catchment than in the catchments of the Gurgler and Venter Ache. This means that glacial outflow should have more influence on simulated discharge at the gauging stations Vent and Obergurgl, which is something what can be observed in Figure 4.7 and 4.8. In these Figures the results of sensitivity analyses are given for gauging station Vent, performed on the same parameters.

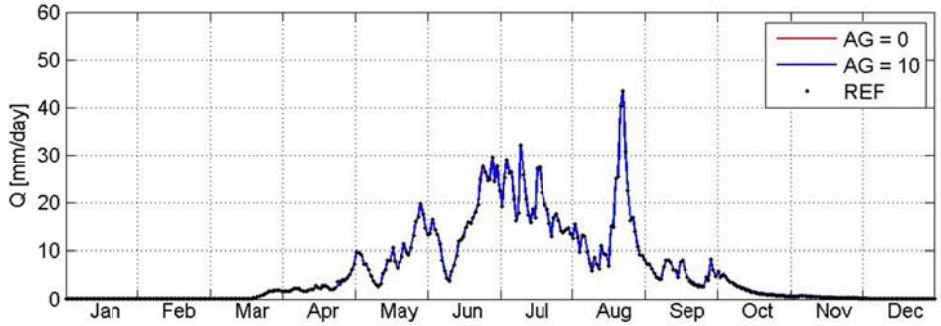

Figure 4.6: *HBV Light Simulations Brunau for AG = 0 mm^{-1} and AG = 10 mm^{-1}.*

Figure 4.7 (top) shows the simulated discharge for two different values of KGmin at gauging station Vent. It can be seen that discharge increases with increasing KGmin during summer period and decreases with increasing KGmin during winter period. The only difference with Brunau is that changes in simulated discharge are more apparent and that especially increases are noticeable over a longer period (May-September instead of June/July), which may be explained by the higher contribution of glacial meltwater to discharge.

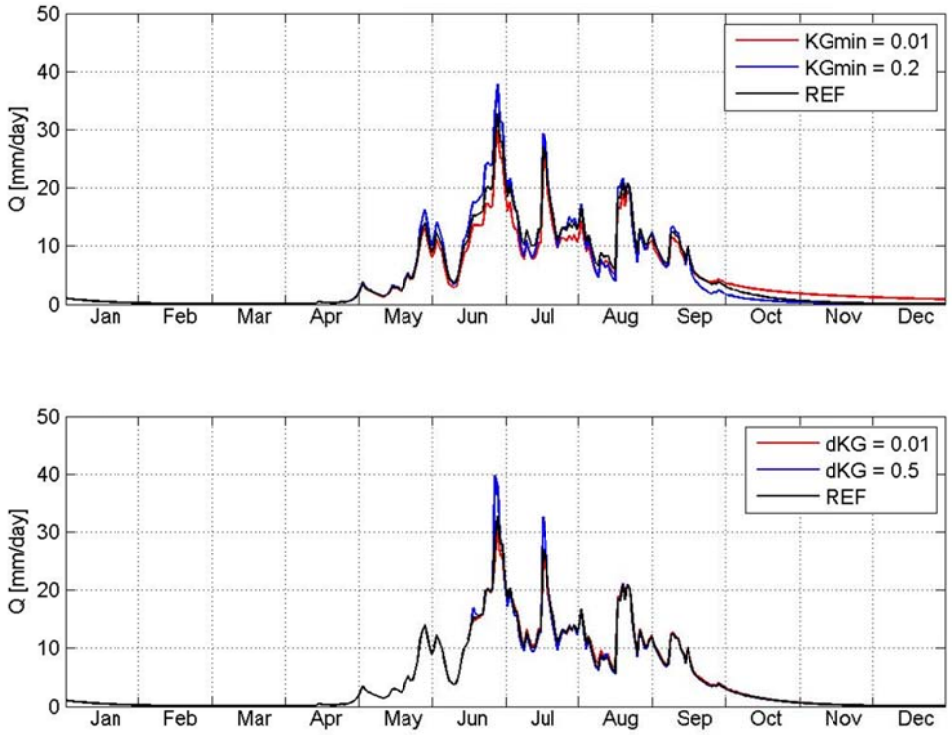

Figure 4.7: *HBV Light Simulations Vent for KGmin = 0.01 d^{-1}, KGmin = 0.2 d^{-1} (top), dKG = 0.01 d^{-1} and dKG = 0.5 d^{-1} (bottom).*

For dKG (see Figure 4.7, bottom), changes are only traceable in June-July with increased simulated discharge with increasing dKG. The explanation for these increases is that with increasing dKG more glacial outflow appears, resulting in higher discharge. A possible reason why these changes are only influential in June-July is that in this period the glacial drainage system is better developed.

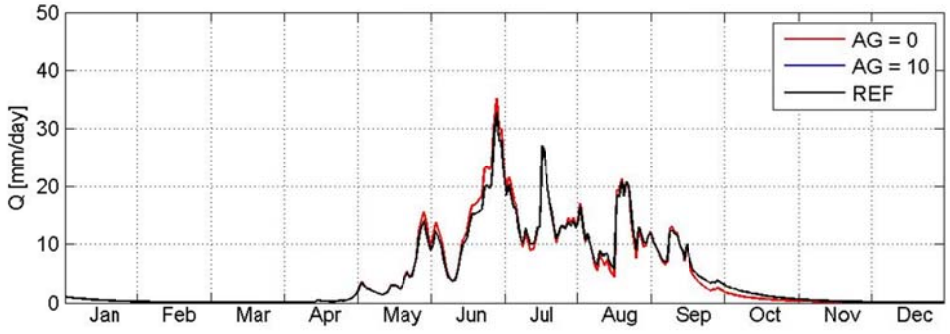

Figure 4.8: *HBV Light Simulations Vent for AG = 0 mm^{-1} and AG = 10 mm^{-1}.*

For AG (see Figure 4.8), differences in simulated discharges are more apparent under peak flow conditions than under low flow conditions, but only when AG = 0 mm^{-1}. Otherwise differences are negligible. The reason why differences only appear for AG = 0 mm^{-1} is that with AG = 0 mm^{-1} dKG becomes operative; implying that the glacial drainage system is well developed. This means glacial outflow is higher for AG = 0 mm^{-1}, resulting in higher simulated discharges. However because the

glacial reservoir is emptying faster, differences in simulated discharge become negative during low flow conditions.

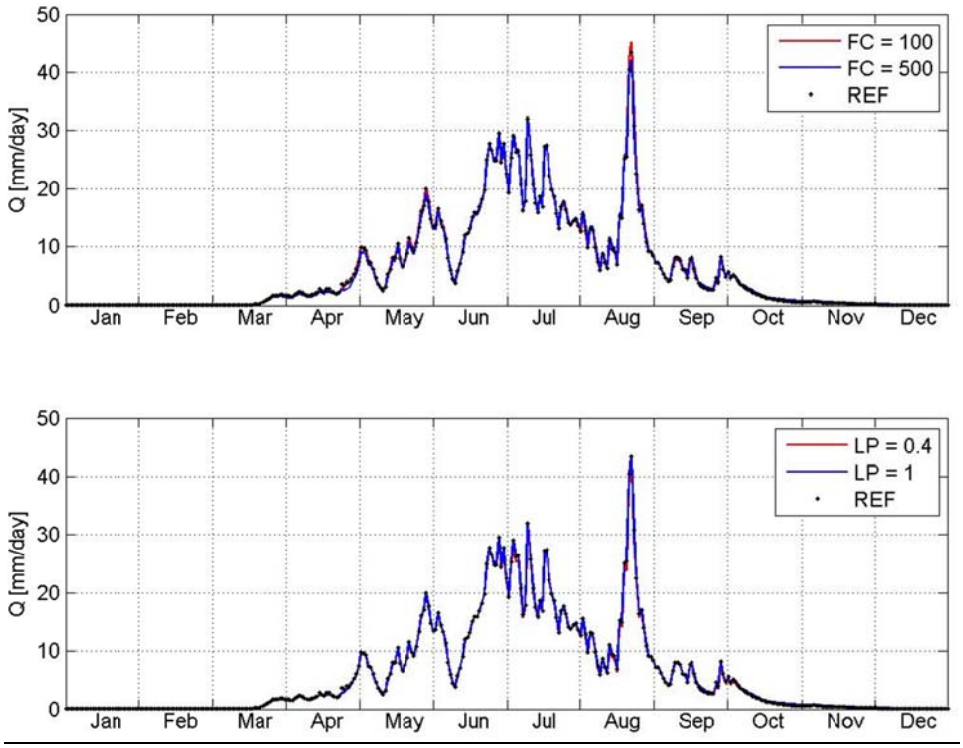

Figure 4.9: *HBV Light Simulations Brunau for FC = 100 mm, FC = 500 mm (top), LP = 0.4 and LP = 1 (bottom).*

Soil Moisture & Response Routine Parameters

For the soil moisture routine it can be expected that simulated discharge values increase with decreasing FC (see Figure 4.9, top), increasing LP (see Figure 4.9, bottom) or decreasing BETA (see Figure 4.10). The changes are however very small.

Simulated discharge values are expected to increase with decreasing FC, because a lower FC means that maximum storage of the soil reservoir is smaller and less soil water is available for evapotranspiration, which means that more water is added to the groundwater reservoirs. This will lead to higher simulated discharge values, which can mainly be observed in August (see Figure 4.9, above).

The reason why simulated discharge values are expected to increase with increasing LP is that LP determines the magnitude of actual evapotranspiration and therefore also how much water is extracted from the catchment. A higher LP entails that the threshold is higher for actual evapotranspiration to be equal to potential evapotranspiration. Therefore actual evapotranspiration is lower in catchments with high LP, resulting in increased discharge. This increase in discharge is however limited since it can barely be observed in Figure 4.9 (bottom).

The increase in simulated discharge due to decrease in BETA can best be explained using Equation 3.3. If BETA decreases the ratio between groundwater recharge and the input to the soil reservoir increases. This means that groundwater recharge increases relatively leading to an increase in simulated discharge, which can mainly be observed in Figure 4.10 as small increases during the summer period.

In Figures 4.11 and 4.12 simulated discharge values are given for two values of UZL (Figure 4.11, top), K_0 (Figure 4.11, bottom) and K_1 (Figure 4.12) respectively.

When looking at the simulated discharge values for two different UZL values it is evident that during peak flow conditions simulated discharge decreases with increasing UZL and that during baseflow conditions simulated discharge increases with increasing UZL. The explanation behind this pattern is that during peak flow conditions under increasing UZL it will take longer before a third

reservoir outflow (also referred as overland flow) can occur. This means only two reservoir outflows are operative, which indirectly results in lower simulated discharge values. Since by increasing UZL the amount of groundwater storage is larger, outflow from groundwater reservoirs will continue for a longer time, meaning that simulated discharge is higher during baseflow conditions.

For decreasing K_0 a similar pattern can be observed as with increasing UZL, with decreasing simulated discharge during peak flow conditions and increasing simulated discharge after peak flow conditions (see Figure 4.11, bottom). The explanation for this pattern is that with low K_0 the outflow is lower during peak flow conditions with the result that groundwater storage increases, resulting in increased simulated discharge after peak flow conditions.

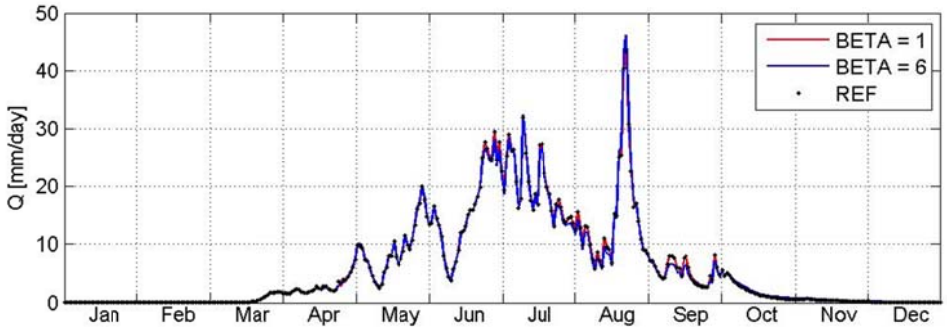

Figure 4.10: *HBV Light Simulations Brunau for BETA= 1 and BETA = 6.*

The same pattern can be observed for K_1 values (see Figure 4.12), although the difference is that changes in simulated discharge are slightly smaller for low K_1 values than for low K_0 values. A possible interpretation for this observation can be that with lower K_1 values the third outflow will receive a relatively higher contribution than with lower K_0, resulting in slightly higher peak discharges for low K_1 than for K_0 and slightly lower discharges after peak flow conditions.

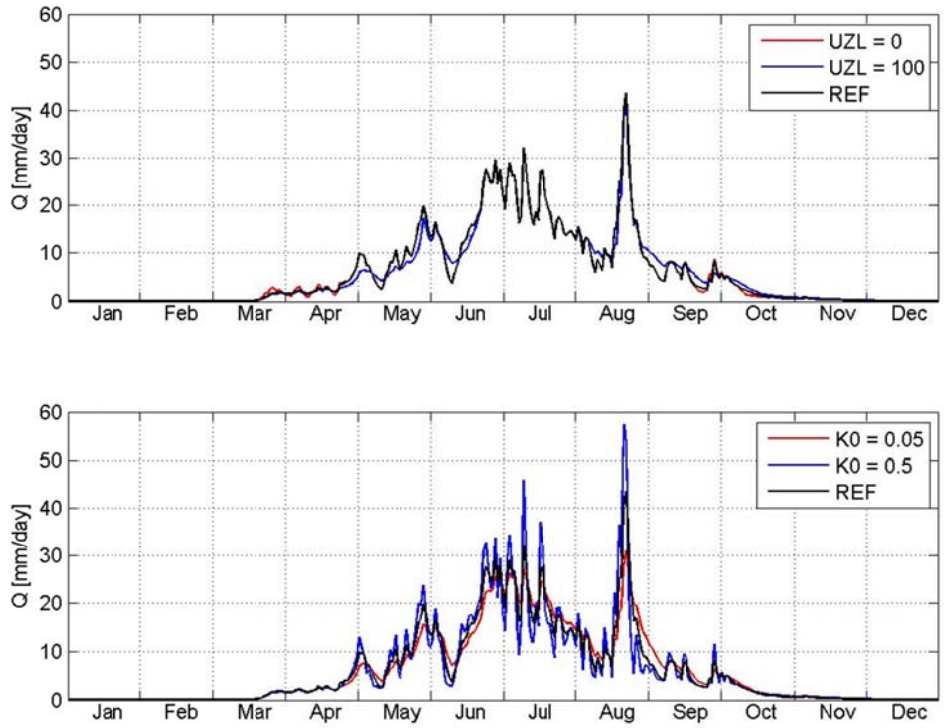

Figure 4.11: *HBV Light Simulations Brunau for UZL = 0 mm, UZL = 100 mm (top), $K_0 = 0.05\ d^{-1}$ and $K_0 = 0.5\ d^{-1}$ (bottom).*

In Figure 4.13 simulated discharge values are given for two values of K_2 (top) and PERC (bottom).

It is evident that almost no changes in simulated discharge are visible with changing K_2. The only observation is that simulated discharge increases slightly during baseflow conditions with decreasing K_2. A possible reason can be that with lower K_2 it takes longer to empty the groundwater reservoirs, resulting in slightly higher simulated discharge values during baseflow conditions in winter period (Oct – Mar).

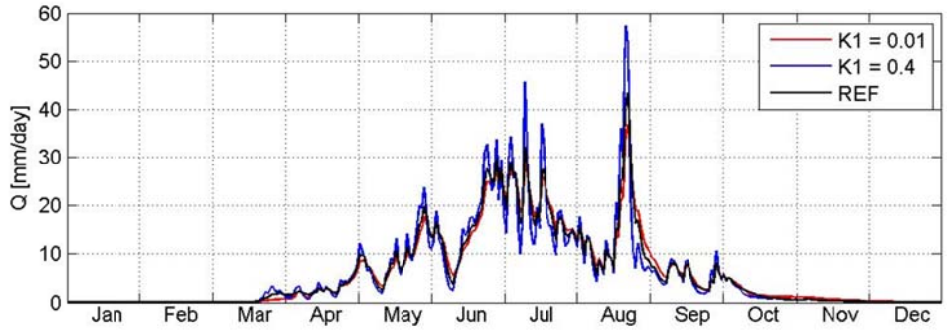

Figure 4.12: *HBV Light Simulations Brunau for K_1= 0.01 d^{-1} and K_1 = 0.4 d^{-1}.*

It is also evident that with lower PERC simulated discharge increases during the melting season and decreases after the melting season with exception of peak flow conditions. Lower PERC will result in a lower discharge contribution of the lower groundwater reservoir with the consequence that the upper groundwater reservoirs may contribute more to simulated discharge. This means that during the melting season, when the groundwater reservoirs are filling, the simulated discharge is generally higher. After the melting season the reservoirs are not filling any more, except during precipitation events and when small amounts of ice melt are entering the groundwater reservoirs. This results in a higher contribution of the lower groundwater reservoir.

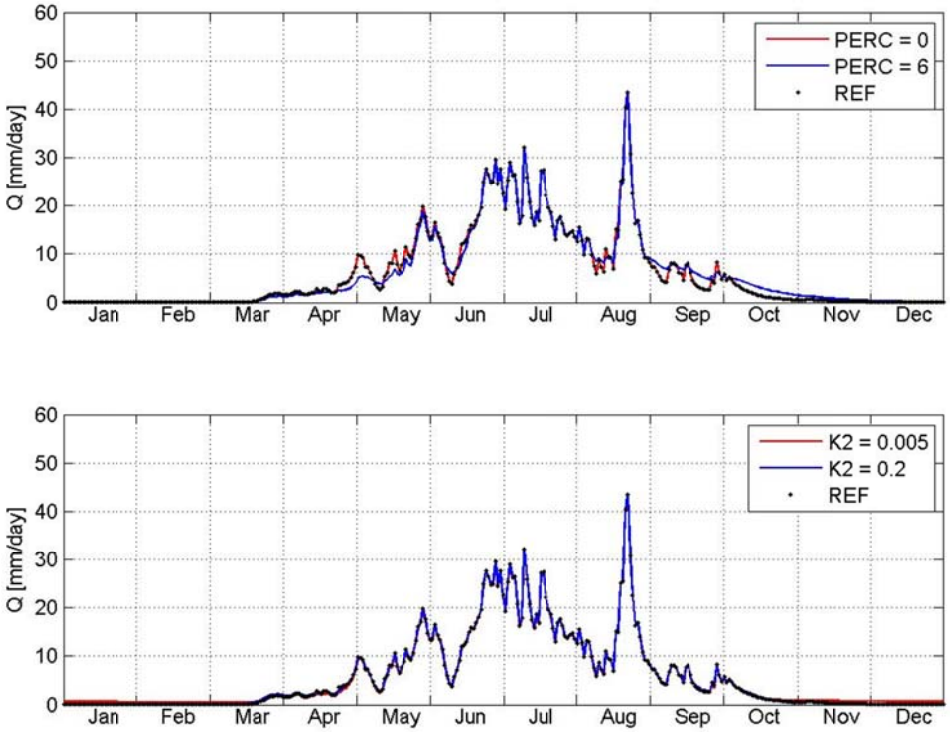

Figure 4.13: *HBV Light Simulations Brunau for PERC = 0 mm d^{-1}, PERC = 6 mm d^{-1} (top), K_2 = 0.005 d^{-1} and K_2 = 0.2 d^{-1} (bottom).*

Routing Routine Parameters

Figure 4.14 illustrates the effect of different MAXBAS values on simulated discharge. It is evident that a higher MAXBAS will lead to lowering peak values and a shift in peak occurrence to later times.

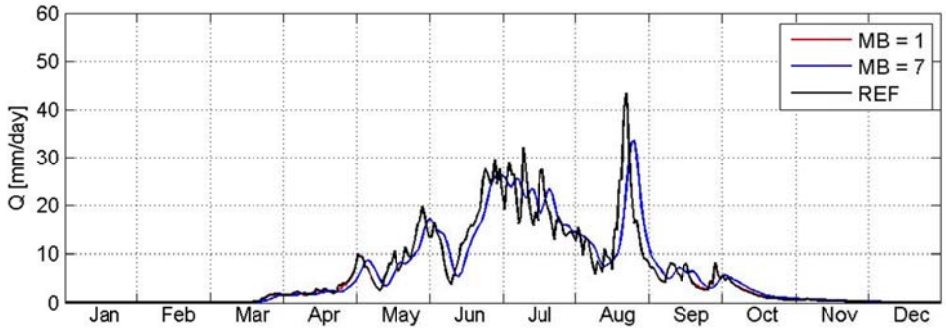

Figure 4.14: *HBV Light Simulations Brunau for MAXBAS = 1 d and MAXBAS = 7 d.*

Summary & Remarks

The sensitivity analysis shows that HBV Light is most sensitive to changes in precipitation and temperature gradients, and snow routine parameters. These parameters are important for the simulation of snow accumulation and -melt and therefore also highly determinative for the amount and timing of discharge. For glacier routine parameters the sensitivity of HBV Light depends on the degree of glaciation in a catchment. In highly glaciated catchments HBV Light behaves more sensitive to parameter changes than in less glaciated catchments. HBV Light is insensitive to the soil moisture routine parameters and for response routine parameters the sensitivity of HBV Light depends on whether outflow is predominantly from the upper or lower groundwater reservoirs. For upper groundwater reservoirs HBV Light behaves more sensitive than for lower groundwater reservoirs. Upper groundwater reservoirs generally react faster on precipitation events than lower groundwater reservoirs. Therefore upper groundwater reservoirs exert more influence on simulated discharge, resulting in a more sensitive behaviour. Finally, HBV Light also behaves sensitive to changes in routing routine parameters.

4.2 Calibration and Validation – Results

From the calibration and validation procedure the following results are obtained. In Table 4.1 the Nash-Sutcliffe efficiency (NSE) values are given for calibration periods of the respective catchments. All catchments scored with efficiency values in the range 0.86-0.87, which can be classified as “good performance” (Helfricht et al., In Press). In Table 4.2 the resulting parameter sets are given for the Ötztaler, Gurgler and Venter Ache.

Table 4.1: *Calibration periods and Nash-Sutcliffe efficiency values.*

(Sub)Catchment	*Calibration Period*	*NSE Calibration*
Ötztaler Ache	*1998-2007*	*0.8695*
Gurgler Ache	*1998-2007*	*0.8576*
Venter Ache	*1993-2002*	*0.8697*

In Table 4.3 the NSE values are given for the validation periods of respective catchments together with the mean differences (expressed in mm and %) between observed and simulated discharge. What concerns the performance of HBV Light, taking NSE values into consideration, HBV Light has a better performance for the second validation period than for the first validation period. A possible explanation for this difference is the lack of meteorological data in the 80s and the 90s. This will be discussed later on in Section 5. The improving performance of HBV Light with time can also be observed in the mean differences, which are generally larger in the first validation period than in the second validation period. The exception however is the catchment of the Gurgler Ache where the

mean difference for 2008-2012 is larger than for 1987-1997. We have no explanation why the mean difference is larger for 2008-2012.

Table 4.2: *Parameters sets resulting from calibration of HBV Light (V1 = Vegetation Zone 1 (Glacial Cover), V2 = Vegetation Zone 2 (Bare Vegetated), V3 = Vegetation Zone 3 (Vegetated).*

	Ötztaler Ache			*Gurgler Ache*			*Venter Ache*		
Catchment Settings									
PGrad	*8.5*			*7.5*			*7.5*		
TGrad	*0.51*			*0.49*			*0.53*		
PElev[1]	*1880*			*1990*			*2230*		
TElev	*0*			*0*			*0*		
	Ötztaler Ache			***Gurgler Ache***			***Venter Ache***		
Snow/Glacier Routine	***V1***	***V2***	***V3***	***V1***	***V2***	***V3***	***V1***	***V2***	***V3***
TT	*-0.7*	*-0.7*	*-0.7*	*-1.1*	*-1.1*	*-1.1*	*-0.6*	*-0.6*	*-0.6*
CFMAX	*3*	*3*	*2*	*3*	*3*	*2*	*3*	*3*	*2*
SFCF	*1*	*1*	*0.9*	*1*	*1*	*0.9*	*1*	*1*	*0.9*
CWH	*0.1*	*0.1*	*0.1*	*0.1*	*0.1*	*0.1*	*0.1*	*0.1*	*0.1*
CFR	*0.05*	*0.05*	*0.05*	*0.05*	*0.05*	*0.05*	*0.05*	*0.05*	*0.05*
CFGlac	*1.7*	*0*	*0*	*1.4*	*0*	*0*	*1.4*	*0*	*0*
CFSlope	*1.7*	*1.7*	*1.7*	*1.9*	*1.9*	*1.9*	*1.9*	*1.9*	*1.9*
	Ötztaler Ache			***Gurgler Ache***			***Venter Ache***		
Soil Moist Routine	***V1***	***V2***	***V3***	***V1***	***V2***	***V3***	***V1***	***V2***	***V3***
FC	*160*[2]	*290*	*450*	*160*[2]	*290*	*450*	*160*[2]	*290*	*450*
LP	*0.95*	*0.8*	*0.7*	*0.95*	*0.8*	*0.7*	*0.95*	*0.8*	*0.7*
BETA	*5*	*3*	*4*	*5*	*3.2*	*4*	*5.5*	*4.3*	*4.5*
Glacier Routine	***Ötztaler Ache***			***Gurgler Ache***			***Venter Ache***		
KG_{min}	*0.2*			*0.2*			*0.2*		
dKG	*0.38*			*0.4*			*0.2*		
AG	*0*			*0*			*0*		
Response Routine	***Ötztaler Ache***			***Gurgler Ache***			***Venter Ache***		
PERC	*3.5*			*4.7*			*6*		
UZL	*100*			*83*			*75*		
K_0	*0.051*			*0.051*			*0.051*		
K_1	*0.027*			*0.01*			*0.011*		
K_2	*0.014*			*0.021*			*0.015*		
Routing Routine	***Ötztaler Ache***			***Gurgler Ache***			***Venter Ache***		
MAXBAS	*1.7*			*1.2*			*1.1*		

[1] For the reference elevation of precipitation the mean elevation of precipitation stations used for IDW has been taken.
[2] In order to calibrate FC for a glacial cover vegetation zone a value has been taken from Hagg (2003). Hagg (2003) conducted a study with HBV-ETH3 in the catchment of the Vernagtbach, which is locacted in the catchment of the Venter Ache. Since the catchment of the Vernagtbach has a glaciation of 78% (Hagg, 2003; Konz et al. 2010) the value of 160 mm is assumed to have a good representation for FC in a glacial cover vegetation zone. In another study, implemented by Braun and Renner (1992) with the same model, a similar value has been used for the catchment of the Massa (Aletsch Glacier Area, Switzerland; glaciation of 66%).

Table 4.3: *Validation Periods, Efficiency (Nash-Sutcliffe) and Mean Difference relative to observed discharge.*

(Sub)Catchment	***Validation Period(s)***	***NSE Validation***	***Mean Difference (mm)***	***Mean Difference (%)***
Ötztaler Ache	*1987-1997*	*0.8486*	*-27*	*-2.6*
	2008-2012	*0.8981*	*-23*	*-2.1*
Gurgler Ache	*1987-1997*	*0.8047*	*-29*	*-1.7*
	2008-2012	*0.8598*	*-179*	*-11.4*
Venter Ache	*1987-1992*	*0.8534*	*-92*	*-6.3*
	2008-2012	*0.8979*	*-35*	*-2.3*

In Figures 4.15, 4.16 and 4.17 the observed and simulated discharge resulting from the second validation period has been plotted along each other showing an excellent fit.

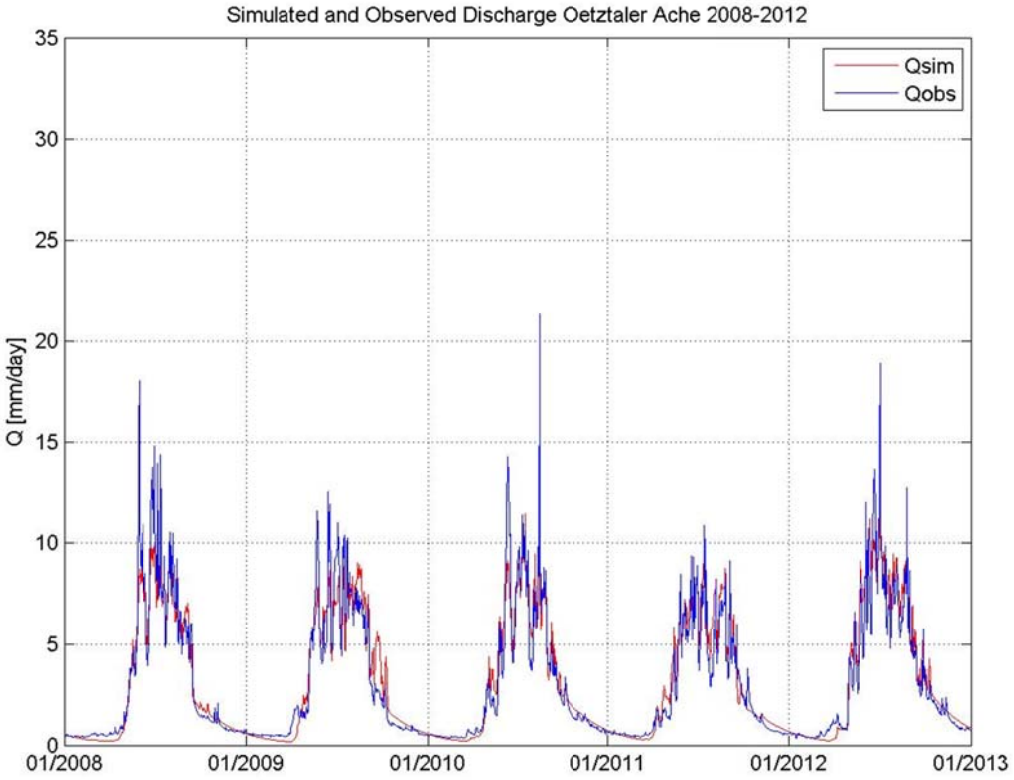

Figure 4.15: *Simulated and Observed Discharge of Ötztaler Ache (Brunau) for validation period 2008-2012.*

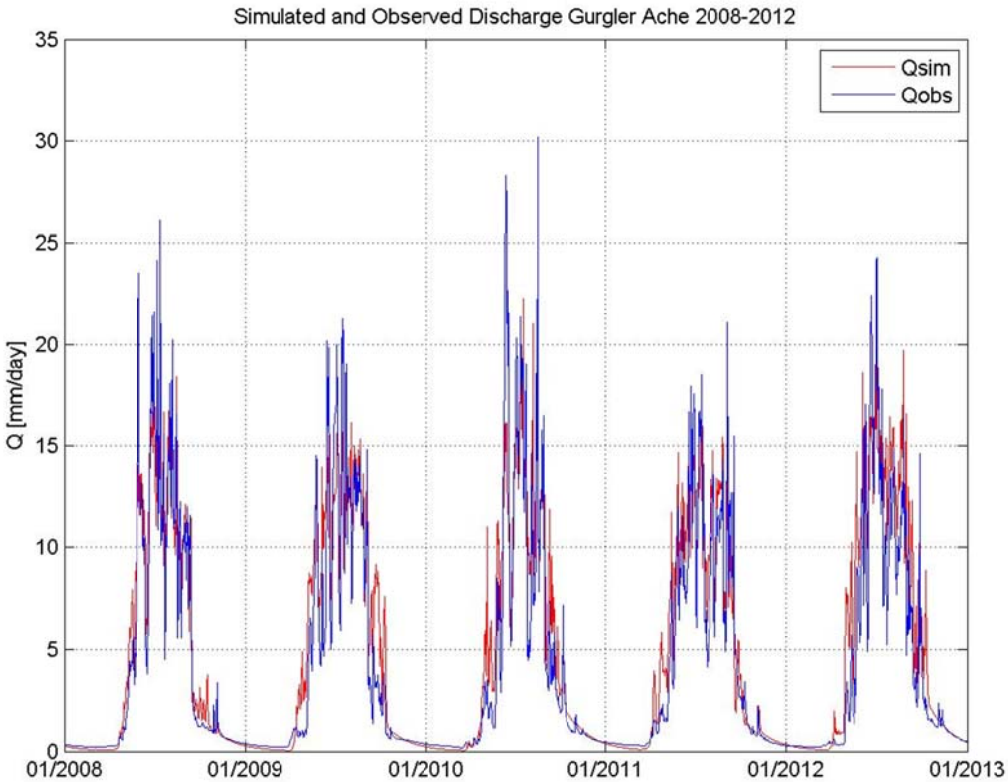

Figure 4.16: *Simulated and Observed Discharge of Gurgler Ache (Obergurgl) for validation period 2008-2012.*

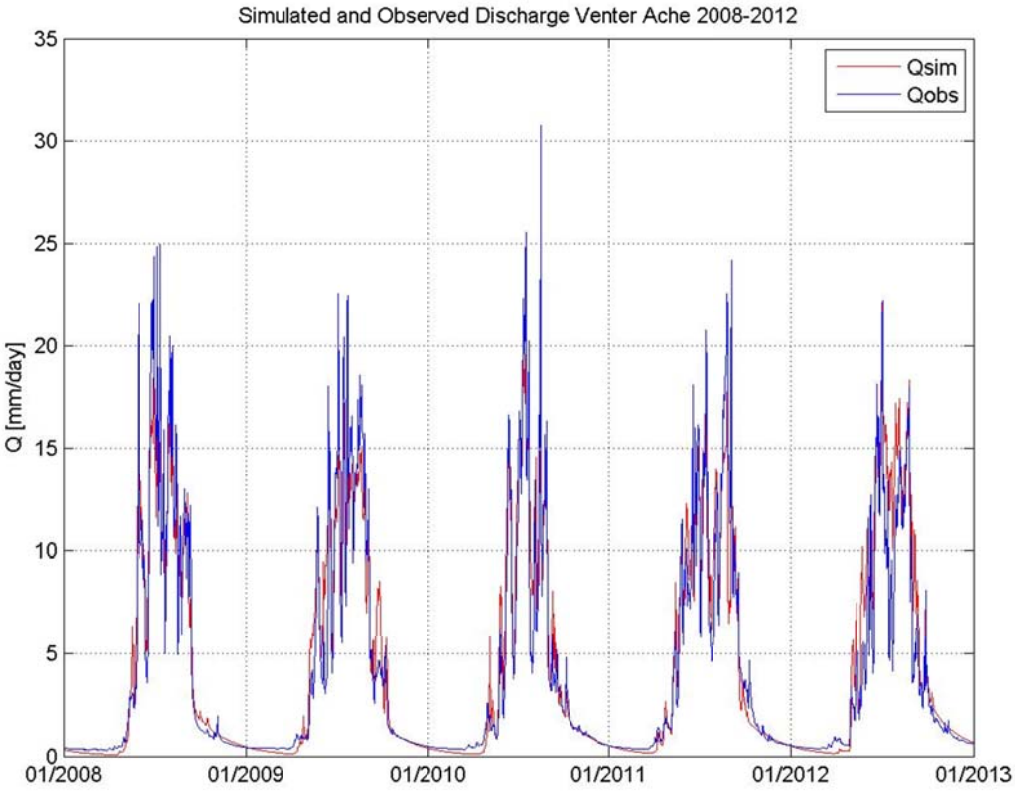

Figure 4.17: *Simulated and Observed Discharge of Venter Ache (Vent) for validation period 2008-2012.*

4.3 Glacier Changes

Using the model of Helfricht (2013) the following results were computed:

- Absolute area-elevation, ice thickness-elevation and volume-elevation distributions.
- Relative area-elevation, ice thickness-elevation and volume-elevation distributions.
- Relative changes in area, ice thickness and volume.
- Ice thickness distributions of 2006, 2025, 2055 and 2085.

In Figure 4.18 the absolute area-elevation, ice thickness-elevation and volume-elevation distributions are given for the period 2005 - 2105. From different distributions a significant decrease in glacial area and volume with time can be observed. According to Figure 4.19, which shows a relative area-elevation, a relative ice thickness-elevation and a relative volume-elevation distribution, the rate of decrease in glacial area and volume is approximately the same for all elevation zones. However the rate of decrease behaves different for the lower elevation zones (2400 -2700 m a.s.l.). In these elevation zones an increase in glacial area and volume (limited to elevation zone 2400 m a.s.l.) relative to the initial area and volume of 2005 is expected for 2015. In the subsequent decades the expectation is that glacial volume and area will decrease again until glaciers start to disappear, which is expected to happen after 2050.

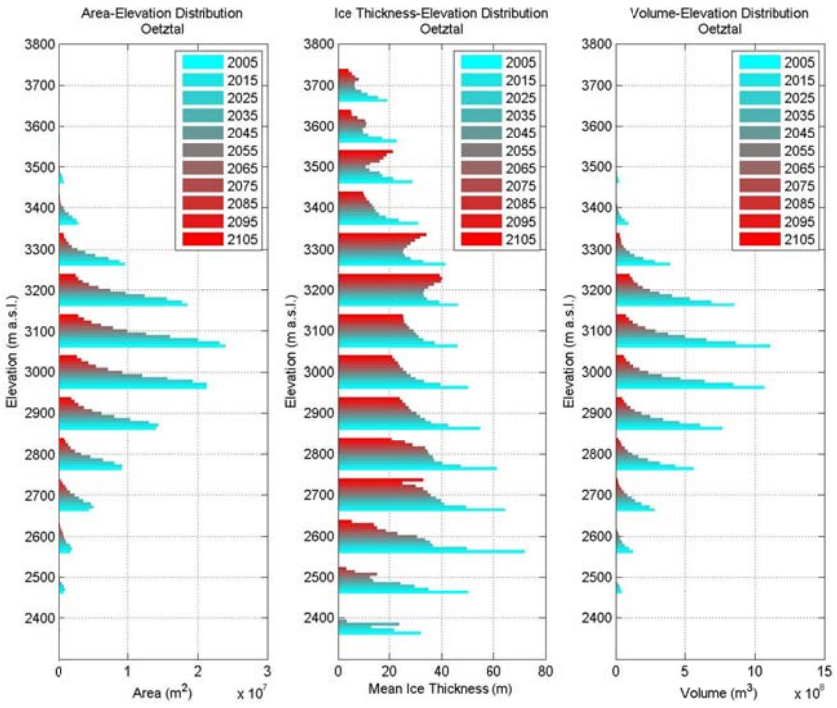

Figure 4.18: *Area-, Ice-thickness- and Volume-Elevation Distribution of glaciers Ötztal (including the glaciers of Ötztaler Ache catchment, which are located in Stubaier and Ötztaler Alps). Based on data of Helfricht (2013).*

Where glacial area and volume show a general decrease with time, the ice thickness distributions show only a general decrease during the first half of the 21st century. During the second half of the 21st century there are elevation zones (e.g. 2400-2600 m a.s.l.) where the reduction of mean ice thickness continues. In other elevation zones (e.g. 3200-3300 m a.s.l.) however the mean ice thickness increases again, i.e. because the reduction rate of area is higher than the reduction rate of ice thickness. Averaging the relative changes in mean ice thickness over all elevation zones it would mean that the relative change in ice thickness is slowly getting constant toward 2100. This can be observed in Figure 4.20, which illustrates relative changes in area, ice thickness and volume with time for a minimum, mean and maximum temperature increase of 0.9 °C, 2 °C and 3 °C respectively. In this figure it is evident that initially volume and ice thickness change relatively with the same rate where the relative change in area is limited. The limited change in area explains why for 2015 a relative increase in area and volume is projected for the lower elevation zones. When ice thickness decreases it means that surface elevation also decreases, leading to a shift in elevation zones. Because glacial area remains relatively constant the shift in elevation zones eventually results in an increase in area in the lowest elevation zones. This can be illustrated by Figure 4.21, which shows the distribution of elevation zones for the Hintereisferner (location, see Figure 2.5) for the years 2005 (top) and 2015 (bottom). It is from this figure evident that the areas covering the elevation zones 2400-2500 m and 2500-2600 m are getting larger in 2015, while areas covering the other elevation zones are getting smaller or remain approximately constant. After glacial area has started to reduce in the lower elevation zones, the relative change in area is getting larger where the relative change in ice thickness is getting smaller. After ~2040 the moment is reached that the relative change in area is expected to be larger than the relative change in ice thickness, which means that area reduction will be stronger than thickness reduction. This is the moment that the ELA is assumed to reach the highest part of the glaciers, the AAR is assumed to be zero and that the runoff regimes are assumed to change (Casassa et al., 2009). The expectation that area reduction will be stronger than thickness reduction after ~2040 may also explain why the mean ice thickness is increasing in some of the elevation zones after ~2040. The stronger area reduction ensures that glaciers concentrate with time to locations with initially the largest ice thicknesses (e.g. Vernagtferner, Hintereisferner and Gurgler

Ferner; see Figure 2.5). Because in other parts of the elevation zones glaciers disappear and the locations with the largest ice thicknesses still have reasonable ice thicknesses, this will lead to an increase in mean ice thickness in the elevation zones to which these locations are restricted. This can be observed very well in Figure 4.22, which present 4 maps of ice thickness distributions for 2006, 2025, 2055 and 2085. These maps demonstrate that there is not much difference between the glacial areas of 2006 and 2025, where the difference is much bigger between 2025 and 2055. Likewise is demonstrated that glaciers in 2085 are restricted to locations where in 2006 the largest ice thicknesses were observed.

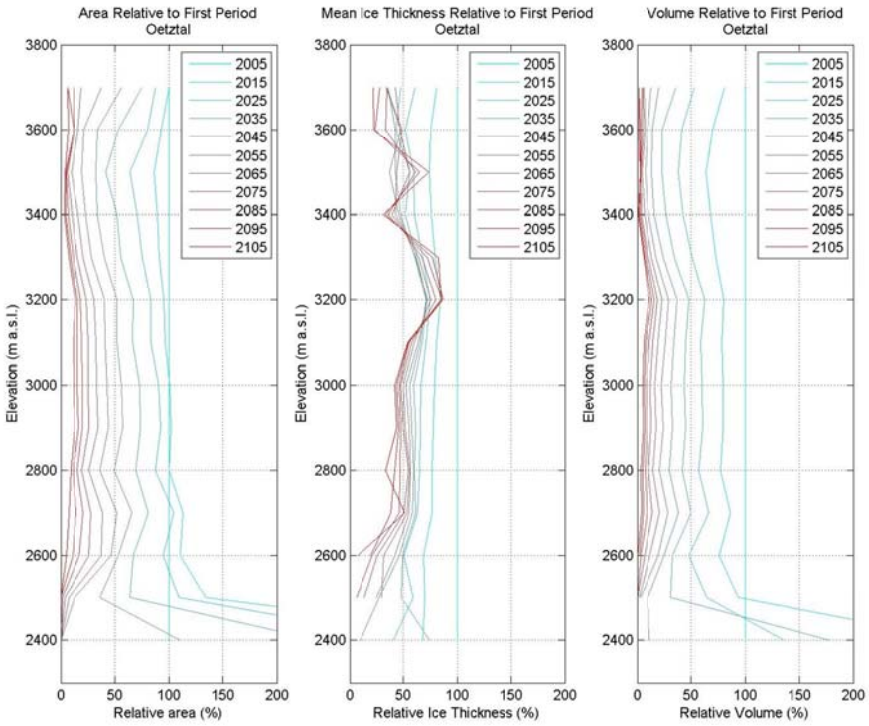

Figure 4.19: *Relative Area-, Ice thickness- and Volume-Elevation distributions of Glaciers Ötztal. Based on data of Helfricht (2013).*

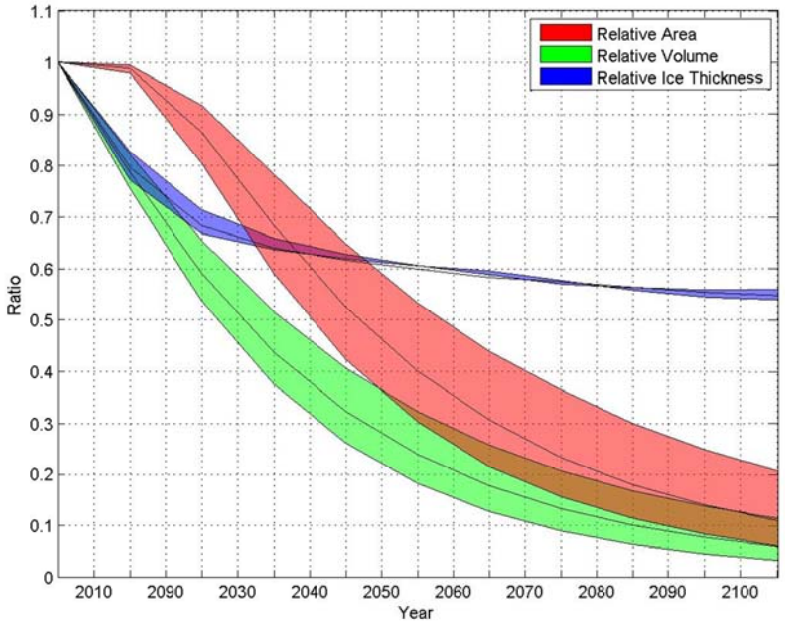

Figure 4.20: *Relative changes in glacial area, ice-thickness and glacial volume with time for a minimum, mean and maximum temperature increase of 0.9 °C, 2 °C and 3 °C respectively. Based on data of Helfricht (2013).*

To obtain a better overview in which magnitude relative changes in glacial area, ice thickness and glacial volume are expected to appear, these relative changes are summarized in Table 4.4 for minimum vs. maximum temperature increase. In this Table (and likewise in Figure 4.20) it is also evident that future ranges for glacial area and volume changes are larger than future ranges for ice-thickness changes, indicating that uncertainty is larger for area and volume changes than for ice-thickness changes.

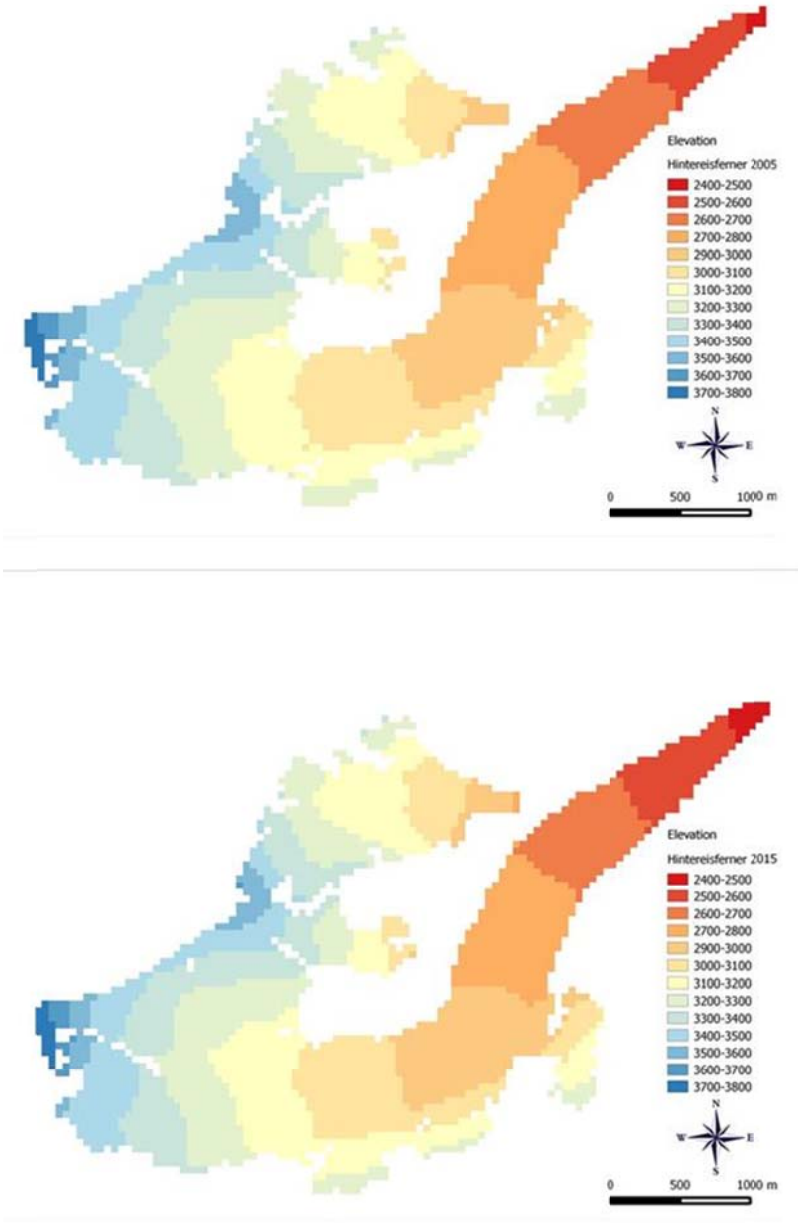

Figure 4.21: *Distribution of Elevation Zones Hintereisferner for 2005 (top) and 2015 (bottom). Based on data of Helfricht (2013).*

Table 4.4: *Relative Area, Volume and Ice Thickness Changes for minimum vs. maximum temperature increase.*

Year	**Relative Area Change (%) +0.9 °C. vs. +3.0 °C**	Relative Thickness Change +0.9 °C. vs. +3.0 °C	**Relative Volume Change +0.9 °C. vs. +3.0 °C**
2025	- 8 % vs. - 20 %	- 29 % vs. - 33 %	- 35 % vs. - 46 %
2055	- 47 % vs. - 70 %	- 40 % vs. - 40 %	- 68 % vs. - 82 %
2085	- 70 % vs. - 89 %	- 44 % vs. - 44 %	- 83 % vs. - 94 %
2105	- 79 % vs. - 94 %	- 44 % vs. - 46 %	- 88 % vs. - 97 %

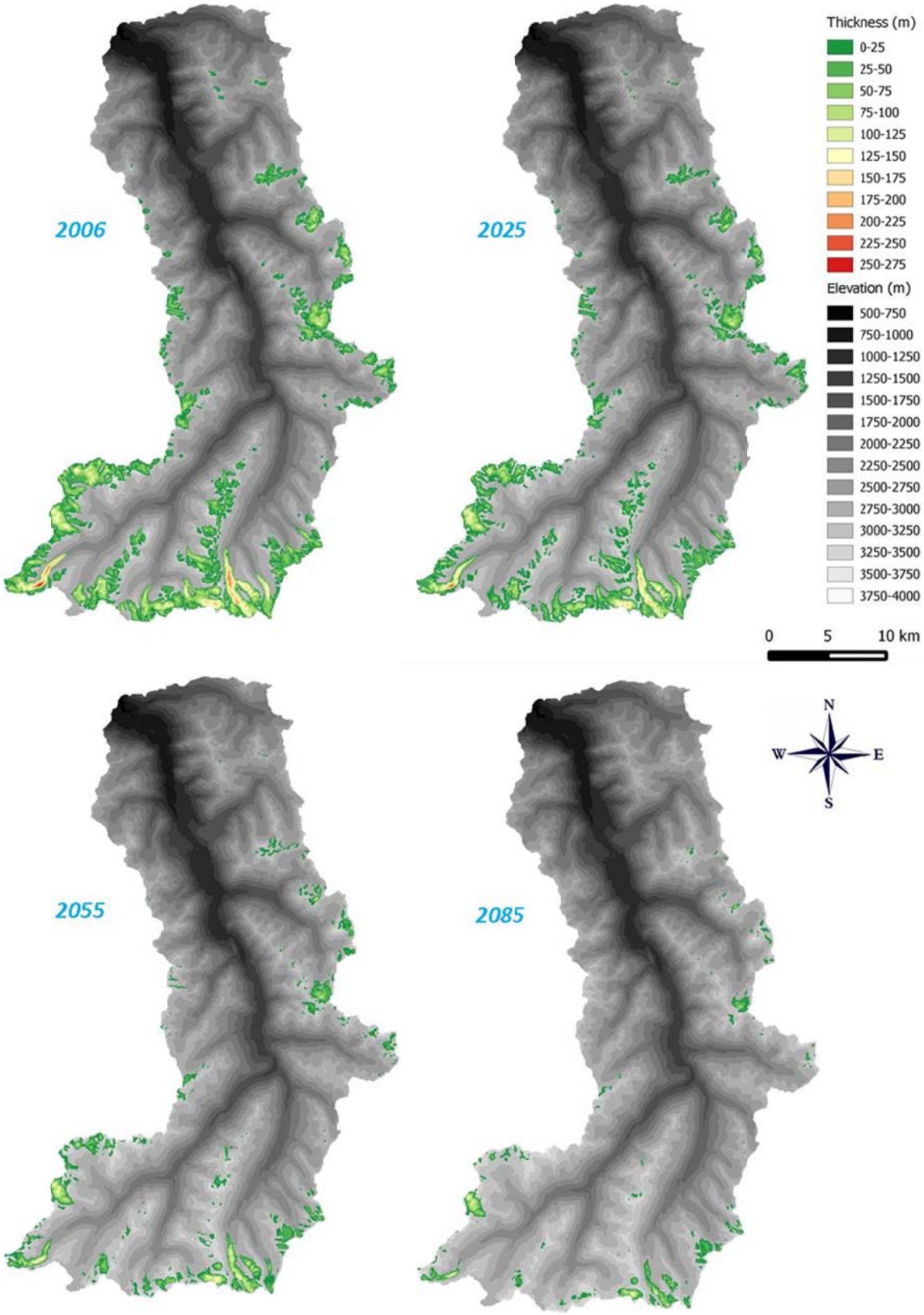

Figure 4.22: *Ice-thickness Distributions of Glaciers in 2006, 2025, 2055 and 2085. The orange-purple distribution represents the elevation distribution extracted from the DTM 2006. The green-blue distribution represents the ice-thickness distribution. Based on data of Helfricht (2013).*

4.4 Hydrological Response

In the following sections changes in hydrologic response to glacier and climatic changes will be presented for each (sub) catchment separately.

4.4.1 Ötztaler Ache

In Figure 4.23a the Pardé coefficients are given for the catchment of the Ötztaler Ache (Brunau) assuming that only the glacier scenarios are valid (Class A). In the reference situation the Pardé coefficients for June and July are higher than in August, which means that a glacio-nival regime is dominating, which is also stated in Section 2.4 and Figure 2.7. The runoff regime will stay approximately the same for scenario A1, while for scenarios A2 and A3 regime will change. Instead of having the highest Pardé coefficient in July, the highest coefficient will shift to June. Because the Pardé coefficient for August is still higher than the coefficient for May and the coefficient for May is higher than for September it can be concluded that the runoff regime will shift from a glacio-nival regime to a nivo-glacial regime. This means that snowmelt will become a more dominating factor in runoff generation of the Ötztaler Ache. In Figure 4.23b the absolute and relative changes are given for the same scenarios. Also in this figure it is evident that the change (absolute and relative) for scenario A1 is limited. For the other scenarios the absolute and relative changes are largest in July and August. In these months a decrease in runoff is expected up to 30% for scenario A2 and up to 40% for scenario A3 with the largest decreases in August. This means that the glacial runoff will become less and the snowmelt will become more dominating, causing the runoff regime to shift from a glacio-nival regime to a nivo-glacial regime.

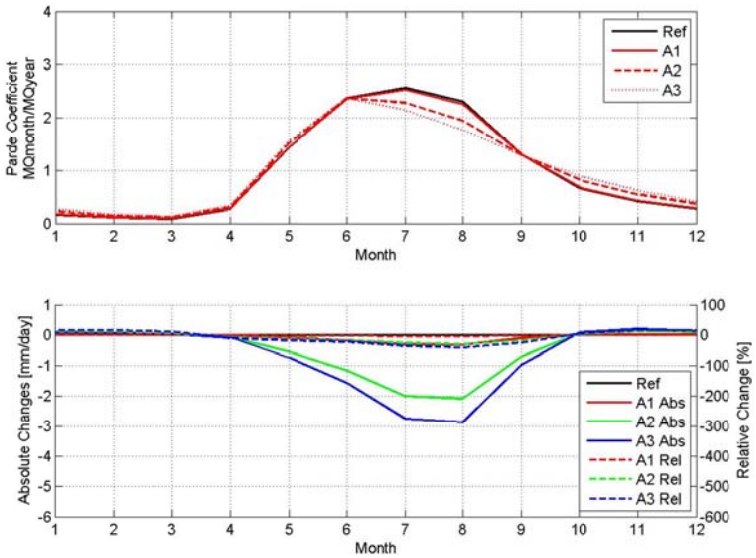

Figure 4.23: *Pardé coefficients of Ötztaler Ache (Brunau) (a), and absolute and relative changes in runoff of Ötztaler Ache relative to the reference condition (b) for scenarios A1, A2, A3 and the reference condition (= Ref). (Abs=Absolute, Rel=Relative).*

In Figure 4.24 the results for the Ötztaler Ache catchment are presented for the climate only-scenarios, i.e. glacial conditions remain constant (Class B). In 4.24a, which illustrates the Pardé coefficients, it is evident that the runoff regime remains constant with time. However this does not mean that the runoff does not change at all. In 4.24b, which gives the absolute and relative changes, we observe an absolute increase in runoff between February and November with largest absolute increases in the period April-September. The relative increase in runoff is expected to be smallest during summer months and to be largest in April. The explanation behind this pattern is that increase of runoff in April is mainly caused by an increase and earlier onset of snowmelt, while during summer months the increase of runoff can be explained by increase in glacier melt due to increase in temperature. Since glacier melt already was a dominating factor the relative change remains limited.

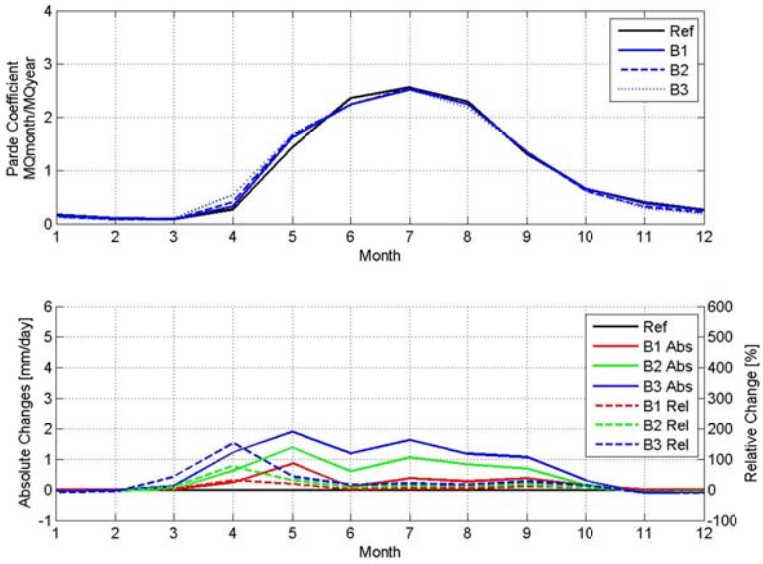

Figure 4.24: *Pardé coefficients of Ötztaler Ache (Brunau) (a), and absolute and relative changes in runoff of Ötztaler Ache relative to the reference condition (b) for scenarios B1, B2, B3 and the reference condition (= Ref). (Abs=Absolute, Rel=Relative).*

When combining glacier and climate scenarios it can be seen that the runoff regime will not change much for scenario C1 (see Figure 4.25a). The only change in runoff, which is expected for C1, is a small absolute and relative increase in runoff in May and September (see Figure 4.25b) that can be explained by increase in snowmelt (May) and glacier melt (September). Absolute and relative increases are also observed for scenarios C2 and C3 with relative increases up to 110% for scenario C3. The difference with absolute/relative increases of scenario C1 is that the relative increases of scenario C2 and C3 will occur in April instead of May. During the summer month's runoff will remain approximately constant for scenario C1 and will decrease for the other scenarios with relative decreases up to 55% in July and August. The combination of decrease in runoff during summer months and increase in runoff during spring period is expected to evolve the existing glacio-nival regime into a moderate nival regime with highest discharges expected in May (see Figure 4.25a).

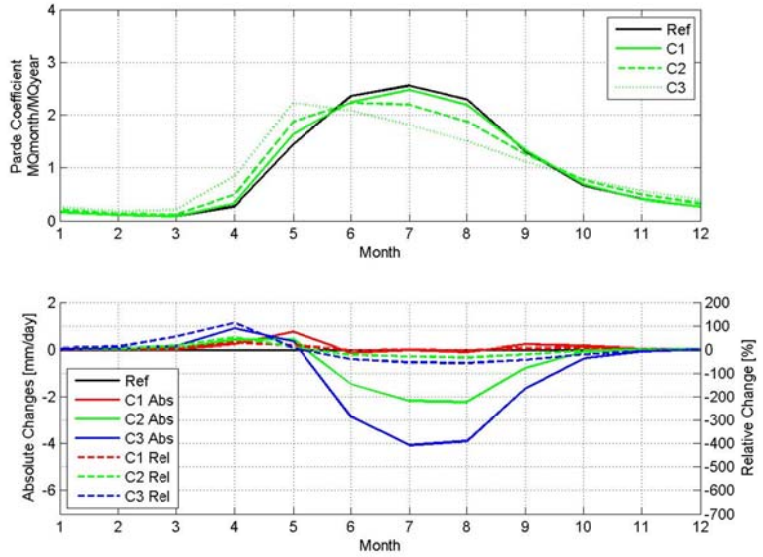

Figure 4.25: *Pardé coefficients of Ötztaler Ache (Brunau) (a), and absolute and relative changes in runoff of Ötztaler Ache relative to the reference condition (b) for scenarios C1, C2, C3 and the reference condition (= Ref). (Abs=Absolute, Rel=Relative).*

From the results of the scenarios with glacier change (Classes A and C) the regime shift, that is expected when glacier area reduction becomes stronger than glacier thickness reduction, can be traced back. When thickness reduction is stronger than area reduction (before ~2040) the results of classes A and C do not show a change in runoff regime. This is different for the period after ~2040, where area reduction becomes stronger, meaning that runoff regimes will shift. This is also what can be observed in the results of classes A and C for the respective time period. This means that the results presented here are in accordance with the results presented in Section 4.3.

4.4.2 Gurgler Ache

In Figure 4.26a the Pardé coefficients are given for the Gurgler Ache (Obergurgl) under assumption of stable climate conditions and changing glacier conditions (Class A). Observing the Pardé coefficients for the reference condition, it can be seen that the runoff regime during reference period is a glacial/ glacio-nival regime, since the Pardé coefficient for July (2.82) is higher than for August (2.56) and the Pardé coefficient for August (2.56) is slightly higher than for June (2.49). The difference is however that small that a glacio-nival regime could be considered to be the regime. For scenarios A1, A2 and A3 the runoff regimes will change in a similar way as the scenarios A1, A2 and A3 of the Ötztaler Ache. This means that for scenario A1 no changes are observed and that for scenarios A2 and A3 the runoff regimes will shift from a glacial/glacio-nival regime to a nivo-glacial regime. The absolute and relative changes for the Gurgler Ache (see Figure 4.26b) are also similar to changes observed for the Ötztaler Ache with no or limited change for scenario A1 and absolute/ relative decrease in runoff during summer months for scenarios A2 and A3. The magnitude of relative decrease is about 30% for scenario A2 and 45% for scenario A3. Additionally, a relative increase in runoff up to 35% is observed for the winter period. A possible explanation for this increase is the decrease in glacial cover leading to a decrease in glacial storage. Since glaciers store large volumes of precipitation during winter period, glaciers ensure low runoff conditions. With decreasing glacial storage it would mean that low runoff conditions could not be ensured any more, leading to an increase in runoff during winter period.

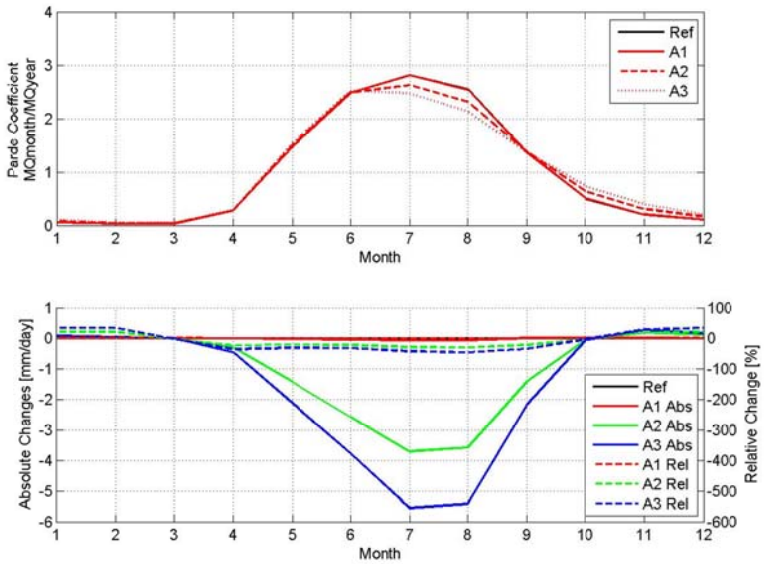

Figure 4.26: *Pardé coefficients of Gurgler Ache (Obergurgl) (a), and absolute and relative changes in runoff of Gurgler Ache relative to the reference condition (b) for scenarios A1, A2, A3 and the reference condition (= Ref). (Abs=Absolute, Rel=Relative).*

In case glacier conditions remain stable and climate conditions will change (Class B) Figure 4.27 shows that also for the Gurgler Ache the runoff regimes will remain unchanged (see Figure 4.27a). However, in terms of absolute and relative changes (Figure 4.27b) there will be an absolute increase for the period February – November, which is higher than the absolute increases for the respective

scenarios of the Ötztaler Ache. The largest relative changes are observed for the same period as the absolute changes with largest relative increases (up to 200%) in March-April. This means that the effect of an earlier onset of snowmelt is noticeable earlier in the catchment of the Gurgler Ache than in the catchment of the Ötztaler Ache where relative increases are largest in April. Next to the relative increases of March-April there is also a relative increase up to 55% expected for October, which can be explained by increase in precipitation projected from the climate scenarios of BOKU (see Section 3.4; Figure 3.5).

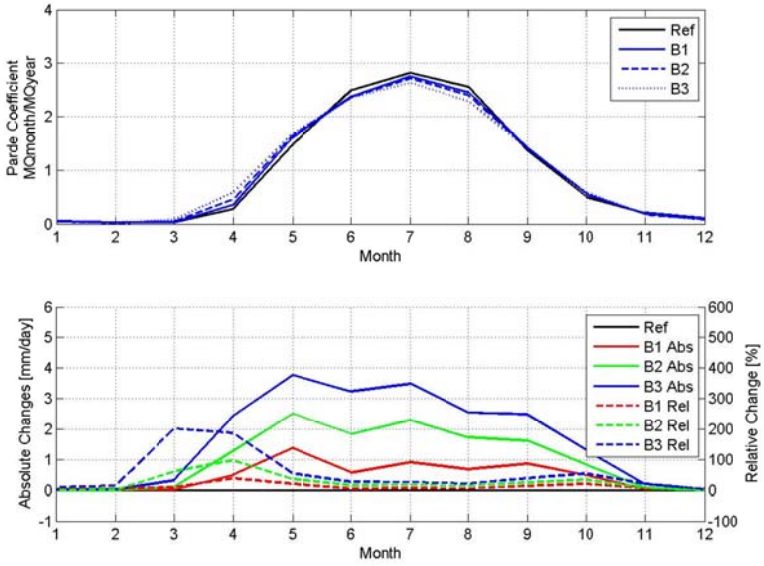

Figure 4.27: *Pardé coefficients of Gurgler Ache (Obergurgl) (a), and absolute and relative changes in runoff of Gurgler Ache relative to the reference condition (b) for scenarios B1, B2, B3 and the reference condition (= Ref). (Abs=Absolute, Rel=Relative).*

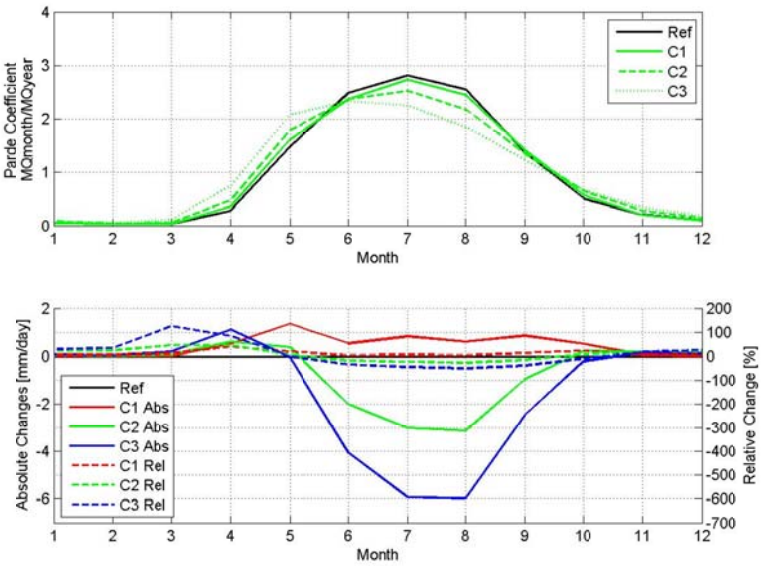

Figure 4.28: *Pardé coefficients of Gurgler Ache (Obergurgl) (a), and absolute and relative changes in runoff of Gurgler Ache relative to the reference condition (b) for scenarios C1, C2, C3 and the reference condition (= Ref). (Abs=Absolute, Rel=Relative).*

In case both glacier and climate conditions will change the runoff regime will shift from a glacio/glacio-nival regime to a nival regime (see Figure 4.28). The absolute changes accompanied with this regime shift will vary from a general increase in runoff for scenario C1 to an increase/ decrease in runoff, for respective spring/summer period, for scenarios C2 and C3. The relative changes will vary from relative increases up to 125% for the spring period, to relative decreases up to

50% for the summer period. The explanation for this pattern is that for scenario C1 the thinning process of glaciers is still dominant above area reduction, leading to an increase in runoff. For scenarios C2 and C3 the area reduction is more dominant than glacier thinning, leading in combination with the earlier onset of snowmelt to a shift in peak discharge from summer period to spring period. This explains why the absolute/ relative changes are negative for summer period and positive for spring period.

4.4.3 Venter Ache

Figure 4.29a shows the Pardé coefficients of the Venter Ache (Vent) for stable climate conditions and changing glacier conditions (Class A). For the reference period Figure 4.29 shows that the runoff regime in the Venter Ache is dominated by a glacial regime with highest Pardé coefficients in July, followed by August and June. In contradiction with the Ötztaler Ache and the Gurgler Ache the regime type will not change with time in the glacier-only scenarios, although for scenario A3 the regime type can be considered to be border case between glacial regime and glacio-nival regime. The reason for this doubt is the same as for the runoff regime of the reference period of the Gurgler Ache. The difference between the Pardé coefficients of June (2.19) and August (2.25) is that small that it is difficult to determine whether the runoff regime a glacial one or a glacio-nival one. The changes in runoff show absolute and relative increases/decreases during the winter period and summer period respectively (see Figure 4.29b). The magnitudes of absolute and relative changes are similar to those of the Gurgler Ache with relative decreases up to 35% for scenario A2 and 50% for scenario A3. The relative increase during the winter period will be up to 55%. The explanation for this increase is the same as for the respective scenarios of the Gurgler Ache. The explanation why this increase is higher than the expected increase in the Gurgler Ache catchment is that (a) the Venter Ache catchment has a higher initial glaciation (32%) than the Gurgler Ache catchment (29%) and (b) the Venter Ache catchment covers a larger area (165 km^2 instead of 72 km^2). These two factors combined are responsible for higher initial glacier storage. For scenario A3 the expectation however is that the glaciation of the Gurgler Ache catchment (9.7%) will remain higher than the glaciation for the Venter Ache (5.2%). This will lead in a relative larger decrease in glacial storage in the Venter Ache catchment, causing the relative increases to be higher than in the Gurgler Ache catchment.

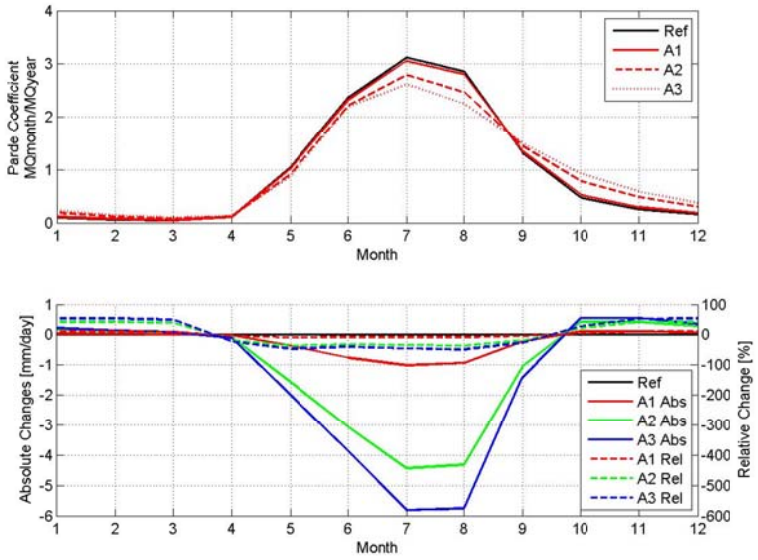

Figure 4.29: *Pardé coefficients of Venter Ache (Vent) (a), and absolute and relative changes in runoff of Venter Ache relative to the reference condition (b) for scenarios A1, A2, A3 and the reference condition (= Ref). (Abs=Absolute, Rel=Relative).*

Figure 4.30 illustrates the runoff regime (Figure 4.30a) and absolute/ relative changes (Figure 4.30b) for stable glacier conditions and changing climate conditions (Class B). Similar to the Ötztaler and Gurgler Ache the runoff regimes will not change under stable glacier conditions. Absolute changes are mainly concentrated in the period March-November and relative changes appear in the same period with the highest relative changes in April, where a relative increase up to 310% is expected. Earlier onset and increase of snowmelt are assumed to be responsible for this increase.

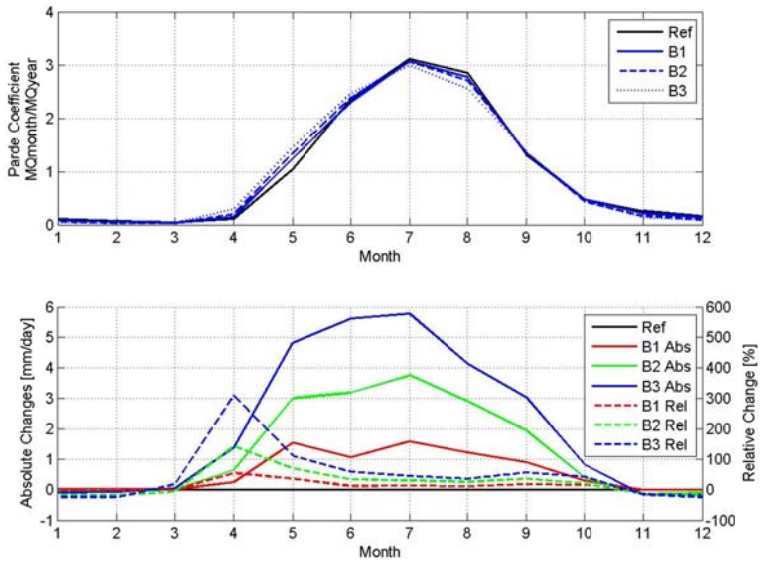

Figure 4.30: *Pardé coefficients of Venter Ache (Vent) (a), and absolute and relative changes in runoff of Venter Ache relative to the reference condition (b) for scenarios B1, B2, B3 and the reference condition (= Ref). (Abs=Absolute, Rel=Relative).*

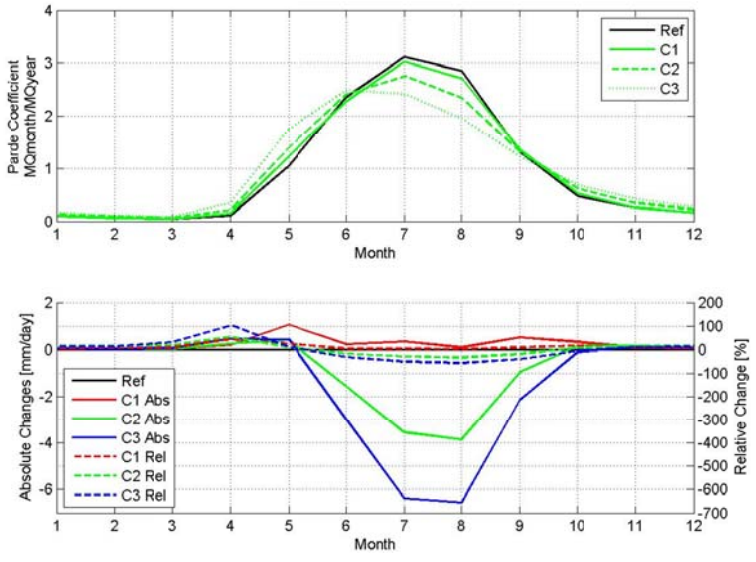

Figure 4.31: *Pardé coefficients of Venter Ache (Vent) (a), and absolute and relative changes in runoff of Venter Ache relative to the reference condition (b) for scenarios C1, C2, C3 and the reference condition (= Ref). (Abs=Absolute, Rel=Relative).*

Combining glacier and climate scenarios indicate that the runoff regime will shift from a glacial regime to a nivo-glacial regime with highest runoff conditions in June (see Figure 4.31a), where snowmelt becomes a more dominated runoff source. The absolute changes accompanied with this regime shift will initially start with an absolute increase for scenario C1 (see Figure 4.31b). The

relative increase for this scenario is limited for the summer period and about 45% in April. Subsequently for scenarios C2 and C3 absolute increases/decreases are projected for April and the period May-October respectively with the largest absolute decreases in July and August. The relative changes vary from up to a 100% increase in April up to a 55% decrease in August. The explanation for these large runoff changes is similar to the explanation for those observed in the Gurgler Ache, which means that initially when the glacier thinning process is more dominated than the area reduction (until ~2040), runoff will increase. When area reduction becomes predominant the runoff is expected to decrease.

4.4.4 Annual Runoff Changes

In Table 4.5 the annual runoff changes, paired with glacial, climate and combined scenarios, are given for each (sub)catchment respectively. Considering glacier change only (Class A), annual runoff will change slightly for scenario A1, but for scenarios A2 and A3 relative decreases up to 35% are projected for the (sub)catchments of the Ötztaler, Gurgler and Venter Ache, which can mainly be explained by the reduction of glacial area. Considering climate change only (Class B), the annual runoff of Brunau, Obergurgl and Vent will increase up to 51% towards the end of the 21st century. The increase and earlier onset of snowmelt during the spring period is considered to be the main cause of this runoff increase. For combined glacier and climate scenarios relative increases up to 9% are projected for scenario C1, while for scenarios C2 and C3 relative decreases up to 35% are projected. The main reason for this difference is the same as for the observed differences between scenario C1 and scenarios C2 and C3 in Obergurgl and Vent. This means that initially when glacier thinning is the dominant process runoff will increase, but when area reduction becomes the dominant process later on runoff will decrease.

Table 4.5: *Annual relative runoff changes for glacier, climate and combined glacier and climate scenarios. The runoff changes were calculated relative to the mean annual runoff of the reference condition.*

Scenarios	Annual Relative Runoff Changes (%)	Annual Relative Runoff Changes (%)	Annual Relative Runoff Changes (%)
Glacier Change	**Ötztaler Ache (Brunau)**	**Gurgler Ache (Obergurgl)**	**Venter Ache (Vent)**
A1	-3 %	-	-6%
A2	-17 %	-23 %	-26 %
A3	-23 %	-34 %	-35 %
Climate Change			
B1	+7 %	+10 %	+14 %
B2	+14 %	+22 %	+31 %
B3	+23 %	+35 %	+51 %
Combined Climate and Glacier Change			
C1	+3 %	+9 %	+6 %
C2	-16 %	-13 %	-18 %
C3	-30 %	-30 %	-35 %

4.4.5 Summary

Future runoff simulations, considering glacier scenarios only, show that highest runoff conditions will shift from July to June in the (sub) catchments of the Ötztaler and Gurgler Ache, meaning that the glacio-nival and glacial/glacio-nival regimes of respective catchments will shift to a nivo-glacial regime. For the Venter Ache, where a glacial/glacio-nival regime is dominant, the expectation is that runoff regime will not change at all. Under climate scenarios only, runoff regimes will not change for all catchments. For combined glacier and climate scenarios the glacio-nival regime of the Ötztaler Ache will shift to a moderate nival regime with highest runoff conditions in May. In the catchments of the Gurgler and Venter Ache the expectation is that the glacial/glacio-nival regime will shift to nival and nivo-glacial regimes in respective catchments with highest runoff conditions in June. The

maximum relative runoff changes, which are paired with glacial, climate and combined far future scenarios, are summarized for all three (sub) catchments in Table 4.6.

Table 4.6: *Maximum relative runoff changes and respective periods for glacier, climate and combined far future scenarios.*

Scenarios	Relative Changes (Period)		Relative Changes (Period)		Relative Changes (Period)	
Glacier A3	**Ötztaler Ache (Brunau)**		**Gurgler Ache (Obergurgl)**		**Venter Ache (Vent)**	
Rel. Increase	15 %	(Nov – Feb)	35 %	(Dec – Feb)	55 %	(Jan – Feb)
Rel. Decrease	40 %	(Aug)	45 %	(Aug)	50 %	(Aug)
Climate B3						
Rel. Increase	150 %	(Apr)	200 %	(Mar)	310 %	(Apr)
Rel. Decrease	10 %	(Dec)	-		25 %	(Dec-Feb)
Combined C3						
Rel. Increase	110 %	(Apr)	125 %	(Mar)	100 %	(Apr)
Rel. Decrease	55 %	(Aug)	50 %	(Aug)	55 %	(Aug)

Relative runoff changes, for glacier scenarios only, can mainly be explained by loss of glacial storage causing runoff to increase relatively during winter, and reduction of glacial area causing runoff to decrease relatively during summer period since less melt water is available. For climate scenarios only, relative changes are mainly caused by earlier onset of snowmelt during spring. Combining earlier onset of snowmelt and reduction of glacial areas generally explain the relative changes of combined glacier and climate scenarios.

4.5 Peak & Low Flow Statistics - Results

In this section the results in relation with peak and low flow statistics will be presented for each (sub) catchment separately.

4.5.1 Ötztaler Ache

Peak Flow

In Figure 4.32 four rose plots are given, representing the reference condition and the scenarios A3, B3 and C3 of gauging station Brunau. It shows that for the reference condition over the period 1987-2012 peak discharges were most common in July, followed by June and August. In the far future this is projected to remain the same for scenario B3, although peak discharges will be more concentrated in July and will be less concentrated in August compared to the reference condition. For scenarios A3 and C3 the peak discharges shift from July to June for A3 and from July to May for C3.

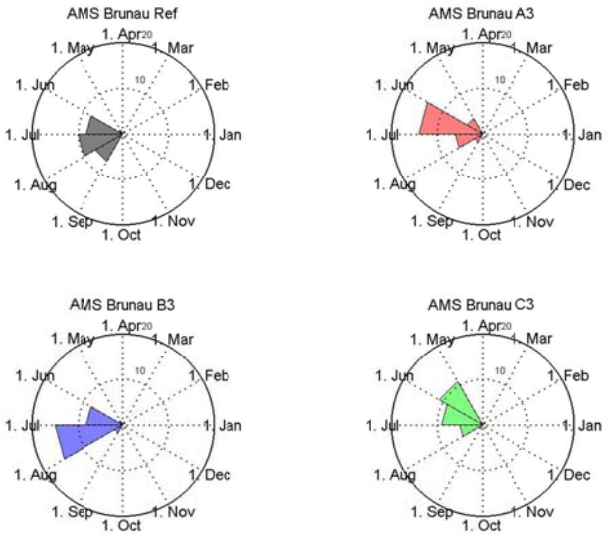

Figure 4.32: *Rose Plots Gauging Station Brunau for reference period and scenarios A3, B3 and C3.*

In Figure 4.33 four rose plots are given for the reference condition and scenarios C1, C2 and C3 of gauging station Brunau. For scenario C1 the peak discharge frequencies will approximately remain the same. The only difference is that the peak discharge frequency is projected to increase for June and May. For C2 and C3 the frequency remains constant for June, increases for May and decreases for July, which eventually will result in peak discharge to become most frequent in May.

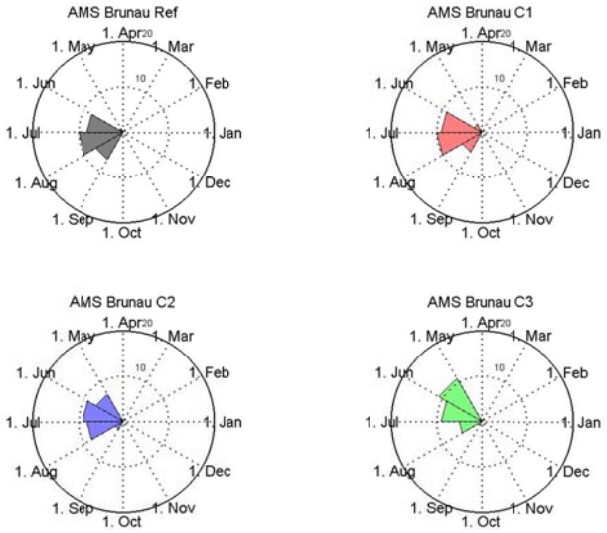

Figure 4.33: *Rose Plots Gauging Station Brunau for reference period and scenarios C1, C2 and C3.*

Low Flow

In Figure 4.34 the Flow Duration Curves (FDCs) of gauging station Brunau are given for the observed discharge and the simulated discharge of the reference condition and scenarios A3, B3 and C3 with a focus on June-August. For observed discharges the Q_{70} (magenta) and Q_{95} (cyan) are ~6 mm d^{-1} and ~3.6 mm d^{-1}. For scenario B3 low flows will become less frequent in summer since both Q_{70} and Q_{95} are expected to shift to higher percentiles respectively. For scenario A3 and C3 low flow conditions will become more frequent into far future. For these scenarios the Q_{70}/ Q_{95} percentiles are expected to shift to lower percentiles.

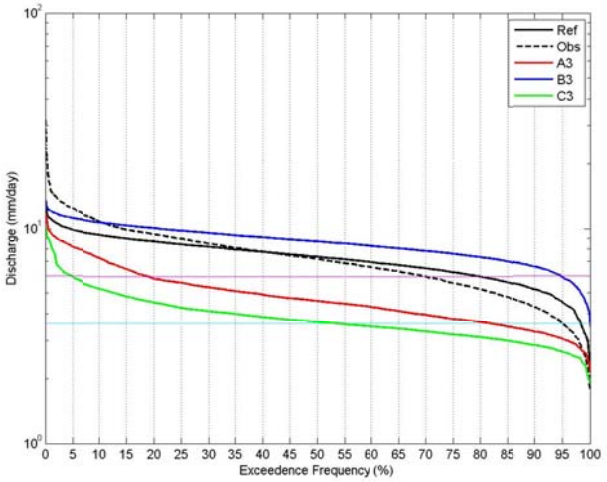

Figure 4.34: *Flow Duration Curves Gauging Station Brunau for reference period and scenarios A3, B3 and C3 with a focus on June-August.*

In Figure 4.35 the FDCs of gauging station Brunau are given for the observed discharge and the simulated discharge of the reference condition and scenarios C1, C2 and C3 with a focus on June-August. It shows that low flow conditions will become less frequent for scenario C1 using both the Q_{70} and Q_{95} as reference level. For scenario C2 low flow conditions will become more frequent using

the Q_{70} as reference level and will remain constant using Q_{95} as reference level. For scenario C3 both the Q_{70} and Q_{95} low flow conditions will become more frequent.

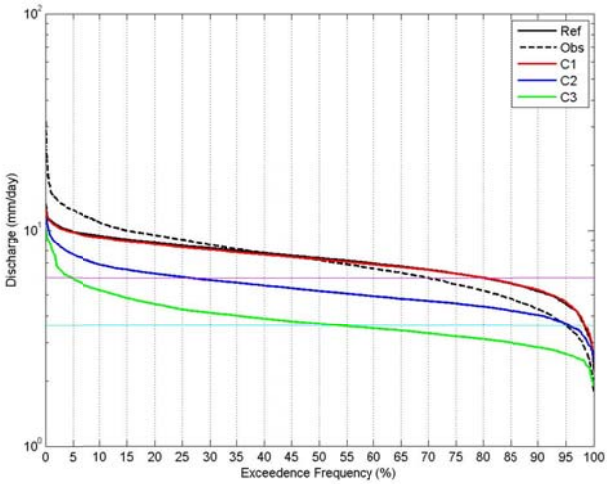

Figure 4.35: *Flow Duration Curves Gauging Station Brunau for reference period and scenarios C1, C2 and C3 with a focus on June-August.*

4.5.2 Gurgler Ache

Peak Flow

In Figure 4.36 four rose plots are given, showing the peak flow statistics of gauging station Obergurgl, for the reference condition and scenarios A3, B3 and C3. For the reference condition peak discharges were most frequent in July followed by August and June. For scenario B3 the frequencies are not expected to change much. The frequency for July and August are a bit lower and a bit higher for June. More changes are however expected for scenarios A3 and C3 where the highest frequencies will shift from July to June for both of the scenarios.

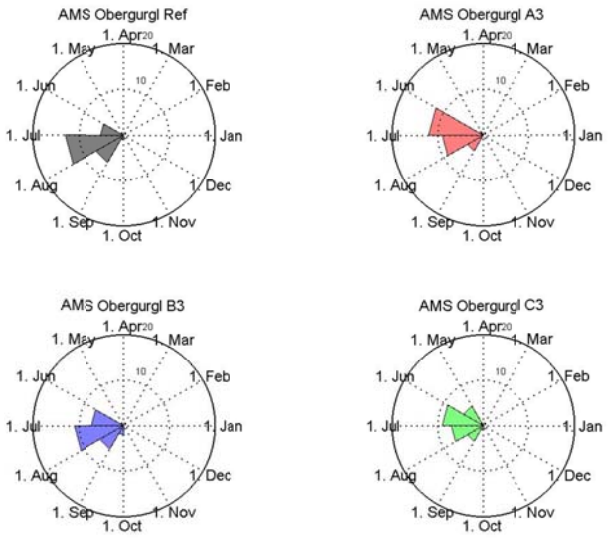

Figure 4.36: *Rose Plots Gauging Station Obergurgl for reference period and scenarios A3, B3 and C3.*

In Figure 4.37 four rose plots are given for the reference condition and scenarios C1, C2 and C3 of gauging station Obergurgl. For scenarios C1 frequencies will be slightly lower in July and higher in September. For other months frequencies will remain approximately constant. Relative to scenario C1, frequencies are expected to increase in June and to decrease in August and September for scenario C2. Relative to scenario C2, the frequencies are expected to remain constant in June and

August, to decrease in July and September and to increase in May. Eventually the result is that highest frequencies shift from July to June.

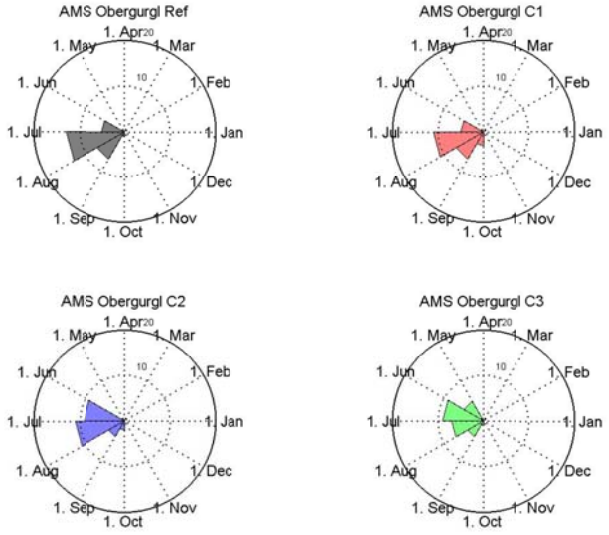

Figure 4.37: *Rose Plots Gauging Station Obergurgl for reference period and scenarios C1, C2 and C3.*

Low Flow

In Figure 4.38 the FDCs of gauging station Obergurgl are given for the observed discharge and the simulated discharge of the reference condition and scenarios A3, B3 and C3 with a focus on June-August. The Q_{70} and Q_{95} of the observed discharge are ~10 mm d^{-1} and ~4.6 mm d^{-1}. Using Q_{70} as reference level low flow conditions will become less frequent for scenario B3 and will become more frequent for scenarios A3 and C3. Using Q_{95} low flow conditions will not appear any more for scenario B3 where for scenarios A3 and C3 low flow conditions will become less frequent.

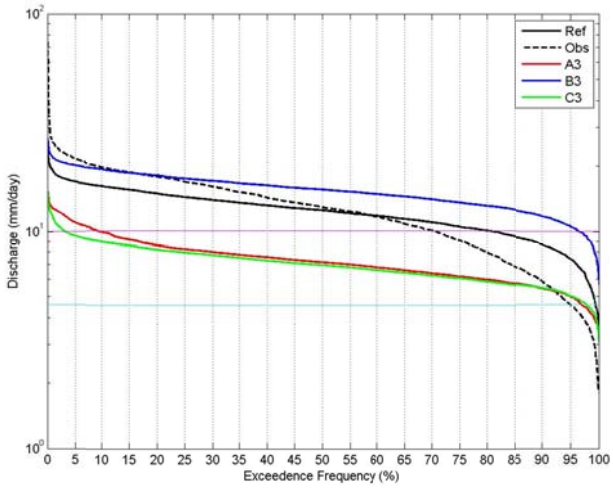

Figure 4.38: *Flow Duration Curves Gauging Station Obergurgl for reference period and scenarios A3, B3 and C3 with a focus on June-August.*

In Figure 4.39 the FDCs of gauging station Obergurgl are given for the observed discharge and the simulated discharge of the reference condition and scenarios C1, C2 and C3 with a focus on June-August. Using Q_{70}, as reference level, low flow conditions will become less frequent for scenario C1 and more frequent for scenarios C2 and C3. Using Q_{95}, as reference level, low flow conditions will become less frequent for scenarios C1, C2 and C3.

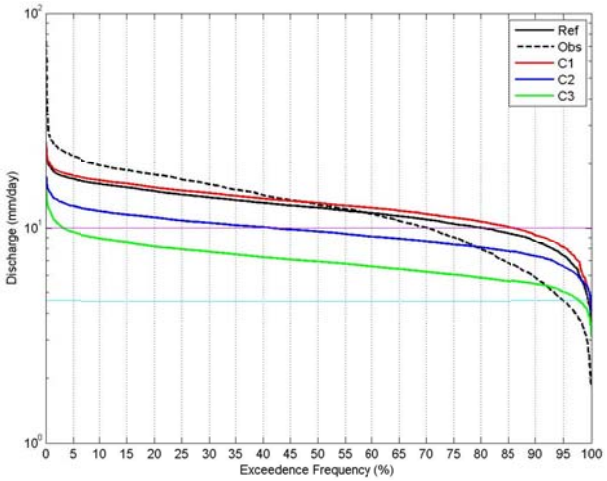

Figure 4.39: *Flow Duration Curves Gauging Station Obergurgl for reference period and scenarios C1, C2 and C3 with a focus on June-August.*

4.5.3 Venter Ache

Peak Flow

In Figure 4.40 four rose plots are given for the reference condition and the scenarios A3, B3 and C3 for gauging station Vent. For scenario B3 the frequency of July will increase relative to the reference condition, while the frequency of August is expected to decrease. For scenario A3 the frequencies remain constant for July, decreases for August and increases for June when compared to the reference condition. For scenario C3 the increase for June is stronger. For July and August frequencies decrease, while they increase in May.

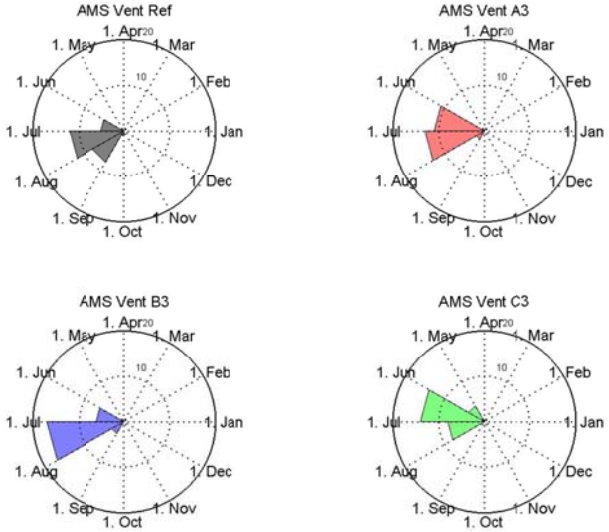

Figure 4.40: *Rose Plots Gauging Station Vent for reference period and scenarios A3, B3 and C3.*

In Figure 4.41 four rose plots are given for the reference condition and the scenarios C1, C2 and C3 for gauging station Vent. Scenario C1 shows an increase in peak discharge frequency for July, and a decrease for June and August when compared to the reference condition. For scenario C2 the frequency of July remains constant relative to scenario C1, while the frequency of August decreases and the frequency of June increases. For scenario C3 frequencies will mainly increase in May and July and decrease in July.

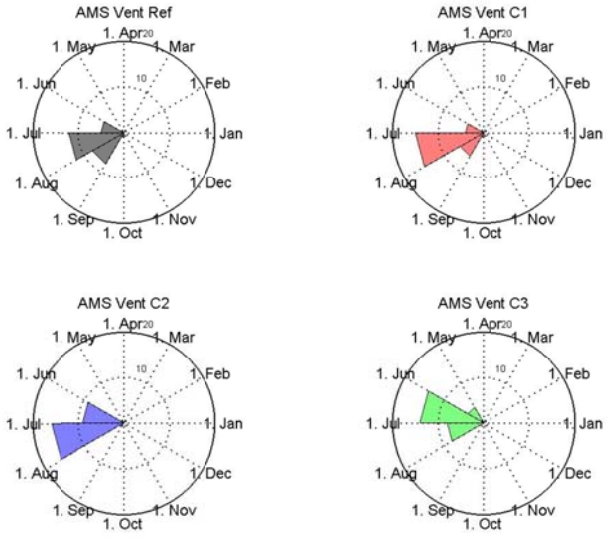

Figure 4.41: *Rose Plots Gauging Station Vent for reference period and scenarios C1, C2 and C3.*

Low Flow

In Figure 4.42 the FDCs of gauging station Vent are given for the observed discharge and the simulated discharge of the reference condition and scenarios A3, B3 and C3 with a focus on June-August. The Q_{70} and Q_{95} of the observed discharge are respectively equal to ~8.3 mm d^{-1} and ~3.5 mm d^{-1}. It is shown that low flow conditions will become less frequent for scenario B3 and will become more frequent for scenarios A3 and C3, using Q_{70} as reference level. Using Q_{95} as reference level results in no significant low flow conditions for scenario B3 while low flow conditions will become less frequent for scenarios A3 and C3.

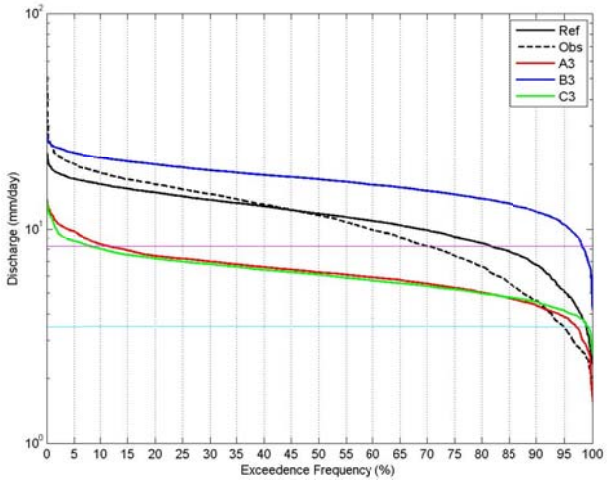

Figure 4.42: *Flow Duration Curves Gauging Station Vent for reference period and scenarios A3, B3 and C3 with a focus on June-August.*

Figure 4.43 shows the Flow Duration Curves (FDCs) of gauging station Vent for the observed discharge and the simulated discharge of the reference condition and scenarios C1, C2 and C3 with a focus on June-August. It shows that low flow conditions will become less frequent for scenario C1 and will become more frequent for scenarios C2 and C3, using Q_{70} as reference level. Using $Q_{95,}$ as reference level, low flow conditions will become less frequent for scenarios C1, C2 and C3.

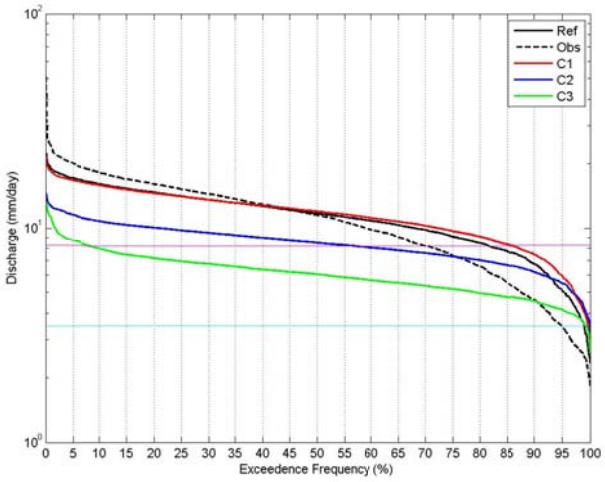

Figure 4.43: *Flow Duration Curves Gauging Station Vent for reference period and scenarios C1, C2 and C3 with a focus on June-August.*

4.5.4 Summary

In Table 4.7 peak flow statistics are summarized for the Ötztaler, Gurgler and Venter Ache catchment. For the reference period and the scenario periods the ranking of months is given associated with highest peak discharge frequencies. When change does not occur in the sequence of months relative to the reference period, but in the magnitude of frequencies, an arrow-like sign is used to clearify whether increase or decrease in frequency has occurred.

Table 4.7: *Ranking of months considering Peak Discharge Frequencies for Brunau, Obergurgl and Vent (↑= more frequent, - = constant and ↓= less frequent).*

Scenario	Ötztaler Ache (Brunau)				Gurgler Ache (Obergurgl)				Venter Ache (Vent)		
Reference	*7*	*6*	*8*		***7***	***8***	***6***		*7*	*8*	*6*
Glacier A3	*6*	*7*	*5*	*8*	***6***	***7***	***8***		*7* ↑	*6*	*8*
Climate B3	*7* ↑	*6* -	*8* ↓		***7*** ↓	***6***	***8***	***9***	*7* ↑	*6*	*8*
Comb C1	*7* -	*6* -	*8* ↓	*5*	***7*** ↓	***8*** -	***6*** -	***9***	*7* ↑	*8* ↓	*6* ↓
Comb C2	*6*	*7*	*5*	*8*	***7*** ↓	***6***	***8***	***9***	*7* ↑	*6*	
Comb C3	*5*	*6*	*7*		***6***	***7***	***5***	***8***	*6*	*7*	*5*

Based on this Table it can be concluded that for the reference period peak discharge is most frequent in July, followed by June and August for present glacio-nival regimes, and by August and June for present glacial/glacio-nival regimes. In the far future the highest frequencies will generally shift from July to June assuming glacier scenarios only. Considering climate scenarios only, peak discharge frequencies will remain highest in July and for combined scenarios the expectation is that highest frequencies will shift from July to May for present glacio-nival regimes or from July to June for present glacial/glacio-nival regimes.

In Table 4.8 low flow statistics are summarized for the Ötztaler, Gurgler and Venter Ache catchment. For Q_{70} and Q_{95} is indicated whether the low flow during summer (June-August) is expected to occur more frequent or less frequent compared to preceding different scenario periods.

Table 4.8: *Change in Low Flow Frequency for Brunau, Vent and Obergurgl with focus on June-August (↑= more frequent, - = constant and ↓= less frequent).*

Scenario	Ötztaler Ache (Brunau)		Gurgler Ache (Obergurgl)		Venter Ache (Vent)	
	Q_{70}	Q_{95}	Q_{70}	Q_{95}	Q_{70}	Q_{95}
Glacier A3	↑	↑	↑	↓	↑	↓
Climate B3	↓	↓	↓	↓	↓	↓
Comb C1	↓	↓	↓	↓	↓	↓
Comb C2	↑	-	↑	↓	↑	↓
Comb C3	↑	↑	↑	↓	↑	↓

Based on this Table it can be concluded that low flow conditions (using the Q_{70} low flow index) will appear more frequently in the Ötztaler, Gurgler and Venter Ache catchments under glacier-only scenarios and combined scenarios for the mid-future and far future. Under climate-only scenarios and combined scenarios low flow conditions will appear less frequent. Using the Q_{95} low flow index low flow conditions will become less frequent for all scenarios in the Venter and Gurgler Ache catchments. In the Ötztaler Ache low flow conditions are expected to appear less frequent under climate-only scenarios and combined scenarios for the near future, remain constant for the combined scenarios for mid future, and more frequent considering glacier-only scenarios and combined scenarios for the far future.

5. Discussion

In this section the outcomes of HBV Light and therewith-related aspects will be discussed. In order to create some structure in this section the following set-up is maintained:

- Discussion about the reliability of HBV Light outcomes.
- Discussion about other factors that may have influenced outcomes.

5.1 Reliability of HBV Light Outcomes

To test the reliability of HBV Light outcomes, they are compared with similar existing studies, which have been implemented in the Ötztaler Alps and other regions of the world. For instance in the Ötztaler Alps a similar study was performed by Helfricht et al. (In Press) using the semi-distributed conceptual model HQSIM. The study areas and scenarios used for HQSIM were the same as the ones used for HBV Light. In Figure 5.1a, 5.1b and 5.1c boxplots are given for projected absolute changes in runoff for the Ötztaler, Gurgler and Venter Ache catchments, which are derived from the combined climate and glacier scenario outcomes of HBV Light and HQSIM. In order to compose these boxplots the mean of absolute runoff changes were determined for each month of the period 2070-2099 (far future). Generally the outcomes of HBV Light show a slightly larger decrease in runoff than the outcomes of HQSIM, especially during late spring and early summer. In the Gurgler and Venter Ache catchments the outcomes of HQSIM show a larger decrease during late summer and early autumn. The ranges of absolute runoff change of HBV Light and HQSIM are similar in the Ötztaler Ache catchment. In the Gurgler and Venter Ache catchments the outcome ranges for HQSIM are larger than the ranges for HBV Light, mainly during summer. This implicates that HQSIM predicts greater variability with respect to discharge than HBV Light in catchments with higher glaciations, when glacier change is expected to have its greatest impact on runoff characteristics.

Huss et al. (2014) performed a study in the catchment of the Findelengletscher (Swiss Alps) by assessing the uncertainties of 21st century runoff in glacierized catchments. In this study several experiments were conducted including experiments with climate scenarios and changes in glacial evolution. The outcomes of this study indicated inter alia that for August runoff would change in the range of -89% and + 22% for 2075. The outcomes of HBV Light are in this range with a projected 40-55% runoff decrease in August for the period 2070-2099.

Likewise as in the European Alps, also similar studies have been implemented in the Central Asian mountain ranges. Hagg et al. (2007) modelled the hydrological response to climate change in the glacierized catchments (7 – 51% glaciation) of the Pamir (Tajikistan) and the Tien Shan (Kyrgyzstan) using two different models. Several scenarios were used including scenarios incorporating 50% glacier loss and 2x CO_2. The outcomes of this study indicate that there is generally a shift in high runoff conditions from mid-late summer to late spring/ early summer under changing climate and changing glacier conditions. Although the scenarios are different, the outcomes of HBV Light still have agreements with the outcomes of Hagg et al. (2007). Another similar study performed in the Central-Asian mountain ranges, is that of Immerzeel et al. (2013) that has been conducted in the Karakoram and Himalayan mountain ranges. In this study two different scenarios were studied, including different possible magnitudes of radiative forcing for 2100 and using an ensemble of GCMs abstracted from CMIP5 (Climate Model Intercomparison Project 5). These scenarios were used for a glaciohydrological model to simulate runoff. The outcomes of this study indicate an increase in total runoff until 2100, which is contradictive with the outcomes of HBV Light in relation with combined glacier and climate scenarios. The reason for this contradiction is that the expected glacier retreat in the Himalayas and Karakoram (33-54% in 2100) is less extreme than the expected glacier retreat in the Ötztaler Alps (79-94% in ~2100). Additionally increasing precipitation toward 2100 will cause more snow accumulation in the Himalayan and Karakoram mountain ranges, resulting in combination with smaller glacial retreat in increasing total runoff. Results of Immerzeel et al. (2013) do agree with this study with regard to runoff increases during spring. In the study of Immerzeel et al. (2013) increases between 126% and 300% are expected in May for the Karakoram mountain

range. The outcomes of HBV Light indicate an increase between 100% and 300% for the period March- May, considering climate scenarios and combined glacier and climate scenarios.

With respect to changes in peak and low flow statistics, the outcomes of this study are comparable with the outcomes of other studies. For instance, Helfricht et al. (In Press) predicted similar changes in peak discharge frequency for 2070-2099 with shifts in highest peak discharge frequency from August to May-July depending on type of scenario (glacier or combined) used and the catchment (Ötztaler Ache, Venter Ache and Gurgler Ache) modelled. The projected increase in low flow frequency with time (under climate and glacier change) is confirmed by inter alia Schädler and Weingartner (2010) who predicted an increase in dry periods during summer of 36% for the Alps in 2050. Unknown however is on which kind of low- flow index this percentage has been based. As shown in this study (Table 4.7), whether Q_{70} or Q_{95} is used as low flow index can yield different results.

In conclusion, comparing the outcomes of HBV Light with other studies shows that their outcomes are often in agreement, although care must be taken due to differences in climate and other local characteristics (e.g. topography). Moreover there are a lot of factors, which possibly have influenced the outcomes of HBV Light and have increased uncertainty concerning these outcomes. Which factors may be responsible for these uncertainties will be discussed in Section 5.2.

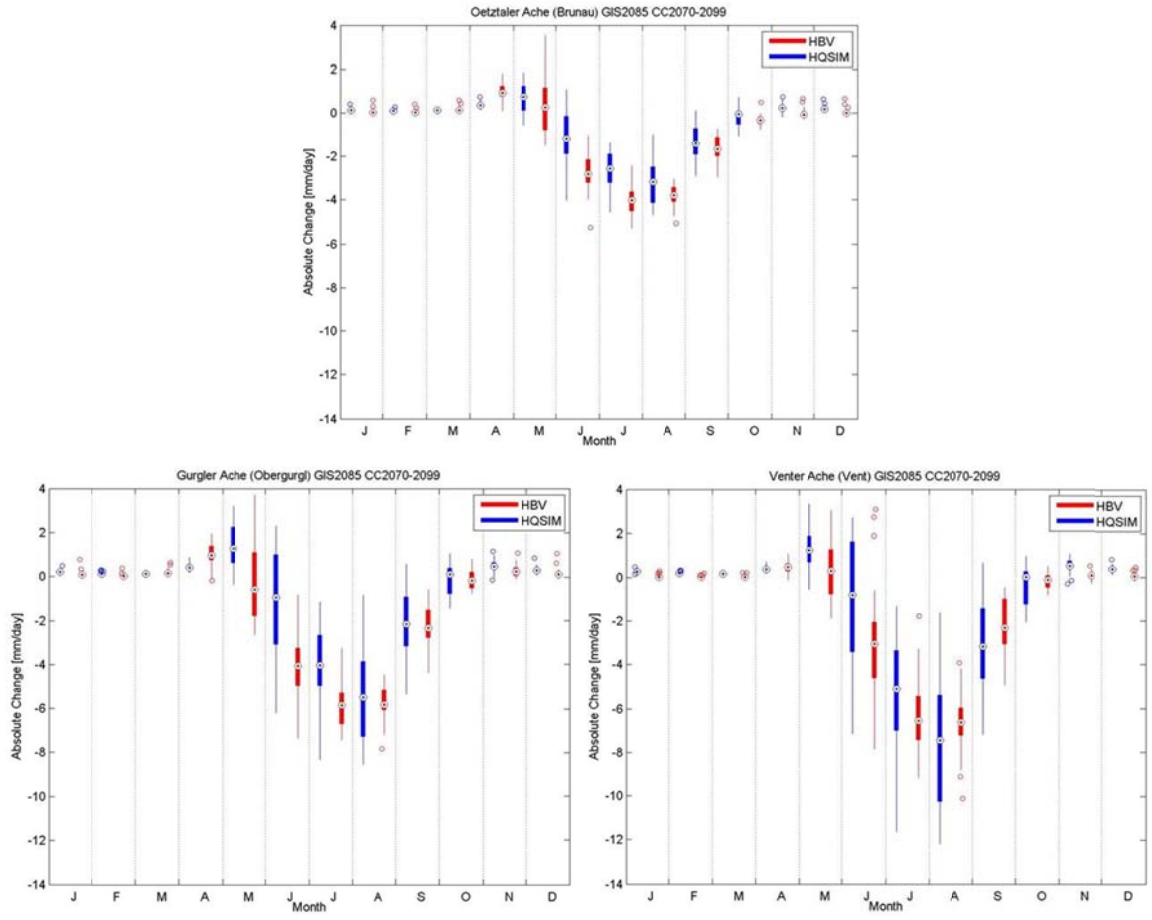

Figure 5.1: *Boxplots for projected absolute changes in runoff for the (a) Ötztaler Ache (Brunau), (b) Gurgler Ache (Obergurgl) and (c) Venter Ache (Vent), derived from the combined glacier and climate scenario outcomes of HBV Light and HQSIM. The boxplots were composed by determination of the mean of absolute runoff changes for each month of the period 2070-2099 (far future). The red boxplots represents HBV Light projected absolute changes; the blue boxplots represent the HQSIM projected absolute changes. The boxes represent the interquartile range; the central mark inside the boxes represents the median; the whiskers represent the range between the minimum value (Q25-1.5*(Q75-Q25)) and Q25 (lower whisker) and the range between Q75 and the maximum value (Q75+1.5*(Q75-Q25)) (upper whisker) and the empty dots represent the outliers.*

5.2 Factors influencing HBV Light Outcomes

5.2.1 Input Data

In order to calibrate HBV Light daily temperature, daily precipitation, daily-observed discharge and potential evapotranspiration were required as input data. Paired with these input data, especially for daily precipitation data, there were a lot of uncertainties, which have possibly exerted influence on the output of HBV Light.

For daily temperature data these uncertainties can mainly be the result of measurement errors and lack of data, something what can be a problem for the implementation of linear regression, especially in the 80s. In Table 5.1 the number of stations available for linear regression (see Ch. 3.2) is given for the period 1986-2012. At the end of 1986 for instance, only 5 stations were available for the western part of Tyrol (exact locations stations, see Appendix II). Although these stations were available, it does not guarantee the completeness and quality of the data sets. Often data gaps appear and data sets are exposed to measurement errors leading to an uncertain course of temperature values and gradients. When the number of stations increases possible measurement errors or data gaps become less influential, meaning that the course of temperature values and gradients may become less uncertain.

Table 5.1: *Number of Precipitation Gauging and Temperature Stations available for 1986-2012.*

Year	Temperature	Precipitation
1986	5	3
1990	14	3
1995	18	6
2000	28	9
2005	34	13
2010	51	16
2012	59	18

Within case of daily precipitation data, uncertainties can be the result of missing data, especially in the 80s and the 90s. Since precipitation has a more heterogeneous behaviour than temperature (due to inter alia the occurrence of convective precipitation events) the use of precipitation data is limited to meteorological stations (if present) located in the study catchments. This limitation reduces the amount of meteorological stations that can be used for IDW (see Ch. 3.2), which can especially be a problem in the 80s and the 90s. In 1986 and 1990 there were for instance only 3 stations available from which 2 stations were located in the northern part of the Ötztaler Ache catchment and 1 was located in the central part (exact locations, see Appendix III). For the Gurgler and Venter Ache there were no stations available at the time. This means that especially for the catchments of the Gurgler and Venter Ache the interpolated precipitation values are more uncertain than the interpolated values in other parts of the Ötztaler Ache catchment. This may explain why the model performance during first validation period, in terms of mean difference (see Section 4.2), is better for the Ötztaler Ache than for the Venter Ache. After 1990 the number of stations available increased from 3 in 1990 to 18 in 2012 and also in the catchments of the Venter and Gurgler Ache stations became available. Thus, the uncertainty of interpolated precipitation values reduces from 1990 on, which may explain why the model performance (in terms of NSE) for all three catchments is better for the second validation period than for the first validation period. The fact that stations also have become available in the catchment of the Venter Ache may also explain why the model performance (in terms of mean difference) has become similar to the model performance of the Ötztaler Ache catchment. For the Gurgler Ache, the model performance (in terms of mean difference) is worse for the second validation period than for the first period. This has possibly to do with the size of the catchment causing the catchment to react differently to e.g. meteorological changes that occur with time.

For daily discharge values uncertainties may be the result of missing data or measurement errors. For instance at the gauging station of Vent observed discharge data is missing from 2003 till 2006, which makes this period unable to use for calibration and validation. Likewise measurement errors can be made, resulting in under- or overestimation of observed discharge and subsequently also will have effect on simulated discharge.

Since potential evapotranspiration is estimated with the "Hamon" method for the entire Ötztaler Ache catchment and therefore is dependent on daily temperature and daily length the uncertainties can mainly be the result of measurement errors and data gaps in daily temperature series, especially when these errors and gaps cover large ranges of temperature series. This can especially be the case in the 80s. Uncertainties can also be the result of the missing link with wind speed, radiation and relative humidity. Since potential evapotranspiration is estimated by using only daily temperature and daily length, factors such as wind speed, radiation and relative humidity are not incorporated. This means that potential evapotranspiration can be underestimated on windy days, i.e. because wind is responsible for the removal of water vapour and therefore prevent air to become saturated, which means that on windy days the evapotranspiration rate can be higher (Allen et al., 1998). On cloudy and humid days potential evapotranspiration can be overestimated. Cloudy conditions mean that solar radiation is adsorbed and reflected partly by clouds, indicating that less radiation is available for evapotranspiration. Subsequently potential evapotranspiration is lower than it would be under clear-sky conditions. Humid conditions mean that air is filled with higher amounts of water vapour than it would be under dry conditions. Subsequently air can be saturated faster under humid conditions, reducing the rate of evapotranspiration (Allen et al., 1998).

5.2.2 Climate and Glacier Scenarios

In order to investigate the hydrological response of the Ötztaler, Venter and Gurgler Ache catchments to future changes in climate and glaciers, climate and glacier scenarios were used for runoff simulations in HBV Light.

The climate scenarios used for this study are developed by using a 'delta change approach' on daily basis in which climate projections of absolute temperature and relative precipitation are used. The modelled absolute temperature changes are quite similar to those of other studies. Schädler and Weingartner (2010) reported temperature increases for northern Switzerland of 1.8 °C and 2.7 °C until 2050 for the winter and summer respectively. The absolute temperature changes used for this study show slightly lower temperature increases of 1.7 °C and 2.3 °C until 2055 (2040-2069) for the winter and summer respectively. Larger differences can be observed between the temperature changes of this study and a study conducted by ETH Zürich and MeteoSwiss where temperature increases were reported for northeast Switzerland of 2.3 °C, 2 °C, 2.6 °C and 2.2 °C until 2060 for winter, spring, summer and autumn respectively (according to SRES A1B; Alpenzeller et al., 2011). This study shows generally lower temperature increases (1.9 °C, 1.4 °C, 2.8 °C and 1.9 °C for the winter, spring, summer and autumn of 2055 respectively) with exception of the summer. The differences between these values are caused by different model approaches since ETH Zürich applied 14 different RCMs derived from the ENSEMBLES project where alpS GmbH and BOKU only used 3 of them.

The modelled relative precipitation changes differ from other studies, especially for the high precipitation increases in autumn. The expected precipitation increases and decreases in winter and summer respectively are in agreement with most studies. Precipitation increases and decreases during winter and summer respectively have been reported by inter alia Heinrich and Gobiet (2011) and Schädler and Weingartner (2010). Heinrich and Gobiet (2011) reported for inter alia Tyrol precipitation increases/decreases of ~4%/ ~7% for the winter/summer of 2035 (2021-2050), based on an ensemble of 22 GCMs, where Schädler and Weingartner (2010) reported precipitation increases/decreases, at the northern side of the Alps, of 8%/ 17% for the winter/summer of 2050. For autumn however the high precipitation increases are more uncertain, i.e. because of the large spread in results between studies. Alpenzeller et al. (2011) reported for instance much smaller

precipitation increases for autumn (0.9 % in northeast Switzerland, for 2060, according to SRES A1B), but also reported precipitation decreases in other regions of Switzerland. Heinrich and Gobiet (2011) reported median precipitation increases of ~3% for 2035, but with outliers to ~17%, which is still lower than the maximum mean precipitation increase shown in this study (~27% in October 2025). The high precipitation increases of the autumn result subsequently in higher uncertainty concerning the runoff changes in the respective period, especially in the Gurgler Ache under the climate-only scenarios (see Section 4.4.2, Figure 4.21).

Other uncertainties in relation with climate scenarios that could have influence on the outcomes of HBV Light are uncertainties in relation with precipitation input data, which are used for the 'delta change approach' to construct daily precipitation data sets for near future, mid future and far future, and uncertainties in relation with downscaling, accuracy and resolution of GCM and RCM output.

The glacier scenarios used for this study are extracted from a model (Helfricht 2013), which is able to derive future ice-thickness, glacial area and volume distributions as a result of climate change. The expected glacier area loss between 79% and 94% for ~2100 are similar to the reported glacier losses of other studies in the Alps. Huss et al. (2014) reported a loss between 63% and 100% for 2100 based on several conducted experiments. Linsbauer et al. (2013) reported losses between 55% and 95% for 2100 based on three different methodological approaches conducted in the Swiss Alps. Although the expected glacier area losses are similar to reported glacier area losses the glacial evolution will remain uncertain. The disadvantage of the model approach, used in this study, is that the approach is very hypothetical. In the model temperature and precipitation data are not included, i.e. the model lacks the possibility to describe glacial accumulation and ablation. Therefore an important aspect is missing in modelling glacial evolution. Furthermore aspects such as glacial movement, glacial energy balance (i.a. albedo) and snow dynamics are missing.

5.2.3 HBV Light Model

In order to model future runoff the newest version of the semi-distributed conceptual model HBV Light was used. The newest version of HBV Light can be considered to be suitable for model exercises in glaciated catchments since this version includes a more improved glacier routine than the previous versions. Despite improvements in the newest version there are still restrictions or inconsistencies.

The first restriction is the missing link with vegetation dynamics. In this study the assumption was made that if glacial cover would disappear the respective vegetation zone would change to a bare vegetated zone. With increasing temperature it is likely that e.g. tree line will shift to higher elevation zones meaning that the vegetated and bare vegetated zones actually should have been larger and smaller respectively. This brings us to the second restriction of the model, which is the limited amount of vegetation zones. In HBV Light only 3 vegetation zones can be used, but in reality there are at least 4 significant vegetation zones, which are glaciated, bare vegetated, alpine meadows and forested. Working with 4 vegetation zones at least enables the possibility to use land cover scenarios in HBV Light, which can contribute to better understanding of the dynamics in a hydrological systems. Approaches where land cover scenarios were used are e.g. the approach of Köplin et al. (2013) who investigated the importance of glacier and forest change in hydrological climate-impact studies by using land cover, climate and glacier scenarios in the PREVAH model.

The third restriction of the model is that only one value can be used for the temperature and precipitation gradients. This is a strong assumption, especially for larger catchment areas, since temperature and precipitation gradients can vary both in space and time. For example when so-called 'inversions' appear, which means that warmer less dense atmospheric layers cover colder more dense atmospheric layers, positive temperature gradients with elevation can be a result. When inversions disappear temperature gradients become negative again. This temporal variability in temperature gradients makes it difficult to use a constant value. Also spatial variation in temperature gradients can occur, which can be caused by steep, rough topography and appearance of valley and katabatic winds (Immerzeel et al., 2014). An additional problem of using constant temperature

gradients is that ice melt can be overestimated. In relation with precipitation gradients, spatial and temporal variability be the result of e.g. difference in precipitation gradients between the windward and leeward side of mountains or due to appearance of convective precipitation events.

The fourth restriction of the model is that the set of potential evapotranspiration values, uploaded in HBV Light as input, is applied over the entire catchment without the possibility to make a distinction of elevation zones. This can lead to overestimation of potential evapotranspiration with increasing elevation, i.e. because with increasing elevation temperature decreases, which subsequently results in decreasing potential evapotranspiration.

The inconsistencies in HBV Light may express themselves in the overestimation of ice melt and underestimation of snowmelt. To illustrate this, two figures are presented. The first figure (Figure 5.2) shows observed and simulated discharge of the Ötztaler Ache catchment (Brunau) for 2008-2012 together with the simulated discharge components. The second figure (Figure 5.3) shows total discharge of the Silvretta catchment (Klosters, Switzerland; catchment area = 103 km^2; glaciation = 7%) for 2010 together with snowmelt and ice melt components. From the differences between these figures it is evident that the glacial component of discharge in Brunau, in comparison with the glacial component observed in Klosters, is rather high and that the snow component is rather low. The main cause of these possible inconsistencies is probably the fact that 2003 is used as calibration year for the simulation of snow, leading to a systematic underestimation of snow accumulation in the model. Systematic underestimation of snow accumulation means that snowmelt is also underestimated and that glaciers in the model are supposed to be covered less by snow, which means more ice melt appears. Subsequently ice melt is overestimated. However we are not sure whether snowmelt is underestimated or ice melt is overestimated since there are no data series of observed runoff components that can be used to compare observed runoff components with simulated runoff components.

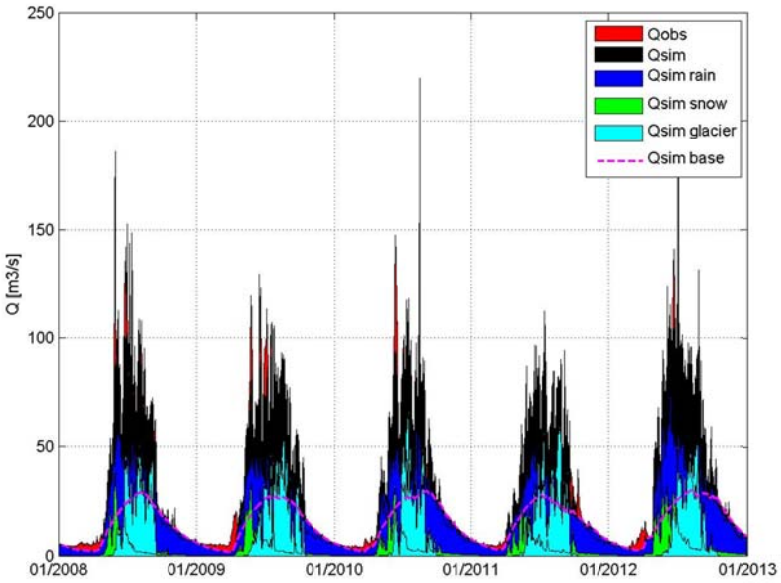

Figure 5.2: *Observed and Simulated Discharge (+ glacial, snow, rain and baseflow components) of the Ötztaler Ache (Brunau) for 2008-2012*

Next to restrictions and inconsistencies of the model there is also uncertainty related to the parameter sets used in the model. The parameter values were obtained by manual calibration, which has disadvantage that parameters can be over-parameterized or inter-correlation can appear between parameters. Also more than one parameter set can result in a good model performance, which makes it more difficult to find a unique parameter set.

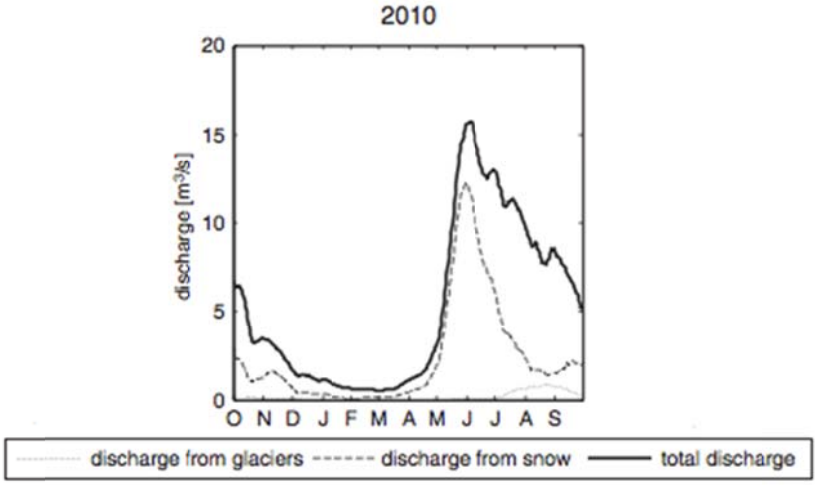

Figure 5.3: *Total Discharge, Discharge from Snow and Discharge from Glaciers of the Silvretta Catchment (Klosters) for 2010. Reference: Junghans et al., 2011*

6. Conclusions

The main aim of this study was to investigate the hydrological response of glacierized catchments in the Ötztaler Alps to future climate change. First glacier changes as a result of climate change were investigated in the Ötztaler/ Stubaier Alps and finally the hydrological response of glacierized catchments was investigated as a result of changes in glaciers and climate. From the study the following conclusions can be drawn:

- Glacier Change: Until ~2040 ice-thickness reduction is expected to be stronger than glacial area reduction. After ~2040 glacial area and volume reduction are expected to remain strong while ice-thickness reduction is expected to cease. The expectation is that in ~2100 less than 20% of the glacial areas (-79% to -94%) and volume (-88% to -97%) of 2006 will be left, assuming that temperature will increase between 0.9 °C and 3 °C until 2055.
- Runoff Change: Future runoff simulations, under glacier-only scenarios, show a relative runoff decrease up to 45% in August with the expectation that the glacio-nival (Ötztaler Ache) and glacial/glacio-nival (Gurgler Ache and Venter Ache) regimes will shift to a nivo-glacial regime (with exception of the Venter Ache catchment). Under climate-only scenarios, future runoff simulations show a relative runoff increase up to 310% in spring without changes in runoff regimes. For the combined scenarios, future runoff simulations show relative runoff increases up to 125% in spring and relative runoff decreases up to 55% in August. Likewise the expectation is that the glacio-nival and glacial/glacio-nival regimes will shift to moderate nival (Ötztaler Ache), nival (Gurgler Ache) and nivo-glacial regimes (Venter Ache).
- Peak Flow: Future peak flow statistics, under combined scenarios, show that flood seasonality will change with decreasing flood risk in July and increasing flood risk in May (Ötztaler Ache) and June (Gurgler and Venter Ache).
- Low Flow: Future low flow statistics, under combined scenarios, show that low flow conditions will appear less frequent in the near future for both Q_{70} and Q_{95}. For the mid-future and far future low flow conditions are expected to appear more frequently (Ötztaler Ache for Q_{70} and Q_{95}; Gurgler and Venter Ache for Q_{70}), with exception of the Gurgler and Venter Ache when using Q_{95} as a low flow index.

7. Recommendations & Further Research

7.1 Management & Policy Recommendations

In this section a set of recommendations focusing on water/water resources management and water policy of alpine valleys is provided.

- Although the observational meteorological network has been improved during last decades there is still a lack of observational data, especially for high altitude areas. Therefore a recommendation is to expand the observational meteorological network. The disadvantage however is that expanding an observational network can be very expensive and therefore is it necessary to develop cheaper instruments with the same or higher level of accuracy. A second alternative would be the set-up of an observational system where local stakeholders are involved. An example of such an observational system is the so-called "DinoLoket" system, which is a Dutch system where underground data like groundwater levels are saved. The advantages of such a system are the low costs (you do not have to pay ownership) and the increased density of data. Disadvantage however is that in mountainous areas the higher elevation zones are less populated, what makes the system less suitable. In these elevation zones an alternative would be to make use of the mountain huts and stations of ski lifts.
- In order to reduce impacts of possible increasing flood frequency the recommendation is to improve flood risk/hazard maps and to develop flood risk management plans according to the European Flood Directive (2007). As a part of the flood risk management plans adaptation measures could be developed in a co-operation with researchers, managers and other stakeholders. This form of co-operation is expected to function effectively because of factors like exchange of information and data. Examples of adaptation measures are evacuation plans, the construction of retention reservoirs, broadening of the floodplains, etc.
- In order to reduce impacts of possible increasing low flow frequency researchers, managers and stakeholders are recommended to cooperate with each other and to develop water plans, which include adaptation measures to improve the impact of low flow. Examples of adaptation measures are the construction of drinking water reservoirs or the development of new water use plans for inter alia the agricultural and energy sectors.
- After development or improvement of adaptation measures/strategies these measures/ strategies should be integrated in existing policy plans. Mainstreaming can be considered to be a strategy for integration of adaptation measures and strategies into existing policy plans.

7.2 Further Research

This study aimed to create a better understanding of how glacierized catchments would respond hydrologically to climate and glacier change. Although the results are sufficiently reliable to extract main trends, there are still a lot of uncertainties, which subsequently means that still a lot of improvements are needed. Therefore the following recommendations are given for further research:

- To create more complete precipitation data sets a recommendation would be to repair incomplete time series with the help of existing complete data sets. With more complete precipitation data sets it is possible to improve spatial interpolation procedures, such as IDW. Tools, which may be proposed to implement these reparations, are Poisson-Gamma distributions.
- Improvements are needed in modelling of glacial evolution. To have a better and more reliable understanding of glacier evolution, aspects such as glacial accumulation and ablation, glacial movement, glacial energy balance and snow dynamics should be incorporated.
- Next to changes in climate and glaciers there are also other important change factors, which are e.g. land cover changes, which can be an influencing factor in runoff evolution, population growth and economic developments (Viviroli et al., 2011). The latter factors are mainly important in terms of water demand. When population growth and economic

developments increase (and therefore also demand of water) and low flow conditions become more frequent, it can possibly lead to water stress conditions during summer. Therefore it can be important to study the effects of land cover change, population growth and economic developments on water demand and low flows.

- To investigate vegetation dynamics and the effects of land cover changes HBV Light should be provided with more vegetation zones. In this manner it is possible, e.g. to divide vegetated zones into alpine meadow vegetation zones and forested vegetation zones. It would also be recommendable to extend HBV Light with a so-called "GSI (Growing Season Index) approach. Förster et al. (2012) used this approach to extend the semi-distributed hydrological model "Panta Rhei" in order to investigate the effect of seasonal vegetation changes on runoff characteristics.
- To relax the assumption of constant temperature and precipitation gradients HBV Light should be improved in such a way that next to using daily temperature and precipitation data as input data, it is also possible to use daily temperature and precipitation gradients as input data.
- To avoid overestimation of potential evapotranspiration with increasing elevation HBV Light should be improved in a way that every elevation zone is equipped with an own set of evapotranspiration values. It can also be an option to extend HBV Light with a Penman-Monteith module, which not only corrects potential evapotranspiration for changes in elevation, but also corrects potential evapotranspiration for changes in wind speed, humidity and radiation (Allen et al., 1998).
- Improvements are needed concerning internal consistencies of the model to avoid overestimation of ice melt and underestimation of snowmelt.
- To investigate whether snowmelt is underestimated or ice melt is overestimated it may be an option to conduct an end-member-mixing-analysis in order to study the contribution of different runoff components. For instance Hunkeler (2013) used this approach to study contributions of rainfall, snowmelt and ice melt to total runoff in the region of the Plaine Morte glacier (Switzerland).

8. References

Abermann, J., Lambrecht, A., Fischer, A., & Kuhn, M. (2009). Quantifying changes and trends in glacier area and volume in the Austrian Ötztal Alps (1969–1997–2006). *The Cryosphere Discussions*, *3*(2), 415-441.

Abermann, J., Seiser, B., Meran, I., Stocker-Waldhuber, M., Goller, M., & Fischer, A. (2012). A new ALS glacier inventory of North Tyrol, Austria, for 2006. *Z. Gletscherkd. Glazialgeol*, *43*(44), 109-119.

Achleitner, S., Schöber, J., Rinderer, M., Leonhardt, G., Schöberl, F., Kirnbauer, R., & Schönlaub, H. (2012). Analyzing the operational performance of the hydrological models in an alpine flood forecasting system. *Journal of Hydrology*, *412*, 90-100.

Allen, R. G., Pereira, L. S., Raes, D., & Smith, M. (1998). Crop evapotranspiration-Guidelines for computing crop water requirements-FAO Irrigation and drainage paper 56. *FAO, Rome*, *300*, 6541.

Appenzeller, C., Bey, I., Croci-Maspoli, M., Fuhrer, J., Knutti, R., Kull, C., & Schaer, C. (2011). Swiss Climate Change Scenarios CH2011. *C2SM, MeteoSwiss, ETH Zurich. NCCR Climate and OcCC, Zurich*.

Alpine Convention (2009). *Water and Water Management Issues – Report on the State of the Alps.* [Online]. Available from: http://www.alpconv.org/en/publications/alpine/Documents/20090625_RSA_II_long.pdf [Accessed on 28th November 2013].

Asztalos, J. (2004). Ein Schnee-und Eisschmelzmodell für vergletscherte Einzugsgebiete (*Diplomarbeit Technische Universität Wien*).

Asztalos, J., Kirnbauer, R., Escher-Vetter, H., & Braun, L. (2007). A distributed energy balance snow and glacier melt model as a component of a flood forecasting system for the Inn River. In *Proceedings of the Alpine* Snow* Workshop, Munich* (pp. 9-17).

Beniston, M. (2011). Alps. In *Encyclopedia of Snow, Ice and Glaciers* (pp. 35-38). Springer Netherlands.

Bergström, S., & Forsman, A. (1973). Development of a conceptual deterministic rainfall-runoff model. *Nordic hydrology*, *4*(3), 147-170.

Bergström, S., Harlin, J., & Lindström, G. (1992). Spillway design floods in Sweden: I. New guidelines. *Hydrological sciences journal*, *37*(5), 505-519.

Bergström, S., & Singh, V. P. (1995). The HBV model. *Computer models of watershed hydrology.*, 443-476.

Bosshard, T., & Zappa, M. (2008). Regional parameter allocation and predictive uncertainty estimation of a rainfall-runoff model in the poorly gauged Three Gorges Area (PR China). *Physics and Chemistry of the Earth, Parts A/B/C*, *33*(17), 1095-1104.

Bosshard, T., Kotlarski, S., Ewen, T., & Schär, C. (2011). Spectral representation of the annual cycle in the climate change signal. *Hydrology & Earth System Sciences Discussions*, *8*(1).

Braun, L. N., & Aellen, M. (1990). Modelling discharge of glacierized basins assisted by direct measurements of glacier mass balance. *IAHS Publ*, *193*, 99-106.

Braun, L. N., & Renner, C. B. (1992). Application of a conceptual runoff model in different physiographic regions of Switzerland. *Hydrological Sciences Journal*, *37*(3), 217-231.

Braun, L. N., Grabs, W., & Rana, B. (1993). Application of a conceptual precipitation-runoff model in the Langtang Kfaola Basin, Nepal Himalaya. In *Snow and Glacier Hydrology (Proceedings of the Kathmandu Symposium)*. IAHS Publ. 218, Wallingford, UK.

Braun, L. N., Weber, M., & Schulz, M. (2000). Consequences of climate change for runoff from Alpine regions. *Annals of glaciology*, *31*(1), 19-25.

Bundesministerium für Land-und Forstwirtschaft (2005). Digitaler Hydrologischer Atlas Österreich (digHAO). Version 2.0.1.

Casassa, G., López, P., Pouyaud, B., & Escobar, F. (2009). Detection of changes in glacial run-off in alpine basins: examples from North America, the Alps, central Asia and the Andes. *Hydrological Processes*, *23*(1), 31-41.

Einarsson, B. & Jónsson, S. (2010). *The effect of climate change on runoff from two watersheds in Iceland.* [Online]. Available from: http://rafhladan.is/bitstream/handle/10802/4478/2010_016.pdf?sequence=1 [Accessed on 11th July 2014].

Farinotti, D., Huss, M., Bauder, A., Funk, M., & Truffer, M. (2009). A method to estimate the ice volume and ice-thickness distribution of alpine glaciers. *Journal of Glaciology*, *55*(191), 422-430.

Farinotti, D., Usselmann, S., Huss, M., Bauder, A., & Funk, M. (2012). Runoff evolution in the Swiss Alps: projections for selected high-alpine catchments based on ENSEMBLES scenarios. *Hydrological Processes*, *26*(13), 1909-1924.

Federer, C. A., & Lash, D. (1978). BROOK: A hydrologic simulation model for eastern forests.

Förster, K., Gelleszun, M., & Meon, G. (2012). A weather dependent approach to estimate the annual course of vegetation parameters for water balance simulations on the meso-and macroscale. *Advances in Geosciences*, *32*(32), 15-21.

Gabbi, J., Farinotti, D., Bauder, A., & Maurer, H. (2012). Ice volume distribution and implications on runoff projections in a glacierized catchment. *Hydrology and Earth System Sciences Discussions*, *9*(6), 7507-7541.

Glen, J. W. (1955). The creep of polycrystalline ice. *Proceedings of the Royal Society of London. Series A. Mathematical and Physical Sciences*, *228*(1175), 519-538.

Gurtz, J., Baltensweiler, A., & Lang, H. (1999). Spatially distributed hydrotope-based modelling of evapotranspiration and runo in mountainous basins. *Hydrological Processes*, *13*, 2751-2768.

Gurtz, J., Zappa, M., Jasper, K., Lang, H., Verbunt, M., Badoux, A., & Vitvar, T. (2003). A comparative study in modelling runoff and its components in two mountainous catchments. *Hydrological Processes*, *17*(2), 297-311.

Hagg, W. (2003). *Auswirkungen von Gletscherschwund auf die Wasserspende hochalpiner Gebiete, Vergleich Alpen-Zentralasien* (Doctoral dissertation, lmu).

Hagg, W., Braun, L. N., Kuhn, M., & Nesgaard, T. I. (2007). Modelling of hydrological response to climate change in glacierized Central Asian catchments. *Journal of Hydrology*, *332*(1), 40-53.

Hamon, W. R. (1961). Estimating potential evapotranspiration. In *Proceedings of the American Society of Civil Engineers*, *87*, 107-120.

HD Tirol (2014). *Hydrographischen Daten Österreichs.* [Online]. Available from: http://ehyd.gv.at [Accessed on 28th February 2014]

Heinrich, G., & Gobiet, G. (2011). Expected climate change and its uncertainty in the Alpine region. WEGC Report to ACRP Nr. 02/2011. *Wegener Center for Climate and Global Change, University of Graz, Austria*.

Helfricht, K. (2013). *Calculation of Ice Thickness Scenarios based on Ice Thickness Distributions and Geodetic Mass Balance.* alpS Center for Climate Change Adaptation, Innsbruck.

Helfricht, K., Schneeberger, K., Welebil, I., Bellinger, J., Schöber, J., Huttenlau, M., Schneider, K., & Formayer, H. (In Press). Abflussszenarien im Einzugsgebiet der Ötz unter Berücksichtigung von zukünftigen Veränderungen der Kryosphäre.

Hunkeler, S. (2013). Bestimmung der Wasserzusammensetzung in den Abflüssen im Gebiet des Plaine-Morte-Gletschers: Durchführung einer End-Member-Mixing-Analyse zur Bestimmung verschiedener Ursprungswasser des Abflusses im Kanton Bern (*Masterarbeit Univerität Bern*).

Hock, R. (1999). A distributed temperature-index ice-and snowmelt model including potential direct solar radiation. *Journal of Glaciology*, *45*(149), 101-111.

Hottelet, C., Braun, L. N., Leibundgut, C., & Rieg, A. (1993). Simulation of snowpack and discharge in an alpine karst basin. In *Snow and Glacier Hydrology (Proceedings of the Kathmandu Symposium)*. IAHS Publ. 218, Wallingford, UK.

Huss, M., Farinotti, D., Bauder, A., & Funk, M. (2008). Modelling runoff from highly glacierized alpine drainage basins in a changing climate. *Hydrological Processes*, *22*(19), 3888-3902.

Huss, M. (2011). Present and future contribution of glacier storage change to runoff from macroscale drainage basins in Europe. *Water Resources Research*, *47*(7).

Huss, M., Zemp, M., Joerg, P. C., & Salzmann, N. (2014). High uncertainty in 21st century runoff projections from glacierized basins. *Journal of Hydrology*, *510*, 35-48.

Immerzeel, W.W., van Beek, L.P.H. & Bierkens, M.F.P. (2010). Climate Change Will Affect the Asian Water Towers*. Science, 328*, 1382-1385.

Immerzeel, W. W., Van Beek, L. P. H., Konz, M., Shrestha, A. B., & Bierkens, M. F. P. (2012). Hydrological response to climate change in a glacierized catchment in the Himalayas. *Climatic change*, *110*(3-4), 721-736.

Immerzeel, W. W., Pellicciotti, F., & Bierkens, M. F. P. (2013). Rising river flows throughout the twenty-first century in two Himalayan glacierized watersheds. *Nature Geoscience*, *6*(9), 742-745.

Immerzeel, W. W., Petersen, L., Ragettli, S., & Pellicciotti, F. (2014). The importance of observed gradients of air temperature and precipitation for modeling runoff from a glacierized watershed in the Nepalese Himalayas. *Water Resources Research*.

Jeelani, G., Feddema, J. J., Veen, C. J., & Stearns, L. (2012). Role of snow and glacier melt in controlling river hydrology in Liddar watershed (western Himalaya) under current and future climate. *Water Resources Research*, *48*(12).

Juen, I., Kaser, G., & Georges, C. (2007). Modelling observed and future runoff from a glacierized tropical catchment (Cordillera Blanca, Perú). *Global and Planetary Change*, *59*(1), 37-48.

Junghans, N., Cullmann, J. & Huss, M. (2011). Evaluating the effect of snow and ice melt in an Alpine headwater catchment and further downstream in the River Rhine. *Hydrological Sciences Journal, 56(6)*, 981-993.

Kaser, G., Großhauser, M., & Marzeion, B. (2010). Contribution potential of glaciers to water availability in different climate regimes. *Proceedings of the National Academy of Sciences*, *107*(47), 20223-20227.

Kirnbauer, R., Schöberl, F., Schönlaub, H., Kleindienst, H., Asztalos, J., Drabek, U., Leonhardt, G., Oberparleiter, C., & Senfter, S. (2007). *Endbericht Phase 1 HOPI HOchwasser Prognosesystem Inn.* alpS Zentrum für Naturgefahren Management (Center for Climate Change Adaptation), Innsbruck.

Kirnbauer, R., Achleitner, S., Schöber, J., Asztalos, J., & Schönlaub, H. (2009). Hochwasservorhersage Inn: Modellierung der Gletscherabflüsse, Mitteilungsblatt des Hydrographischen Dienstes in Osterreich, Nr. 86, 109–130.

Kleindienst, H. (1996). Erweiterung und Erprobung eines anwendungsorientierten hydrologischen Modells zur Gangliniensimulation in kleinen Wildbacheinzugsgebieten. *Unpublished Diploma Thesis, University München*.

Klok, L., & Roelofsma, K. (1999). Modelling of glacier and snow melt processes within the hydrological catchment model WaSiM-ETH. *Sectie Waterhuishouding.*

Klok, E. J., Jasper, K., Roelofsma, K. P., Gurtz, J., & Badoux, A. (2001). Distributed hydrological modelling of a heavily glaciated Alpine river basin. *Hydrological Sciences Journal*, *46*(4), 553-570.

Koboltschnig, G. R., Schoner, W., Zappa, M., & Holzmann, H. (2007). Contribution of glacier melt to stream runoff: if the climatically extreme summer of 2003 had happened in 1979. *Annals of Glaciology*, *46*(1), 303-308.

Koboltschnig, G. R., Schöner, W., Zappa, M., Kroisleitner, C., & Holzmann, H. (2008). Runoff modelling of the glacierized Alpine Upper Salzach basin (Austria): Multi-criteria result validation. *Hydrological Processes*, *22*(19), 3950-3964.

Köplin, N., Schädler, B., Viviroli, D., & Weingartner, R. (2013). The importance of glacier and forest change in hydrological climate-impact studies. *Hydrology and Earth System Sciences*, *17*(2), 619-635.

Konz, M., & Seibert, J. (2010). On the value of glacier mass balances for hydrological model calibration. *Journal of Hydrology*, *385*(1), 238-246.

Kuhn, M., Nickus, U., & Pellet, F. (1982). *Die Niederschlagsverhältnisse im inneren Ötztal.* [Online]. Available from: http://epic.awi.de/32636/2/Kuhn_etal_1982.pdf [Accessed on 29th May 2014].

Lambrecht, A., & Kuhn, M. (2007). Glacier changes in the Austrian Alps during the last three decades, derived from the new Austrian glacier inventory. *Annals of Glaciology*, *46*(1), 177-184.

Land Tirol (2006). Digitales Geländemodell Tirol [Online]. Available from: https://www.tirol.gv.at/data/datenkatalog/geographie-und-planung/digitales-gelaendemodell-tirol/ [Accessed on: 15th July 2014].

Lebensministerium (2010). *Hydrographisches Jahrbuch von Österreich 2010.* [Online]. Available from: http://www.bmlfuw.gv.at/wasser/wasser-oesterreich/wasserkreislauf/hydrographische_daten/jahrbuecher/JB2010.html [Accessed on 29th January 2014].

Lindström, G., Johansson, B., Persson, M., Gardelin, M., & Bergström, S. (1997). Development and test of the distributed HBV-96 hydrological model. *Journal of hydrology*, *201*(1), 272-288.

Linsbauer, A., Paul, F., Machguth, H., & Haeberli, W. (2013). Comparing three different methods to model scenarios of future glacier change in the Swiss Alps. *Annals of Glaciology*, *54*(63), 241-253.

Lutz, A. F., Immerzeel, W. W., Gobiet, A., Pellicciotti, F., & Bierkens, M. F. P. (2013). Comparison of climate change signals in CMIP3 and CMIP5 multi-model ensembles and implications for Central Asian glaciers. *Hydrology and Earth System Sciences*, *17*(9), 3661-3677.

Lutz, A. F., Immerzeel, W. W., Shrestha, A. B., & Bierkens, M. F. P. (2014). Consistent increase in High Asia's runoff due to increasing glacier melt and precipitation. *Nature Climate Change*.

Mader, H., Steidl, T., & Wimmer, R. (1996). *Abflußregime Österreichischer Fließgewässer*. Umweltbundesamt.

Martinec, J. (1975). Snowmelt Runoff Model for Stream Flow Forecasts*. Nordic Hydr*, *6(3),* 145-154.

Martinec, J., Rango, A. & Roberts R. (2008). *Snowmelt Runoff Model (SRM) User's Manual.* [Online]. Available from: http://www.mastergardeners.nmsu.edu/pubs/research/water/srmspecrep100.pdf [Accessed on 1st November 2013].

Middelkoop, H. (2008). Climate Change and Hydrological Impact Studies. In Bierkens, M.F.P., Dolman, A.P., Troch, P.A. (eds.). *Climate and the Hydrological Cycle.* IAHS Press, Oxfordshire.

Nash, J., & Sutcliffe, J. V. (1970). River flow forecasting through conceptual models part I—A discussion of principles. *Journal of hydrology*, *10*(3), 282-290.

Oltchev, A., Cermak, J., Gurtz, J., Tishenko, A., Kiely, G., Nadezhdina, N., ... & Gravenhorst, G. (2002). The response of the water fluxes of the boreal forest region at the Volga's source area to climatic and land-use changes. *Physics and Chemistry of the Earth, Parts A/B/C*, *27*(9), 675-690.

Parajka, J., & Blöschl, G. (2006). Validation of MODIS snow cover images over Austria. *Hydrology & Earth System Sciences Discussions*, *3*(4).

Pardé, M. (1947). Fleuves et Rivieres, sec. *Edn. Colin, Parris*.

Pellicciotti, F., Bauder, A., & Parola, M. (2010). Effect of glaciers on streamflow trends in the Swiss Alps. *Water Resources Research*, *46*(10).

Schädler, B., & Weingartner, R. (2010). Impact of climate change on water resources in the alpine regions of Switzerland. In *Alpine Waters* (pp. 59-69). Springer Berlin Heidelberg.

Schneeberger, C., Blatter, H., Abe-Ouchi, A., & Wild, M. (2003). Modelling changes in the mass balance of glaciers of the northern hemisphere for a transient 2× CO2 scenario. *Journal of Hydrology*, *282*(1), 145-163.

Schöber, J., Achleitner, S., Kirnbauer, R., Schöberl, F., & Schönlaub, H. (2010). Hydrological modelling of glacierized catchments focussing on the validation of simulated snow patterns-applications within the flood forecasting system of the Tyrolean river Inn. *Advances in Geosciences*, *27*, 99-109.

Schulla, J. (1997). *Hydrologische Modellierung von Flussgebieten zur Abschätzung der Folgen von Klimaänderungen* (Doctoral dissertation, Diss. Naturwiss. ETH Zürich, Nr. 12018, 1997. Ref.: H. Lang; Korref.: W. Kinzelbach; Korref.: R. Schulze).

Seibert, J. (1997). Estimation of parameter uncertainty in the HBV model. *Nordic Hydrology*, *28*(4), 247-262.

Seibert, J. (1999). Regionalisation of parameters for a conceptual rainfall-runoff model. *Agricultural and Forest Meteorology*, *98*, 279-293.

Seibert, J. (2005). *HBV light version 2, User's Manual.* [Online] Available from: http://www.geo.uzh.ch/fileadmin/files/content/abteilungen/h2k/Docs_download/HBV_manual_2005.pdf [Accessed on 11th November 2013]

Seibert, J., & Vis, M. J. P. (2012). Teaching hydrological modeling with a user-friendly catchment-runoff-model software package. *Hydrology and Earth System Sciences*, *16*(9), 3315-3325.

Seibert, J. & Vis, M. J. P. (2014). HBV Light. Version 4.0.0.7.

Smakhtin, V. U. (2001). Low flow hydrology: a review. *Journal of hydrology*, *240*(3), 147-186.

Sorg, A., Huss, M., & Stoffel, M. (2013, April). How much water will glaciers in the Chon Kemin valley (Tien Shan mountains, Kyrgyzstan) provide in the future?. In *EGU General Assembly Conference Abstracts 15*, 5479).

Stahl, K., Moore, R. D., Shea, J. M., Hutchinson, D., & Cannon, A. J. (2008). Coupled modelling of glacier and streamflow response to future climate scenarios. *Water Resources Research*, *44*(2).

Steele-Dunne, S., Lynch, P., McGrath, R., Semmler, T., Wang, S., Hanafin, J., & Nolan, P. (2008). The impacts of climate change on hydrology in Ireland. *Journal of Hydrology*, *356*(1), 28-45.

Ragettli, S., and F. Pellicciotti (2012), Calibration of a physically based, spatially distributed hydrological model in a glacierized basin: On the use of knowledge from glaciometeorological processes to constrain model parameters. *Water Resources Research*, *48*.

Ragettli, S., F. Pellicciotti, R. Bordoy, and W. W. Immerzeel (2013), Sources of uncertainty in modeling the glaciohydrological response of a Karakoram watershed to climate change. *Water Resources Res*earch, *49*.

Rögnvaldsson, Ó., Jónsdóttir, J. F., & Ólafsson, H. (2007). Numerical simulations of precipitation in the complex terrain of Iceland Comparison with glaciological and hydrological data. *Meteorologische Zeitschrift*, *16*(1), 71-85.

Verbunt, M., Gurtz, J., Jasper, K., Lang, H., Warmerdam, P., & Zappa, M. (2003). The hydrological role of snow and glaciers in alpine river basins and their distributed modeling. *Journal of hydrology*, *282*(1), 36-55.

Verbunt, M., Walser, A., Gurtz, J., Montani, A., & Schär, C. (2007). Probabilistic flood forecasting with a limited-area ensemble prediction system: selected case studies. *Journal of Hydrometeorology*, *8*(4), 897-909.

Viviroli, D., & Weingartner, R. (2004). The hydrological significance of mountains: from regional to global scale. *Hydrology and Earth System Sciences Discussions*, *8*(6), 1017-1030.

Viviroli, D., Dürr, H. H., Messerli, B., Meybeck, M., & Weingartner, R. (2007). Mountains of the world, water towers for humanity: Typology, mapping, and global significance. *Water Resources Research*, *43*(7).

Viviroli, D., Zappa, M., Gurtz, J., & Weingartner, R. (2009). An introduction to the hydrological modelling system PREVAH and its pre-and post-processing-tools. *Environmental Modelling & Software*, *24*(10), 1209-1222.

Viviroli, D., Archer, D. R., Buytaert, W., Fowler, H. J., Greenwood, G. B., Hamlet, A. F., ... & Woods, R. (2011). Climate change and mountain water resources: Overview and recommendations for research, management and policy. *Hydrology & Earth System Sciences*, *15*(2).

Wehren, B., Weingartner, R., Schädler, B., & Viviroli, D. (2010). General Characteristics of Alpine Waters. In *Alpine Waters* (pp. 17-58). Springer Berlin Heidelberg.

WMO (2008). *Manual on Low Flow Estimation and Prediction.* [Online]. Available from: http://www.wmo.int/pages/prog/hwrp/publications/low-flow_estimation_prediction/WMO%201029%20en.pdf [Accessed on 7th May 2014]

ZAMG (2013). *Klimadaten von Österreich 1971 – 2000.* [Online]. Available from: http://www.zamg.ac.at/fix/klima/oe71-00/klima2000/klimadaten_oesterreich_1971_frame1.htm [Accessed on 4th December 2013].

Zappa, M., Rotach, M. W., Arpagaus, M., Dorninger, M., Hegg, C., Montani, A. & Wunram, C. (2008). MAP D-PHASE: real-time demonstration of hydrological ensemble prediction systems. *Atmospheric Science Letters*, *9*(2), 80-87.

Appendices

Appendix I: Hydrographic Map

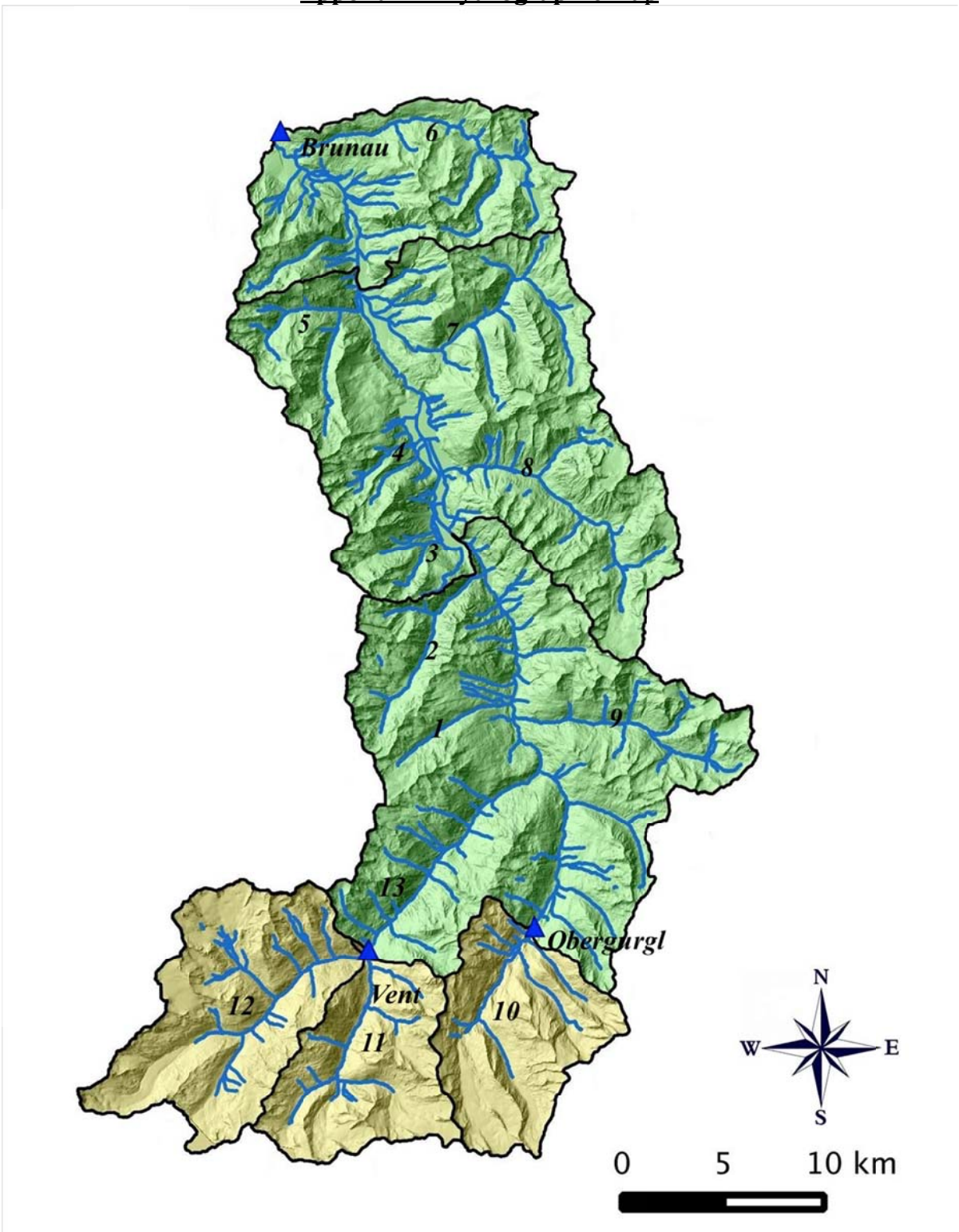

Hydrographic map of Ötztaler Ache catchment. The numbers are representing the main tributaries of the catchment.
1 = Rettenbach, 2 = Pollesbach, 3 = Poltbach, 4 = Unterriederbach, 5 = Leierstalbach, 6 = Stuibenbach, 7 = Hairlachbach, 8 = Fischbach, 9 = Windache, 10 = Gurgler Ache, 11 = Niedertalbach, 12 = Rofenache and 13 = Venter Ache

Appendix II: Temperature Measurements West Tyrol 1986-2012

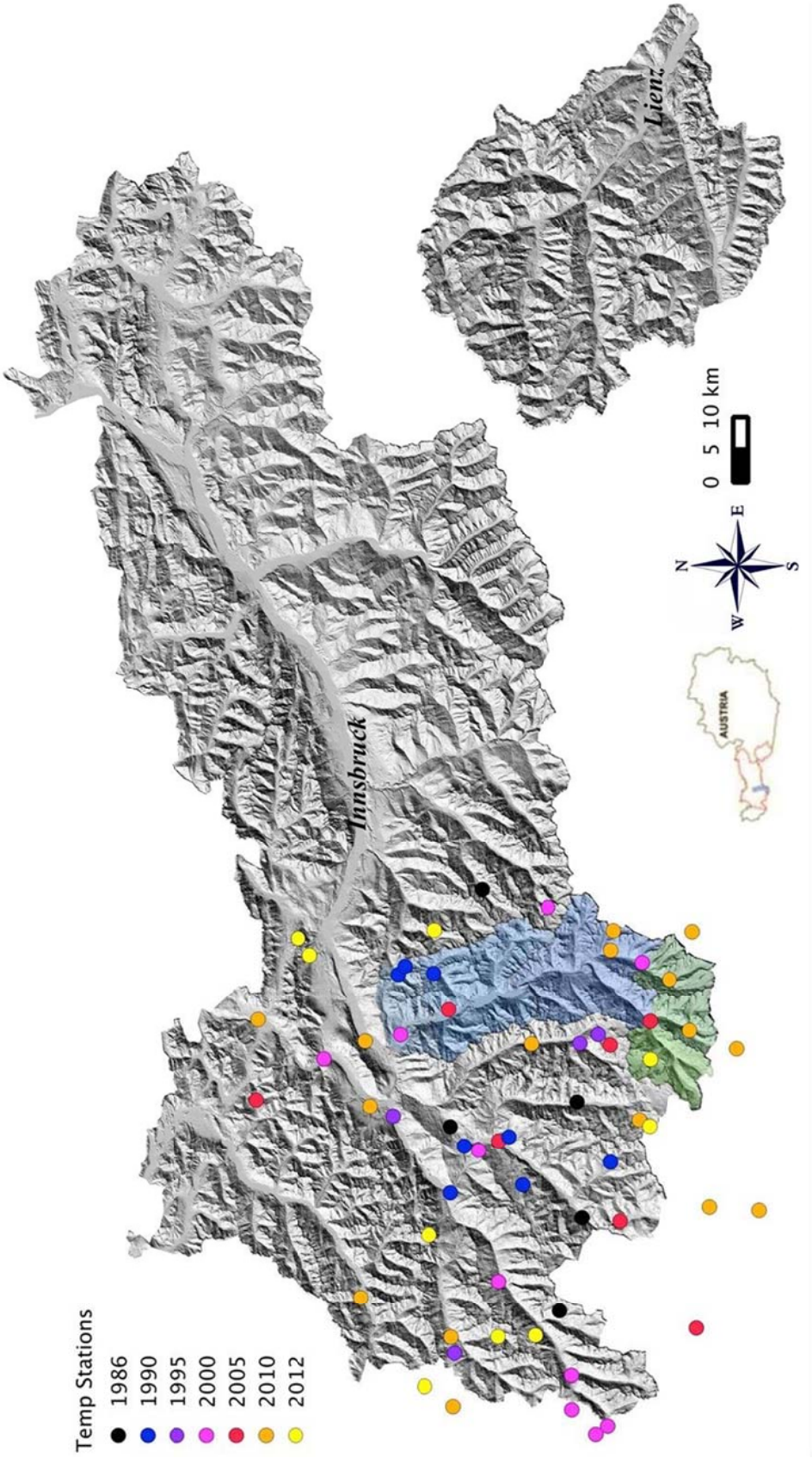

Appendix III: Precipitation Measurements Ötztal 1986-2012